



Virginia Commonwealth University  
VCU Scholars Compass

---

Theses and Dissertations

Graduate School

---

2011

## Drug Design, Biological Activity, and Metabolic Consequences of Cytotoxic Platinum Compounds: Utilizing Fluorescent Tagging to Understand Drug Action and Metabolism

Brad Benedetti  
*Virginia Commonwealth University*

Follow this and additional works at: <https://scholarscompass.vcu.edu/etd>

 Part of the [Chemistry Commons](#)

© The Author

---

Downloaded from

<https://scholarscompass.vcu.edu/etd/195>

This Dissertation is brought to you for free and open access by the Graduate School at VCU Scholars Compass. It has been accepted for inclusion in Theses and Dissertations by an authorized administrator of VCU Scholars Compass. For more information, please contact [libcompass@vcu.edu](mailto:libcompass@vcu.edu).

**Drug Design, Biological Activity, and Metabolic Consequences of  
Cytotoxic Platinum Compounds: Utilizing Fluorescent Tagging to  
Understand Drug Action and Metabolism**

A dissertation submitted in partial fulfillment of the requirements for the degree of Doctor  
of Philosophy at Virginia Commonwealth University

By

Brad T. Benedetti

B.S., Hampden-Sydney College, Hampden-Sydney, Virginia

May, 2006

Director: Dr. Nicholas P. Farrell

Professor

Department of Chemistry  
Virginia Commonwealth University  
Richmond, Virginia

April, 2011

## Acknowledgements

This dissertation, as with all things in life, is the result of a combination of people and events that if alone could not have been possible. I first want to thank my advisor, Dr. Nicholas Farrell, for allowing me the opportunity to work on this project and to be involved with research of this caliber. He has given me the opportunity to grow as a researcher and an individual, as well as the scientific freedom to follow my interests and ideas, no matter how far off based they may have been. And for this I will always be grateful. I would also like to thank Dr. Yun Qu, for her constant support over the years, and for being not just a colleague, but a true friend. As I mentioned earlier, this work could not have been completed without the advice and direction of numerous post-docs and graduate students. I want to thank all present and past group members as well as my committee members for providing me with excellent guidance and mentorship over the last five years.

I would also like to thank, more than words can describe, the support, guidance, and love of my mother, Debra, and my brother, Cory. They continued to believe in me, regardless of the situation or circumstances, or the extended amount of time obtaining a Ph.D. requires. I also want to thank my wife, Ana Paula, for her patience and enduring love during the last 3 years. I could not have achieved the goals and dreams that I have achieved in my life without her love and support.

I would like to make a special acknowledgement and 'thank you' to my father, William "Biff" Benedetti. I thank him for the love and guidance he has provided me throughout my entire life. My passion and dedication to the field of cancer research unfortunately became a greater calling in 2005, when he was diagnosed with prostate cancer. Sadly, he became a victim of this tragic disease on Nov. 15<sup>th</sup> 2011. The research of this work, as well as my passion for a treatment of this disease, is dedicated to him. He will be greatly missed, but his memory lives on forever in our hearts and minds.

## Table of Contents

|                       |      |
|-----------------------|------|
| List of Tables        | vii  |
| List of Figures       | viii |
| List of Abbreviations | xi   |
| Abstract              | xiii |

### **Chapter 1: Cancer and Platinum Based Chemotherapeutics**

|   |    |
|---|----|
| Cancer  | 1  |
| Cisplatin and Platinum Analogs                              | 1  |
| Trans-Platinum Compounds                                    | 7  |
| Polynuclear Platinum Compounds                              | 9  |
| Non-Covalent Polynuclear Platinum Compounds                 | 9  |
| Pharmacological Factors Affecting Platinum Based Treatments | 14 |
| Fluorescence Cellular Imaging of Platinum Compounds         | 17 |
| Concluding Remarks and Project Overview                     | 18 |
| List of References  | 21 |

### **Chapter 2: Modulation of protein-drug deactivation through carboxylate ligand modification in a series of cytotoxic trans-platinum planar amine compounds**

|                        |    |
|------------------------|----|
| Abstract               | 29 |
| Introduction           | 30 |
| Results and Discussion | 32 |

|                      |    |
|----------------------|----|
| Conclusion           | 48 |
| Material and Methods | 48 |
| List of References   | 52 |

### **Chapter 3: Pharmacokinetic Studies of Polynuclear Platinum Complexes with Plasma and Human Serum Albumin: Implications for Drug Design and Delivery**

|                        |    |
|------------------------|----|
| Abstract               | 55 |
| Introduction           | 56 |
| Results and Discussion | 62 |
| Conclusion             | 79 |
| Material and Methods   | 79 |
| List of References     | 83 |

### **Chapter 4: Effects of non-covalent platinum drug-protein interactions on drug efficacy: Use of fluorescent conjugates as probes for drug metabolism**

|                        |     |
|------------------------|-----|
| Abstract               | 87  |
| Introduction           | 88  |
| Results and Discussion | 91  |
| Conclusion             | 109 |
| Material and Methods   | 110 |
| List of References     | 117 |

## **Chapter 5: Design, Synthesis, and Anticancer Activity of Fluorescent-Based Dual Function *trans*-Platinum-NBD Complexes**

|                        |     |
|------------------------|-----|
| Introduction           | 124 |
| Results and Discussion | 128 |
| Conclusion             | 137 |
| Material and Methods   | 138 |
| List of References     | 143 |

## **Chapter 6: Conclusion**

### **Appendix A: TriplatinNC, a Nucleolar-Targeting Agent, Disrupts rRNA**

#### **Transcription Leading to G1 Arrest and p53-independent Apoptosis**

|                        |     |
|------------------------|-----|
| Abstract               | 149 |
| Introduction           | 150 |
| Results and Discussion | 154 |
| Summary                | 173 |
| Material and Methods   | 176 |
| List of References     | 180 |

### **Appendix B: Pre-association of polynuclear platinum anticancer agents on a protein, human serum albumin. Implications for drug design**

|              |     |
|--------------|-----|
| Abstract     | 185 |
| Introduction | 186 |

|                        |            |
|------------------------|------------|
| Results and Discussion | 190        |
| Conclusion             | 200        |
| Experimental           | 201        |
| List of References     | 205        |
| <b>Vita</b>            | <b>210</b> |

## List of Tables

|                  |   | <b>Page</b> |
|------------------|---|-------------|
| <b>Table 2.1</b> | Effects of ligand substitution on methionine binding  | 39          |
| <b>Table 2.2</b> | Effects of serum binding on efficacy of trans-platinum compounds in A2780 ovarian carcinoma cells | 43          |
| <b>Table 5.1</b> | Binding affinities calculated by fluorometric titration   | 130         |
| <b>Table 5.2</b> | Cytotoxic activity of the Trans-NBD complexes and linkers   | 132         |
| <b>Table 5.3</b> | Cell accumulation and DNA binding for the Trans-NBD series  | 134         |
| <b>Table A.1</b> | Effect of cisplatin and TriplatinNC against the 2008 ovarian tumor xenograft mouse model          | 175         |



## List of Figures

|                   |  | <b>Page</b> |
|-------------------|--|-------------|
| <b>Figure 1.1</b> | Chemical Structures of Clinical Platinum Chemotherapeutics                               | 5           |
| <b>Figure 1.2</b> | DNA adducts formed after Cisplatin treatment   | 6           |
| <b>Figure 1.3</b> | Chemical structures of Trans-Platinum anticancer compounds                               | 8           |
| <b>Figure 1.4</b> | Chemical Structures Selected Covalent and Non-Covalent<br>Polynuclear Platinum Compounds | 11          |
| <b>Figure 1.5</b> | Long-Range DNA-Adducts formed by BBR3464   | 12          |
| <b>Figure 1.6</b> | Crystal Structure of TriplatinNC Interactions with DNA                                   | 13          |
| <b>Figure 2.1</b> | Structures of trans-platinum planar amine (TPA) carboxylate<br>compounds studied         | 35          |
| <b>Figure 2.2</b> | NMR Spectra of NAM with t-Pt(4-pic)NH <sub>3</sub> OFm                                   | 36          |
| <b>Figure 2.3</b> | NMR Spectra of NAM with t-Pt(4-pic)NH <sub>3</sub> OAc                                   | 37          |
| <b>Figure 2.4</b> | <sup>195</sup> Pt NMR Spectra of t-Pt(4-pic)NH <sub>3</sub> OAc reaction with NAM        | 38          |
| <b>Figure 2.5</b> | Effects of ligand substitution on HSA protein binding                                    | 41          |
| <b>Figure 2.6</b> | Influence of protein binding on platinum cellular uptake                                 | 45          |
| <b>Figure 2.7</b> | Influence of protein binding on DNA platination  | 47          |
| <b>Figure 3.1</b> | Chemical Structures of Cisplatin and Polynuclear<br>Platinum Compounds                   | 60          |
| <b>Figure 3.2</b> | Chemical Structures of Selected Polynuclear Platinum Compounds                           | 61          |
| <b>Figure 3.3</b> | Effects of mouse plasma binding on drug availability                                     | 63          |
| <b>Figure 3.4</b> | Effects of human plasma binding on drug availability                                     | 66          |
| <b>Figure 3.5</b> | Human Plasma Binding with BBR3610 and derivatives  | 67          |

|                    |   |     |
|--------------------|---|-----|
| <b>Figure 3.6</b>  | Human Plasma Binding with SET3007 and derivatives   | 68  |
| <b>Figure 3.7</b>  | “Pre-Association” Effects and Significance of Electrostatic Interactions on Human Serum Albumin Binding | 71  |
| <b>Figure 3.8</b>  | Crystal structure of human serum albumin  | 73  |
| <b>Figure 3.9</b>  | Effects of Cysteine and Methionine peptide blocking on BBR3464-HSA binding                              | 74  |
| <b>Figure 3.10</b> | Charge density structure of human serum albumin   | 77  |
| <b>Figure 3.11</b> | Electrostatic Effects on HSA Global Structure   | 78  |
| <b>Figure 4.1</b>  | Effect of BSO on platinum drug-induced cytotoxicity   | 93  |
| <b>Figure 4.2</b>  | Effects of protein binding on free drug availability  | 95  |
| <b>Figure 4.3</b>  | Influence of protein binding on platinum drug efficacy  | 97  |
| <b>Figure 4.4</b>  | Influence of protein binding on platinum cellular uptake  | 100 |
| <b>Figure 4.5</b>  | Influence of protein binding on DNA platination   | 102 |
| <b>Figure 4.6</b>  | MTT cytotoxicity assay of fluorescent platinum derivatives  | 106 |
| <b>Figure 4.7</b>  | Confocal laser scanning micrographs of A2780 cells  | 107 |
| <b>Figure 4.8</b>  | Role of protein binding on the cellular localization and distribution of cisplatin and TriplatinNC      | 108 |
| <b>Figure 5.1</b>  | General Chemical Structure of Trans-NBD Compounds   | 127 |
| <b>Figure 5.2</b>  | Confocal laser scanning micrographs of A2780 and HCT116 cells after incubation with Trans-NBD compounds | 136 |
| <b>Figure A.1</b>  | Structures of BBR3464, TriplatinNC and the Phosphate Clamp  | 153 |
| <b>Figure A.2</b>  | Fluorescently-tagged TriplatinNC localizes to the nucleolus   | 155 |
| <b>Figure A.3</b>  | MTT Assay of Fluorescently Tagged Compounds   | 156 |

|                    |   |     |
|--------------------|---|-----|
| <b>Figure A.4</b>  | TriplatinNC competitively inhibits TBP-DNA interaction and interferes with rRNA transcription                                   | 159 |
| <b>Figure A.5</b>  | TBP Binding Assay with TriplatinNC and AH44   | 160 |
| <b>Figure A.6</b>  | TriplatinNC induces G1 cell cycle arrest  | 161 |
| <b>Figure A.7</b>  | Flow Cytometry; Cell cycle analysis of HCT116 cells treated with Cisplatin  | 164 |
| <b>Figure A.8</b>  | Flow Cytometry; Cell cycle analysis of HCT116, HCT116 p53 <sup>-/-</sup> , and HCT116 p21 <sup>-/-</sup> cells                  | 165 |
| <b>Figure A.9</b>  | TriplatinNC causes rapid proliferative arrest and cell death  | 167 |
| <b>Figure A.10</b> | Clonogenic Survival Assay; Comparison of colonies formed in HCT116 p53 <sup>+/+</sup> cells and HCT116 p53 <sup>-/-</sup> cells | 168 |
| <b>Figure A.11</b> | TriplatinNC induces activation of caspases independent of p53   | 171 |
| <b>Figure A.12</b> | Western Blot; Comparison of BID (p22) and the active form, tBID (p15) proteins in HCT116  | 172 |
| <b>Figure A.13</b> | Antitumor activity of TriplatinNC against 2008 ovarian tumor human xenograft model  | 174 |
| <b>Figure B.1</b>  | Structures of pairs of trinuclear and dinuclear compounds studied for pre-association effects on human serum albumin (HSA)      | 189 |
| <b>Figure B.2</b>  | Changes in fluorescence of HSA treated with trinuclear platinum compounds   | 191 |
| <b>Figure B.3</b>  | CD spectra of HSA incubated with compounds  | 193 |
| <b>Figure B.4</b>  | Nano-ESI-MS of rHSA incubated with platinum compounds   | 195 |
| <b>Figure B.5</b>  | Changes in fluorescence of HSA treated with dinuclear   |     |

platinum compounds 197

**Figure B.6** ICP-OES analysis of Pt content in ultrafiltrate of BBR3464 and  
Ia after incubation with HSA for selected time points 199

### List of Abbreviations

|                  |  |
|------------------|--|
| 5-FU             | 5-Fluorouracil   |
| A                | Adenine (nucleobase)                                     |
| bp               | Base Pair  |
| C                | Cytosine (nucleobase)                                    |
| Cisplatin/c-DDP  | cis-diamminedichloroplatinum(II)                         |
| °C               | Degrees Celsius  |
| Carboplatin      | cis-diammine-1,1-cyclobutane dicarboxylateplatinum(II)   |
| CD               | Circular Dichroism                                       |
| D <sub>2</sub> O | Deuterium Oxide  |
| Da               | Dalton   |
| DDD              | Dickerson-Drew Dodecamer                                 |
| DLT              | Dose limiting toxicity                                   |
| DNA              | Dideoxyribonucleic Acid                                  |
| Ds               | Double Stranded DNA                                      |
| ESI-MS           | Electrospray Ionization Mass Spectrometry                |
| G                | Guanine (nucleobase)                                     |
| GSH              | Glutathione  |
| HSA              | Human Serum Albumin                                      |
| HMG              | High Mobility Group                                      |
| IC <sub>50</sub> | Concentration to inhibit 50% of cell growth              |
| ICP-OES          | Inductively Coupled Plasma-Optical Emission Spectroscopy |
| Isq              | Isoquinoline   |

|             |  |
|-------------|--|
| ITC         | Isothermal Titration Calorimetry                                 |
| Ka          | Association Constant   |
| Kb          | Kilobase   |
| kDa         | Kilodalton   |
| M           | Molar  |
| m/z         | Mass-to-Charge Ratio   |
| mM          | Millimolar   |
| MRP         | Multi-drug resistance-associated protein                         |
| MS          | Mass Spectrometry  |
| NAC         | N-Acetyl Cysteine  |
| NAM         | N-Acetyl Methionine  |
| NBD         | 4-Chloro-7-nitro-2,1,3-benzoxadiazole                            |
| NMR         | Nuclear Magnetic Resonance                                       |
| Oxaliplatin | [(1R,2R)-cyclohexane-1,2-diamine](ethanedioato-O,O')platinum(II) |
| PBS         | Phosphate Buffered Saline  |
| PDB ID      | Protein Database Identification Number                           |
| PPC         | Polynuclear Platinum Compounds                                   |
| ppm         | Parts per Million  |
| Pt          | Platinum   |
| Ss          | Single Stranded DNA  |
| T           | Thymine (nucleobase)   |
| TPA         | Trans-Planar Amine   |
| Transplatin | trans-diamminedichloroplatinum(II)                               |

## Abstract

### **Drug Design, Biological Activity, and Metabolic Consequences of Cytotoxic Platinum Compounds: Utilizing Fluorescent Tagging to Understand Drug Action and Metabolism**

A dissertation submitted in partial fulfillment of the requirements for the degree of Doctor of Philosophy at Virginia Commonwealth University

By  
Brad T. Benedetti

Director: Dr. Nicholas P. Farrell  
Professor  
Department of Chemistry, Virginia Commonwealth University

April, 2011

Platinum drugs are among the most commonly used chemotherapeutics for the treatment of testicular, head and neck, ovarian, small cell lung, and colorectal carcinomas. Although the current set of platinum chemotherapeutics has proven somewhat successful, the overall success of platinum based drugs is limited due to acquired drug resistance and a limited range of tumor types that are treatable with the current regime. The development of novel cytotoxic platinum based compounds, both *trans*- and polynuclear, provides for the promising treatment of clinical platinum drug resistant tumors. While the cytotoxic activity of platinum drugs provides for a hopeful outlook, the ultimate factors that affect the success of chemotherapeutics are the fine balance between cytotoxic activity and metabolic deactivation.

In general, this work reports the drug design/drug action, and pharmacokinetic consequences of anticancer compounds aimed to fight mechanisms of cisplatin resistance. In the first project, we report the biological and biophysical studies aimed at

understanding and improving upon the pharmacokinetic properties of chemotherapeutics; specifically, understanding their interactions with serum proteins. This work resulted in the discovery of using carboxylate ligands to modulate the reactivity of trans-platinum based compounds towards sulfur containing proteins with consequent effects on drug efficacy. In addition, we report an in depth look into the biological consequences of non-covalent platinum drug-protein interactions on drug efficacy, and introduce the use of novel Platinum-NBD fluorescent conjugates as probes for drug metabolism. In the second project we report the design, synthesis, and biological consequences of fluorescent drug derivatives based on the NBD fluorophore, for use in understanding drug action and drug metabolism. As a result of this fluorescent drug labeling, TriplatinNC, a non-covalent platinum based chemotherapeutic, was found to specifically target nucleolar DNA/RNA, due to its high charge, and inhibit ribosomal RNA production in cancer cells. The use of fluorescent derivatization also resulted in the development of a series of novel water-soluble *trans*-platinum complexes, with greater cytotoxicity than cisplatin. Therefore, these data resulted in the understanding of, and improvement upon the pharmacokinetic profile of platinum chemotherapeutics, as well as the development of novel fluorescent platinum conjugates with novel metabolic and cytotoxic profiles.



## Chapter 1: Cancer and Platinum Based Chemotherapeutics

### 1.1 Cancer

Despite an enormous amount of research being committed to the treatment of cancer over the last few decades, cancer still remains a worldwide killer. Deaths from cancer account for 23% of the total deaths in the United States, second only to heart disease.<sup>1</sup> While the number of deaths resulting from heart disease have been drastically reducing over the years, the total number of deaths from cancer remains constant. Cancer is described as a class of diseases in which a group of cells display uncontrolled growth and invasion that intrudes upon and destroys adjacent tissues. To date, there are multiple treatments available to fight the spread of cancer, including, surgery, chemotherapy, immunotherapy, and radiation therapy.<sup>2</sup> Among the most commonly used chemotherapeutics for the prevention and treatment of cancer are Taxol, Cisplatin, Carboplatin, 5-FU and Doxorubicin.<sup>3</sup>

### 1.2 Cisplatin and Platinum Analogs

Cisplatin, *c*-DDP, *cis*-PtCl<sub>2</sub>(NH<sub>3</sub>)<sub>2</sub> was first synthesized by Michel Peyrone in 1845<sup>4</sup>, but remained relatively unnoticed until the early 1960's when Barnett Rosenberg, a professor of biophysics and chemistry at Michigan State University, began to investigate the effect of electrical currents on bacterial cell growth.<sup>5</sup> (Figure 1.1) He discovered that after treatment with electrical current from "inert" platinum electrodes *E. coli* were produced that were 300 times their normal length. This treatment had successfully prevented cell division, but not other growth processes and ultimately led to the

elongation. Eventually, it was determined that the electric field applied to the E. Coli was not the cause of the elongation and that it was in fact the production of a platinum complex formed during reaction between the platinum electrodes and components of the media containing the bacteria. This platinum complex was eventually determined to be *cis*-PtCl<sub>2</sub>(NH<sub>3</sub>)<sub>2</sub>, cisplatin. The serendipitous discovery of cisplatin changed the face of anti-tumour treatment of the 1970's.<sup>6</sup> Cisplatin was eventually found to be highly effective against multiple tumor lines and entered into clinical trials in 1971 and was licensed solely to Bristol-Myers Squibb in 1977.<sup>7</sup>

The cytotoxicity of cisplatin is accepted to result mainly from the formation of bifunctional 1,2-intrastrand DNA crosslinks with purine bases, resulting in the inhibition of DNA synthesis and replication.<sup>8</sup> The most notable crosslinks seen are the 1-2-intrastrand G-G adducts which form nearly 90% of the adducts. Also possible is the formation of 1-2-interstrand adducts, but to a much lesser extent. (Figure 1.2) The DNA-reactive platinum species are considered to be monoquo and diaquo complexes – in general [Pt(amine)<sub>2</sub>(H<sub>2</sub>O)<sub>2</sub>]<sup>2+</sup> or [Pt(amine)<sub>2</sub>(Cl)(H<sub>2</sub>O)]<sup>+</sup> – produced upon hydrolysis of the administered drugs, and the chemistry of these species has been well examined.<sup>9</sup> Following Cisplatin-DNA binding, the subsequent adduct is recognized by a high mobility group (HMG)-domain protein, which binds tightly to the Cisplatin-DNA complex.<sup>10-11</sup> This adduct formation causes de-stacking of the nucleotide bases, resulting in the DNA helix becoming kinked. Therefore it is postulated that this interaction could potentially provide a “shielding” effect from typical DNA repair protein pathways.<sup>12</sup> This inhibition of traditional DNA repair pathways results in the induction

cell signaling pathways, generally, p53, Bcl-2, caspases, and MAPK pathways, eventually leading to an apoptotic response.<sup>13</sup>

With the success of platinum based chemotherapy following the introduction of cisplatin in to the clinics in 1978, the development of subsequent platinum regimes has spiked tremendously. Although this large amount of research has resulted in many promising compounds, only two subsequent platinum drugs, carboplatin and oxaliplatin, have been successfully approved for anti-cancer use by the FDA.<sup>7</sup> (Figure 1.1) Carboplatin, invented by Rosenberg and his colleagues, was developed primarily to decrease the toxic side effects associated with cisplatin treatment, and is currently the only other platinum chemotherapeutic effective against a wide range of tumor types.<sup>14-15</sup> The addition of the bidentate cyclobutanedicarboxylate leaving group is more stable than the chloride groups of cisplatin, therefore slowing down the reactivity in the bloodstream and allowing more drug to reach the tumor intact.<sup>14</sup> Oxaliplatin, the most recent platinum compound to be introduced to the clinics, was approved in across Europe in 1996 and in the United States in 2000 for use against advanced colorectal carcinoma.<sup>14,16</sup> To date, Oxaliplatin is the only platinum chemotherapeutic to be approved for use against colorectal tumors.<sup>16</sup>

Following the development of cisplatin and initial studies on the general structure activity relationship of subsequent compounds, a set of rules was established to aid in the discovery of new platinum chemotherapeutics.<sup>17</sup> These rules state that the compound(s) should have (1) two ammine groups in the *cis* geometry (2) two leaving groups also in the *cis* geometry (3) leaving groups which are only moderately easy to remove and (4) neutral charge.<sup>18</sup> All current clinical platinum chemotherapeutics have

followed these rules. Unfortunately the success of platinum based chemotherapeutics is limited due to eventual acquired drug resistance and a limited range of tumor types that are treatable with the current regime. Therefore, the current research motivation is to find new platinum based drugs which exert a uniquely distinct mode of DNA binding, which could overcome clinical resistance to the currently used platinum drugs.

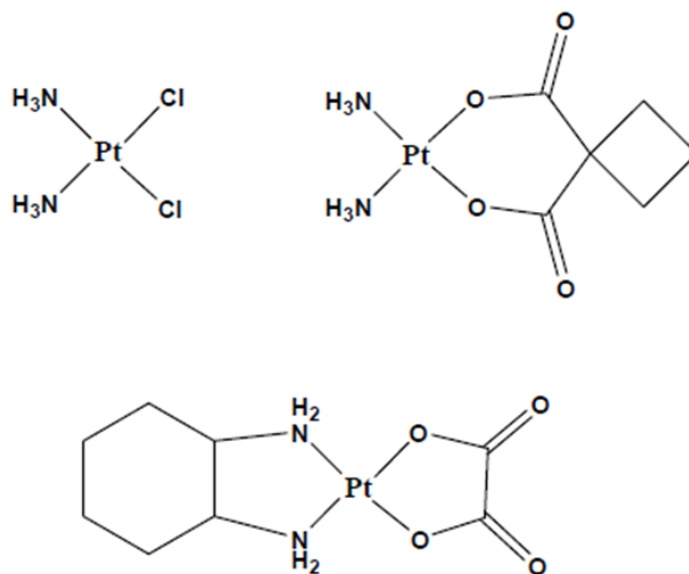


**Figure 1.1** Chemical Structures of Clinical Platinum-Based Chemotherapeutics: *Cisplatin* (top left), *Carboplatin* (top right), and *Oxaliplatin* (bottom)

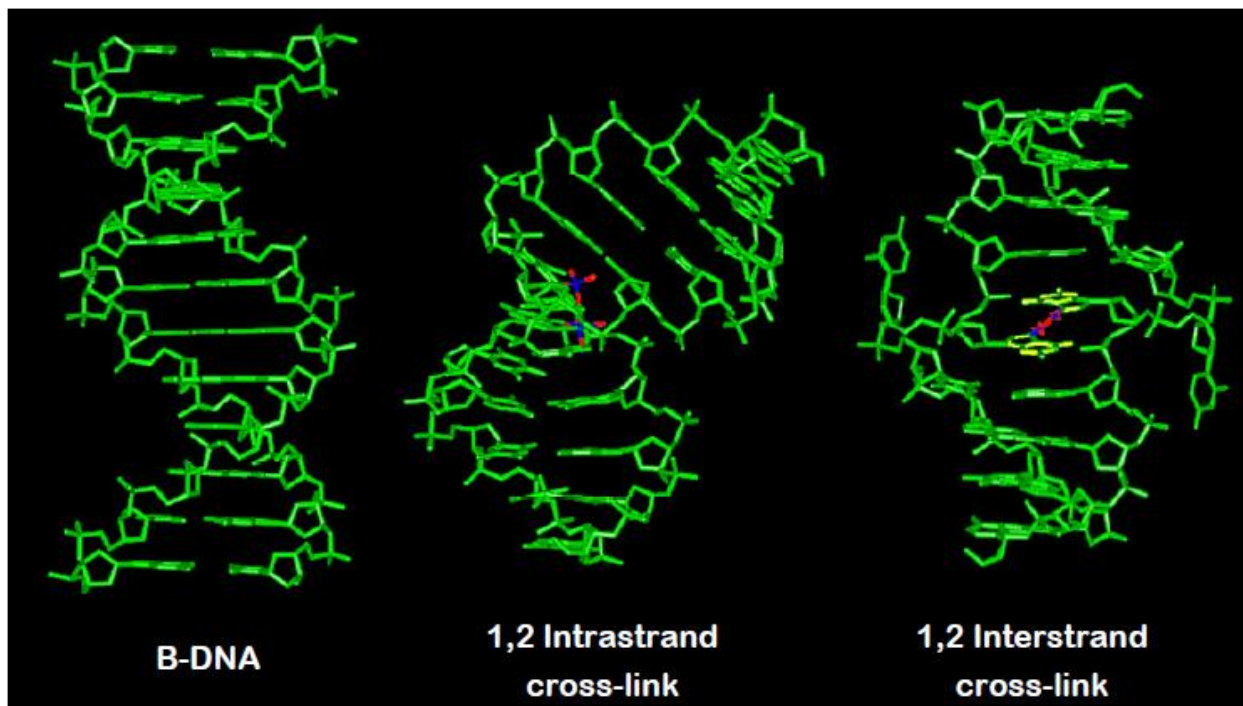
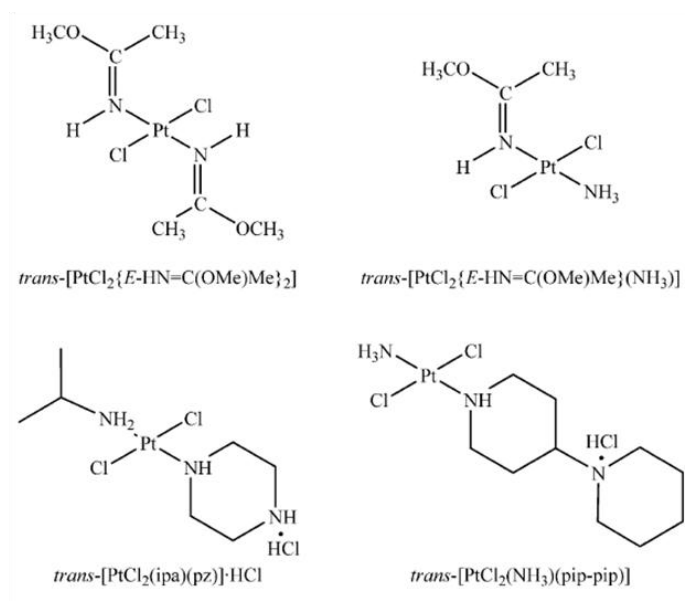
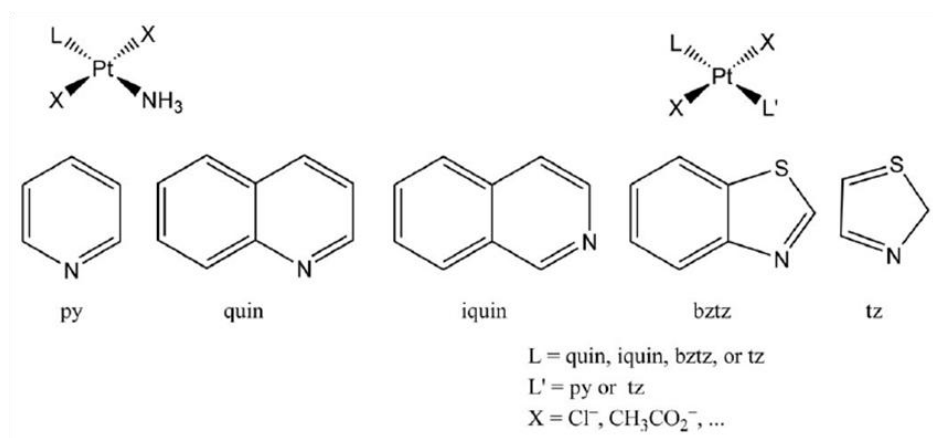


Figure 1.2 DNA adducts formed after treatment of Cisplatin

### 1.3 Trans-Platinum Compounds

One common feature among current clinical platinum therapeutics is the bis, *cis* orientation of the labile leaving groups. The *trans* isomer of cisplatin, *trans*-[PtCl<sub>2</sub>(NH<sub>3</sub>)<sub>2</sub>] is much less toxic than the *cis* counterparts, presumably due to its inability to form 1,2-intrastrand cross links between the N7 atoms of adjacent guanines in double strand DNA.<sup>19-20</sup> Although transplatin itself is clinically inactive, substitution of one of the NH<sub>3</sub> groups with a planar heterocyclic ligand such as pyridine, thiazole, quinoline, isoquinoline, etc., yields a class of active transplanaramine platinum chemotherapeutics (TPA's). (Figure 1.3) These TPA compounds possess substantially enhanced cytotoxicity profiles as compared to the "parent" *trans*-[PtCl<sub>2</sub>(NH<sub>3</sub>)<sub>2</sub>], with IC<sub>50</sub> values in the 1-10μM range across numerous tumor cell lines.<sup>21</sup> Most interestingly, TPA compounds usually exhibit no cross resistance with cisplatin or oxaliplatin and thus demonstrate a unique cytotoxicity profile across the NCI tumor panel.<sup>22</sup> The use of other carrier ligands such as iminoethers, heterocyclic aliphatic amines, and aliphatic amines, has also been used to produce a wide range of *trans*-platinum compounds with potential chemotherapeutic application.<sup>23-24</sup> The use of carboxylates as leaving groups for TPA's has also been used, first introduced to address the low aqueous solubility of TPA's.<sup>25</sup> These carboxylate derivatives have shown similar cytotoxicities to their parent chlorides.<sup>26-27</sup> The use of carboxylate ligands also results in increased cellular accumulation even in cisplatin and oxaliplatin-resistant cell lines.<sup>26-27</sup> In attempts to optimize drug design, previous studies in our group have shown that the use of formate as leaving group gives enhanced cytotoxicity in comparison to acetate.<sup>28</sup>



**Figure 1.3** Chemical structures of selected Trans-Platinum based anticancer compounds.<sup>29</sup>



## 1.4 Polynuclear Platinum Compounds

Polynuclear platinum compounds represent a distinct class of anticancer drugs, whose structural and biological effects differ drastically from the classical mononuclear platinum family of compounds, (cisplatin, carboplatin, etc.).<sup>12,30</sup> The first clinical compound resulting from this research, BBR3464, is a tri-nuclear, bi-functional DNA binding agent with an overall charge of 4+. (Figure 1.4) BBR3464, the only non-cisplatin-like molecule to enter human clinical trials, and has promising activity in cisplatin-resistant, cisplatin-sensitive and p53 mutant tumors.<sup>31-33</sup> BBR3464 is also forty to eighty fold more potent on a molar basis than cisplatin.<sup>34</sup> BBR3464 is capable of forming long range DNA adducts, including 1,4 and 1,6 inter-strand crosslinks. (Figure 1.5) The nature of these long-range adducts provides the basis for the enhanced cytotoxic nature of the compound and also for the ability BBR3464 to effectively treat cisplatin resistant tumors.<sup>35-36</sup>

## 1.5 Non-Covalent Polynuclear Platinum Compounds

Most platinum chemotherapeutics bind to DNA in a covalent manner by formation of a Pt-DNA adduct. Replacement of the chloride leaving groups of BBR3464 with substitutionally 'inert' ammine ligands or 'dangling' amines,  $\text{H}_2\text{N}(\text{CH}_2)_6\text{NH}_3^+$ , gives 'non-covalent' polynuclear platinum compounds; most notably TriplatinNC. (Figure 1.4) TriplatinNC is a highly positively charged, (+8) non-covalent derivative of the phase II clinical platinum drug, BBR3464.<sup>37</sup> The crystal and molecular structure of TriplatinNC associated with a double-stranded B-DNA dodecamer  $5'\text{-d}(\text{CGCGAATTCGCG})_2$  at 1.2 Å resolution (PDB:2DYW), shows formation of phosphate clamps, involving two modes

of DNA binding: "backbone-tracking", by following along the phosphate backbone of one strand, or "groove-spanning", by crossing over the minor groove to interact with both strands.<sup>38</sup> (Figure 1.6) The phosphate clamp motif is a discrete third mode of DNA binding, distinct from intercalation or minor groove binding. These interactions are mediated through hydrogen bonding, and are analogous to the "arginine fork", an important motif for protein-DNA interactions, where positively charged guanidino groups of arginine, interact with negatively charged oxygens of DNA phosphate.<sup>39-41</sup> TriplatinNC has significantly higher cellular accumulation than either BBR3464 or cisplatin, and in some cases equivalent or greater cytotoxicity than cisplatin.<sup>42-43</sup>

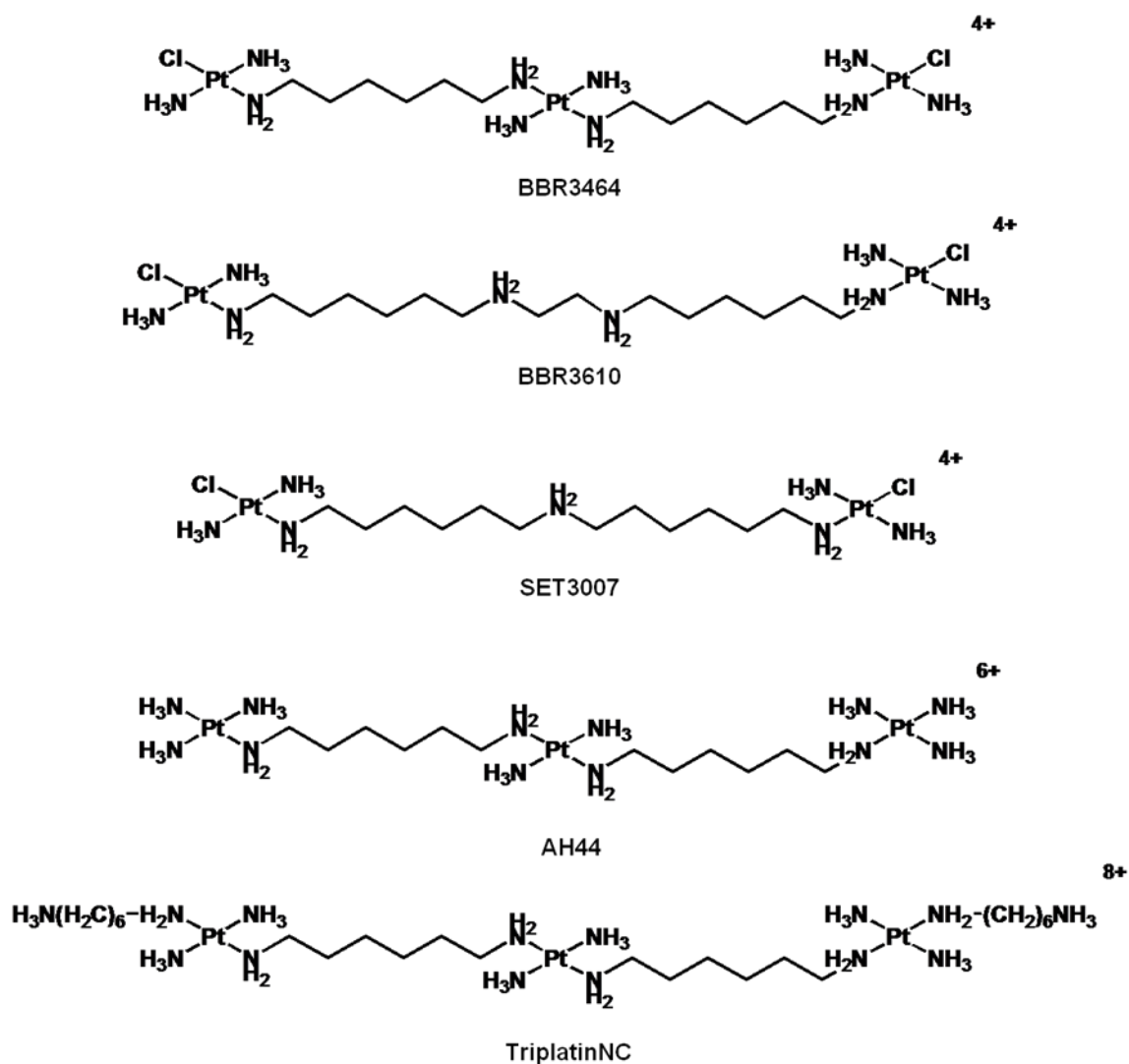


**Figure 1.4** Chemical Structures Selected Covalent and Non-Covalent DNA Binding Platinum Drugs

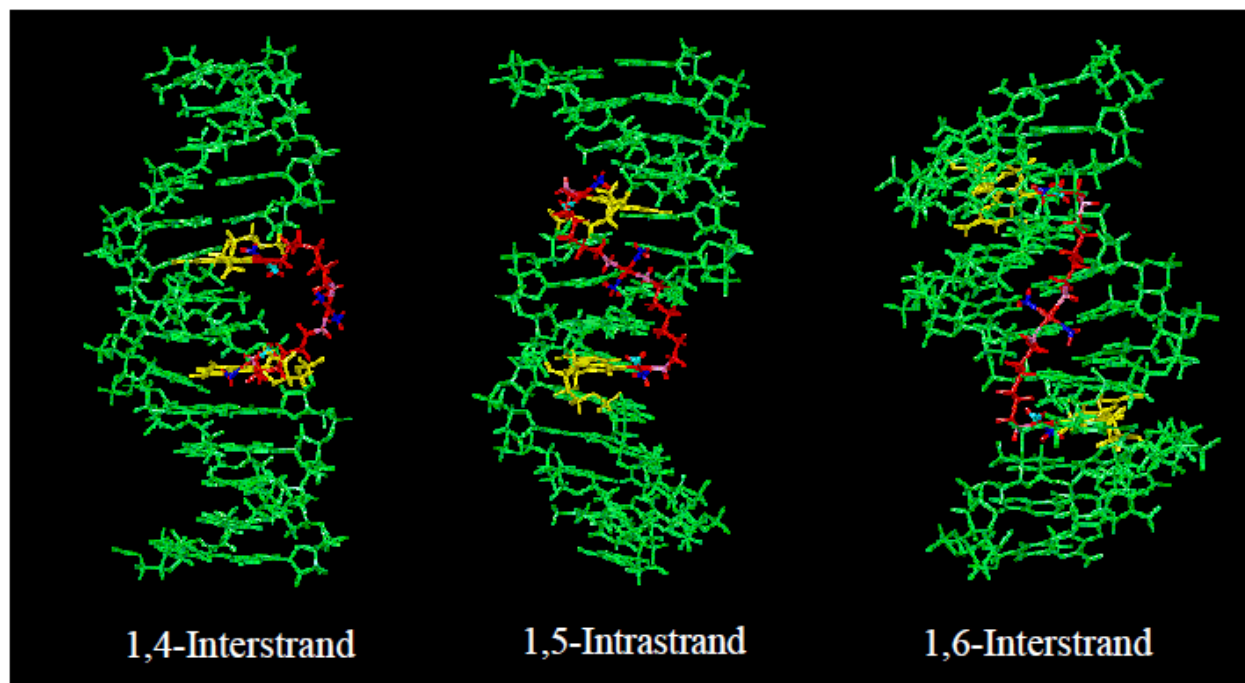


Figure 1.5 Long-Range DNA-Adducts formed by BBR3464

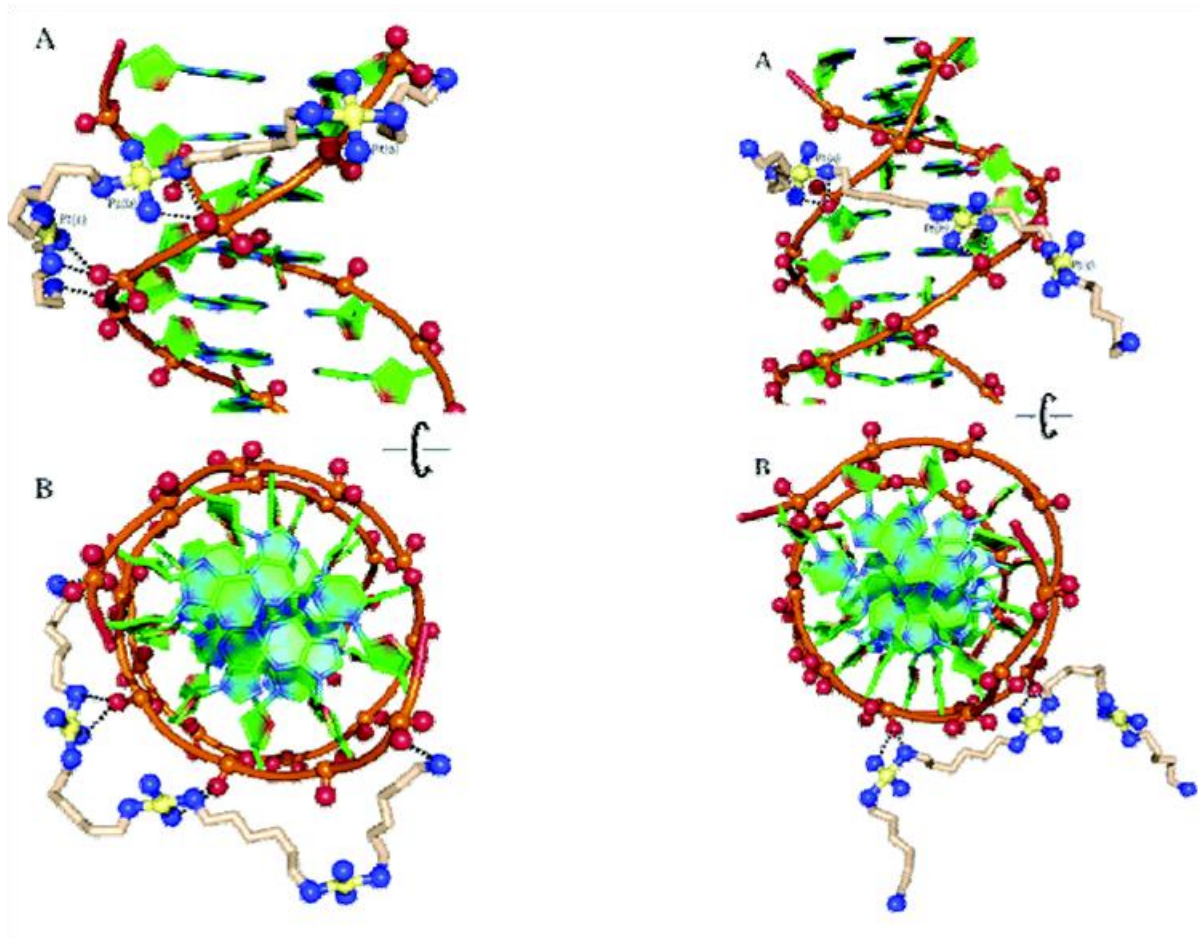


Figure 1.6 Crystal Structure of TriplatinNC Interactions with DNA<sup>44</sup>

## 1.6 Pharmacological Factors Affecting Platinum Based Treatments

There are four main factors which control the pharmacokinetics of compounds in biological systems. These factors include but are not limited to, absorption, distribution, metabolism, and elimination. These four criteria greatly affect the bioavailability and kinetics of drug exposure towards the biological system of interest.

Absorption refers to the ability of a drug, following administration, to effectively reach the systemic circulation; either by passing through intestinal cell membranes in the case of orally administered compounds or other natural membranes such as the blood brain barrier.<sup>45</sup> Once in systemic circulation, the process of metabolism begins to decompose the compounds of interest into drug metabolites. If the metabolites of the compound are 'inert' after metabolism, a large portion of the pharmacological effect is thus diminished and the drug administered can no longer be distributed to the site of action. Metabolism can occur by reactions with liver redox enzymes such as cytochrome P450 and through interactions with proteins in the blood stream.<sup>46</sup> Prolonged elimination half-lives can result in reduced tolerability of the administered drug in patients, often warranting removal of compounds of interest from clinical trials. About 75% of drug candidates do not enter clinical trials due to pharmacokinetics problems in pre-clinical studies. Also, about 40% of molecules that fail in clinical trials do so because of pharmacokinetics problems.<sup>46</sup>

In addition to the pharmacokinetic properties that affect all administered drugs, the three major pharmacological factors affecting the success of any type of platinum-based cancer therapy are cellular uptake, the frequency and the type of DNA adducts formed and metabolic deactivation. Metabolic deactivation is mediated through

interactions of the small molecules with biomolecules, specifically sulfur-containing amino acids in proteins, and these interactions may contribute to the toxic side effects associated with platinum based treatments.<sup>47-48</sup> From a solely chemical standpoint, these metals, following aquation, would be expected to act as soft Lewis acids and to form stable complexes with S or N donors found in proteins.<sup>49</sup> Thus, the rate of hydrolysis of the leaving ligand greatly affects the amount of protein binding.

One of the most plausible extracellular non-DNA targets for platinum compounds is blood serum. Serum is the liquid portion of blood, approximately 55% of the total volume, excluding red and white blood cells, containing all plasma proteins at a concentration of 70 g/L.<sup>50</sup> These proteins include fibrinogen, globulins, and human serum albumin (HSA). Albumin, the most abundant plasma protein and the most likely candidate for drug metabolic interactions, is a 585 amino acid, 66 kDa, single chain protein involved in transportation of numerous drugs and ligands.<sup>51-52</sup> HSA is largely  $\alpha$ -helical and contains 17 disulfide bridges and only one free cysteine, Cys-34. This residue, along with Met-298 is speculated as the primary binding sites of cisplatin.<sup>53</sup> It is mainly accepted, in the case of most Pt-compounds, that once coordinated to S or N donors in plasma proteins or other biomolecules, platinum compounds are effectively 'deactivated' and eliminated from the body; thus never reaching their desired site of action.<sup>48</sup> Severe nephrotoxicity has also been associated with interactions of platinum anti-tumor compounds with thiol groups of proteins.<sup>54</sup>

Plasma proteins in the systemic circulation are not the only 'deactivator' or scavenger of platinum chemotherapeutics. Once removed from the systemic circulation and inside the cellular target there are a large number of molecules, in a high enough

concentration, to interact with the platinum moiety.<sup>55</sup> Among these biomolecules of interest is the tri-peptide glutathione (GSH). Glutathione has been chosen due to its role as a determinant of cellular sensitivity to a wide variety of drugs and cytotoxic agents. The normal intracellular concentration of GSH ranges from 5 to 10 mM<sup>56</sup>, therefore the binding of platinum-containing drugs to GSH is highly probable. Studies of interactions between GSH and *c*-DDP/transplatin showed the formation of a 1:1 Pt-GSH species in the case of the *trans*- isomer, and eventual liberation of the NH<sub>3</sub> ligand to form a 1:2 Pt-GSH species in the case of *c*-DDP.<sup>57-58</sup> Also, clinical and preclinical studies of cellular systems with elevated levels of GSH have show to be more resistant, in varying degrees, to *c*-DDP.<sup>59</sup> Studies with polynuclear platinum compounds have similarly shown the formation of Pt-GSH species in varying ratios, but ultimately, the interactions of these platinum compounds may be expected to follow that of cisplatin and its mononuclear analogues.<sup>60-61</sup> Ultimately, therapeutic efficiency will be reflected as a balance between metabolic deactivating interactions and biological consequences of DNA toxicity.

In an effort to improve the therapeutic efficiency, by minimizing interactions with plasma proteins, novel formulations of platinum compounds have been developed.<sup>62</sup> One pathway to minimize metabolic interactions can be through replacement of the most commonly used –Cl leaving group with other, more stable ligands. Cell Therapeutics Inc. (CTI) is currently evaluating a derivative of the polynuclear platinum compound BBR3610 and has shown that replacement of the –Cl ligand with a carboxylate, such as butyrate or capronate, results in much lower plasma binding *in vitro*, while still retaining its cytotoxicity profile *in vivo*.<sup>63</sup> This ‘carboxylate’ strategy has



also been employed to improve the pharmacokinetic properties of mono-nuclear trans-platinum compounds.<sup>25</sup> In these trans-platinum compounds, carboxylate groups were added at first to simply enhance aqueous solubility, but have also been shown to decrease the rate of hydrolysis, therefore possibly allowing for decreased metabolic deactivation.

### 1.8 Fluorescence Cellular Imaging of Platinum Compounds

The use of molecular imaging techniques, such as fluorescence confocal microscopy, is an important tool in the understanding of platinum drug trafficking and intracellular distribution. Primarily, it is necessary to understand the ability of each compound to effectively penetrate the cell be delivered to the desired site of interest, in most cases, nuclear DNA. Moreover, information regarding the subcellular compartments, transporters, and receptors with which these drugs localize can provide vital information explaining metabolic deactivation, resistance mechanisms, and toxicity. Hambley has summarized recent fluorescent approaches to monitoring platinum trafficking.<sup>64</sup> Previous attempts at “tagging” platinum compounds have yielded cisplatin derivatives in which FITC and Alexa based fluorophores have been utilized. These derivatives tend to mimic the biological properties of the fluorescent “tag” rather than the platinum moiety itself.<sup>64</sup> A number of platinum complexes incorporating fluorescent probes have been developed not just to monitor the localization of cisplatin, but rather as a class of potentially chemotherapeutic platinum drugs in their own right with the aim of combining the benefits of intercalating agents with those of platinum complexes.<sup>65-66</sup> The main objective to successfully create fluorescently labeled compounds that truly

mimic the biological properties of the parent compound is to minimize the size of the fluorescent probe and retain the original structure and solubility properties after conjugation.

### 1.7 Concluding Remarks and Project Overview

Despite an enormous amount of research being committed to the treatment of cancer over the last few decades, cancer still remains a worldwide killer. Although the current set of platinum chemotherapeutics has proven somewhat successful, the overall success of platinum based chemotherapeutics is limited due to eventual acquired drug resistance and a limited range of tumor types that are treatable with the current regime. The development of novel cytotoxic platinum based compounds, *trans*- and polynuclear, provides for promising treatment of clinical “platin” drug resistant tumors. While the cytotoxicity activity of many platinum drugs provides for a hopeful outlook, the ultimate factors affecting the success of chemotherapeutics are the fine balance between cytotoxic activity and metabolic deactivation. By finding this balance, it may be possible to defer many of the toxic side effects associated with chemotherapeutics, and thus provide for substantial increases in mean tolerated dosages, thus, facilitating the better development of platinum compounds for the treatment and prevention of cancer.

The long term objective of this thesis was to evaluate, understand, and improve the pharmacokinetic profile of platinum chemotherapeutics through the use of standard biological and chemical protocols and through the development of novel fluorescent imaging assays. Chapter 1 of this thesis presents an overview of platinum

chemotherapeutics and the role of metabolism in the overall activity of these compounds.

Chapter 2 presents a series of cytotoxic *trans*-platinum compounds, in which we evaluate the ability of using carboxylate ligands to modulate the reactivity of the compounds towards sulfur containing proteins and consequently the biological effect on drug efficacy. The work in this chapter has been completed and is in submission to Dalton Transactions.

In Chapter 3, the interactions of various polynuclear platinum complexes with mouse plasma, human plasma, and human serum albumin were studied. The implications for protein pre-association and plasma stability of polynuclear platinum compounds, both covalent and non-covalent are discussed.

Chapter 4 builds on the biophysical studies observed in Chapter 3 and takes an in depth look into the biological consequences of non-covalent platinum drug-protein interactions on drug efficacy. This chapter also introduces the use of novel Platinum-NBD fluorescent conjugates as probes for drug metabolism. This work has been completed and is in submission to Molecular Pharmaceutics.

Chapter 5 reports the anticancer activity and primary insights into the mechanism of action of a series of novel water-soluble *trans*-platinum complexes that incorporate an amino ligand composed of an aliphatic carbon chain and a planar fluorophore intercalator, NBD. This work has been completed and is in submission to JACS.

Appendix 1 is a completed manuscript, in submission to PNAS, which discusses the biological consequences and mechanism of action of TriplatinNC, based on the fluorescent tagging of this compound with the NBD fluorophore. Appendix 2 is also a

completed manuscript, published in Dalton Transactions, which focuses on the biophysical aspects of the pre-association of polynuclear platinum anticancer agents on a protein, human serum albumin and the implications for drug design.

### 1.9 List of References

1. Anand, P., *et al.* Cancer is a Preventable Disease that Requires Major Lifestyle Changes. *Pharmaceutical Research* **25**, 2097-2116 (2008).
2. Vogel, V.G., *et al.* Effects of Tamoxifen vs Raloxifene on the Risk of Developing Invasive Breast Cancer and Other Disease Outcomes. *JAMA: The Journal of the American Medical Association* **295**, 2727-2741 (2006).
3. Joensuu, H. Systemic chemotherapy for cancer: from weapon to treatment. *The Lancet Oncology* **9**, 304-304 (2008).
4. Peyrone, M. Ueber die Einwirkung des Ammoniaks auf Platinchlorür. *Justus Liebigs Annalen der Chemie* **51**, 1-29 (1844).
5. Rosenberg, B., Van Camp, L. & Krigas, T. Inhibition of Cell Division in *Escherichia coli* by Electrolysis Products from a Platinum Electrode. *Nature* **205**, 698-699 (1965).
6. Rosenberg, B., Vancamp, L., Trosko, J.E. & Mansour, V.H. Platinum Compounds: a New Class of Potent Antitumour Agents. *Nature* **222**, 385-386 (1969).
7. Alderden, R.A., Hall, M.D. & Hambley, T.W. The Discovery and Development of Cisplatin. *Journal of Chemical Education* **83**, 728-null (2006).
8. Jamieson, E.R. & Lippard, S.J. Structure, Recognition, and Processing of Cisplatin-DNA Adducts. *Chem Rev* **99**, 2467-2498 (1999).
9. Berners-Price, S.J. & Appleton, T.G. *Platinum-Based Drugs in Cancer Therapy*, (Humana Press, Totowa, NJ, 2000).

10. Jordan, P. & Carmo-Fonseca, M. Cisplatin inhibits synthesis of ribosomal RNA in vivo. *Nucleic Acids Research* **26**, 2831-2836 (1998).
11. Rice, J.A., Crothers, D.M., Pinto, A.L. & Lippard, S.J. The major adduct of the antitumor drug cis-diamminedichloroplatinum(II) with DNA bends the duplex by approximately equal to 40 degrees toward the major groove. *Proceedings of the National Academy of Sciences* **85**, 4158-4161 (1988).
12. Farrell, N. *Metal Ions in Biological Systems*, (Marcel Dekker, Inc., New York, 2004).
13. Pasetto, L.M., D'Andrea, M.R., Brandes, A.A., Rossi, E. & Monfardini, S. The development of platinum compounds and their possible combination. *Critical Reviews in Oncology/Hematology* **60**, 59-75 (2006).
14. Lebwohl, D. & Canetta, R. Clinical development of platinum complexes in cancer therapy: an historical perspective and an update. *Eur J Cancer* **34**, 1522-1534 (1998).
15. Weiss, R.B. & Christian, M.C. New Cisplatin Analogues in Development: A Review. *Drugs* **46**, 360-377 (1993).
16. Judson, I. & Kelland, L.R. New Developments and Approaches in the Platinum Arena. *Drugs* **59**, 29-36 (2000).
17. Cleare, M.J. & Hoeschele, J.D. Studies on the antitumor activity of group VIII transition metal complexes. Part I. Platinum (II) complexes. *Bioinorganic Chemistry* **2**, 187-210 (1973).
18. Hambley, T.W. The influence of structure on the activity and toxicity of Pt anti-cancer drugs. *Coordin Chem Rev* **166**, 181-223 (1997).

19. Brabec, V., Nepelchova, K., Kasparkova, J. & Farrell, N. Steric control of DNA interstrand cross-link sites of trans platinum complexes: specificity can be dictated by planar nonleaving groups. *J Biol Inorg Chem* **5**, 364-368 (2000).
20. Wang, D. & Lippard, S.J. Cellular processing of platinum anticancer drugs. *Nat Rev Drug Discov* **4**, 307-320 (2005).
21. Ma, E.S.F., *et al.* Enhancement of Aqueous Solubility and Stability Employing a Trans Acetate Axis in Trans Planar Amine Platinum Compounds while Maintaining the Biological Profile. *Journal of Medicinal Chemistry* **48**, 5651-5654 (2005).
22. Fojo, T., *et al.* Identification of non-cross-resistant platinum compounds with novel cytotoxicity profiles using the NCI anticancer drug screen and clustered image map visualizations. *Crit Rev Oncol Hematol* **53**, 25-34 (2005).
23. Radulovic, S., Tesic, Z. & Manic, S. Trans-platinum complexes as anticancer drugs: recent developments and future prospects. *Curr Med Chem* **9**, 1611-1618 (2002).
24. Coluccia, M. & Natile, G. Trans-platinum complexes in cancer therapy. *Anticancer Agents Med Chem* **7**, 111-123 (2007).
25. Bulluss, G.H., *et al.* trans-Platinum Planar Amine Compounds with [N2O2] Ligand Donor Sets: Effects of Carboxylate Leaving Groups and Steric Hindrance on Chemical and Biological Properties. *Inorg Chem* **45**, 5733-5735 (2006).
26. Ma, E.S., *et al.* Enhancement of aqueous solubility and stability employing a trans acetate axis in trans planar amine platinum compounds while maintaining the biological profile. *J Med Chem* **48**, 5651-5654 (2005).

27. Quiroga, A.G., Pérez, J.M., Alonso, C., Navarro-Ranninger, C. & Farrell, N. Novel Transplatinum(II) Complexes with [N2O2] Donor Sets. Cellular Pharmacology and Apoptosis Induction in Pam 212-ras Cells. *Journal of Medicinal Chemistry* **49**, 224-231 (2005).
28. Aris, S.M., Gewirtz, D.A., Ryan, J.J., Knott, K.M. & Farrell, N.P. Promotion of DNA strand breaks, interstrand cross-links and apoptotic cell death in A2780 human ovarian cancer cells by transplatinum planar amine complexes. *Biochemical Pharmacology* **73**, 1749-1757 (2007).
29. Aris, S.M. & Farrell, N.P. Towards Antitumor Active trans-Platinum Compounds. *European Journal of Inorganic Chemistry* **2009**, 1293-1302 (2009).
30. Farrell, N. *Platinum-Based Drugs in Cancer Therapy*, (Humana Press, 2000).
31. Manzotti, C., *et al.* BBR 3464: A Novel Triplatinum Complex, Exhibiting a Preclinical Profile of Antitumor Efficacy Different from Cisplatin. *Clinical Cancer Research* **6**, 2626-2634 (2000).
32. Perego, P., *et al.* A novel trinuclear platinum complex overcomes cisplatin resistance in an osteosarcoma cell system. *Mol Pharmacol* **55**, 528-534 (1999).
33. Pratesi, G., *et al.* A novel charged trinuclear platinum complex effective against cisplatin-resistant tumours: hypersensitivity of p53-mutant human tumour xenografts. *Br J Cancer* **80**, 1912-1919 (1999).
34. Sessa, C., *et al.* Clinical and pharmacological phase I study with accelerated titration design of a daily times five schedule of BBR3464, a novel cationic triplatinum complex. *Ann Oncol* **11**, 977-983 (2000).



35. Wheate, N.J. & Collins, J.G. Multi-nuclear platinum complexes as anti-cancer drugs. *Coordin Chem Rev* **241**, 133-145 (2003).
36. Wheate, N.J. & Collins, J.G. Multi-Nuclear Platinum Drugs: A New Paradigm in Chemotherapy. *Current Medicinal Chemistry - Anti-Cancer Agents* **5**, 267-279 (2005).
37. Harris, A.L., *et al.* Synthesis, characterization, and cytotoxicity of a novel highly charged trinuclear platinum compound. Enhancement of cellular uptake with charge. *Inorg Chem* **44**, 9598-9600 (2005).
38. Komeda, S., *et al.* A Third Mode of DNA Binding: Phosphate Clamps by a Polynuclear Platinum Complex. *Journal of the American Chemical Society* **128**, 16092-16103 (2006).
39. Calnan, B.J., Tidor, B., Biancalana, S., Hudson, D. & Frankel, A.D. Arginine-mediated RNA recognition: the arginine fork. *Science* **252**, 1167-1171 (1991).
40. Mangrum, J.B. & Farrell, N.P. Excursions in polynuclear platinum DNA binding. *Chemical Communications* **46**, 6640-6650 (2010).
41. Terrier, P., Tortajada, J., Zin, G. & Buchmann, W. Noncovalent Complexes Between DNA and Basic Polypeptides or Polyamines by MALDI-TOF. *Journal of the American Society for Mass Spectrometry* **18**, 1977-1989 (2007).
42. Harris, A.L., Ryan, J.J. & Farrell, N. Biological consequences of trinuclear platinum complexes: comparison of  $[\{\text{trans-PtCl}(\text{NH}_3)_2\}_2\mu\text{-(trans-Pt}(\text{NH}_3)_2(\text{H}_2\text{N}(\text{CH}_2)_6\text{-NH}_2)_2)]^{4+}$  (BBR 3464) with its noncovalent congeners. *Molecular Pharmacology* **69**, 666-672 (2006).

43. Harris, A.L., *et al.* Synthesis, characterization, and cytotoxicity of a novel highly charged trinuclear platinum compound. Enhancement of cellular uptake with charge. *Inorganic Chemistry* **44**, 9598-9600 (2005).
44. Komeda, S., *et al.* A third mode of DNA binding: Phosphate clamps by a polynuclear platinum complex. *J Am Chem Soc* **128**, 16092-16103 (2006).
45. Castillo-Garit, J.A., Marrero-Ponce, Y., Torrens, F. & García-Domenech, R. Estimation of ADME properties in drug discovery: Predicting Caco-2 cell permeability using atom-based stochastic and non-stochastic linear indices. *Journal of Pharmaceutical Sciences* **97**, 1946-1976 (2008).
46. Silverman, R.B. *The Organic Chemistry of Drug Design and Drug Action*, (Elsevier Academic Press, Oxford, 2004).
47. Safirstein, R., *et al.* Cisplatin nephrotoxicity. *Am J Kidney Dis* **8**, 356-367 (1986).
48. Wang & Guo, Z. The role of sulfur in platinum anticancer chemotherapy. *Anticancer Agents Med Chem* **7**, 19-34 (2007).
49. Esposito, B.P. & Najjar, R. Interactions of antitumoral platinum-group metallodrugs with albumin. *Coordin Chem Rev* **232**, 137-149 (2002).
50. Espósito, B.P. & Najjar, R. Interactions of antitumoral platinum-group metallodrugs with albumin. *Coordination Chemistry Reviews* **232**, 137-149 (2002).
51. Carter, D.C. & Ho, J.X. Structure of Serum-Albumin. *Adv Protein Chem* **45**, 153-203 (1994).
52. Peters, T. Serum-Albumin. *Adv Protein Chem* **37**, 161-245 (1985).

53. Ivanov, A.I., *et al.* Cisplatin binding sites on human albumin. *J Biol Chem* **273**, 14721-14730 (1998).
54. Borch, R.F. & Pleasants, M.E. Inhibition of cis-platinum nephrotoxicity by diethyldithiocarbamate rescue in a rat model. *Proc Natl Acad Sci U S A* **76**, 6611-6614 (1979).
55. Reedijk, J. Why Does Cisplatin Reach Guanine-N7 with Competing S-Donor Ligands Available in the Cell? *Chemical Reviews* **99**, 2499-2510 (1999).
56. Kosower, N.S. & Kosower, E.M. The glutathione status of cells. *Int Rev Cytol* **54**, 109-160 (1978).
57. Appleton, T.G., Connor, J.W., Hall, J.R. & Prenzler, P.D. NMR Study of the reactions of the cis-diamminediaquaplatinum(II) cation with glutathione and amino acids containing a thiol group. *Inorg Chem* **28**, 2030-2037 (1989).
58. Berners-Price, S.J. & Kuchel, P.W. Reaction of cis- and trans-[PtCl<sub>2</sub>(NH<sub>3</sub>)<sub>2</sub>] with reduced glutathione studied by <sup>1</sup>H, <sup>13</sup>C, <sup>195</sup>Pt and <sup>15</sup>N-{<sup>1</sup>H} DEPT NMR. *J Inorg Biochem* **38**, 305-326 (1990).
59. Eastman, A. *Biomedical Mechanisms of the Platinum Antitumor Drugs*, (IFI. Press Limited, Oxford, 1986).
60. Oehlsen, M.E., Hegmans, A., Qu, Y. & Farrell, N. A Surprisingly Stable Macrochelate Formed from the Reaction of Cis Dinuclear Platinum Antitumor Compounds with Reduced Glutathione. *Inorg Chem* **44**, 3004-3006 (2005).
61. Oehlsen, M.E., Qu, Y. & Farrell, N. Reaction of polynuclear platinum antitumor compounds with reduced glutathione studied by multinuclear (<sup>1</sup>H, <sup>1</sup>H-<sup>15</sup>N

- gradient heteronuclear single-quantum coherence, and  $^{195}\text{Pt}$  NMR spectroscopy. *Inorg Chem* **42**, 5498-5506 (2003).
62. Zutphen, S.v. & Reedijk, J. Targeting platinum anti-tumour drugs: Overview of strategies employed to reduce systemic toxicity. *Coordin Chem Rev* **249**, 2845-2853 (2005).
63. Gatti, L., *et al.* Novel Bis-platinum Complexes Endowed with an Improved Pharmacological Profile. *Molecular Pharmaceutics* **7**, 207-216 (2009).
64. Klein, A.V. & Hambley, T.W. Platinum Drug Distribution in Cancer Cells and Tumors. *Chemical Reviews* **109**, 4911-4920 (2009).
65. Kalayda, G., *et al.* Dinuclear platinum complexes with N, N'-bis(aminoalkyl)-1,4-diaminoanthraquinones as linking ligands. Part II. Cellular processing in A2780 cisplatin-resistant human ovarian carcinoma cells: new insights into the mechanism of resistance. *J Biol Inorg Chem* **9**, 414-422 (2004).
66. Kalayda, G.V., Jansen, B.A.J., Wielaard, P., Tanke, H.J. & Reedijk, J. Dinuclear platinum anticancer complexes with fluorescent N,N'-bis(aminoalkyl)-1,4-diaminoanthraquinones: cellular processing in two cisplatin-resistant cell lines reflects the differences in their resistance profiles. *J Biol Inorg Chem* **10**, 305-315 (2005).

## Chapter 2: Modulation of protein-drug deactivation through carboxylate ligand modification in a series of cytotoxic *trans*-platinum planar amine compounds

Brad T. Benedetti, Susana Quintal, and Nicholas P. Farrell\*

Department of Chemistry and Massey Cancer Center

Virginia Commonwealth University, Richmond, Virginia. USA

Submitted to Dalton Transactions, 2011

### **Abstract**

Transplatinum planaramine (TPA) compounds which possess carboxylate ligands in the *trans* position have been shown to be potential antitumor drugs in a variety of cell types, including cisplatin and oxaliplatin resistance cell lines.<sup>1-3</sup> In this work, we ask whether the nature and stability of the carboxylate ligand can be tuned in an attempt to manipulate the extent of serum protein binding; and consequently influence cytotoxicity, cellular drug accumulation and DNA adduct formation. Monitoring the interactions of selected TPA's with N-Acetyl Methionine (NAM) by <sup>1</sup>H and <sup>195</sup>Pt NMR show large differences in rate of sulfur binding. TPA containing acetate ligands show a much lower sulfur binding rate than those possessing formate leaving groups. The same trend was seen after acetate and formate TPA compounds were incubated with human serum albumin and the reaction was monitored for 24hrs. To understand whether *in vitro* results could be translated *in vivo*, MTT cytotoxicity assays were

conducted for each compound, before and after incubation with whole serum. Both the formate and acetate compounds,  $t\text{-Pt}(4\text{-pic})\text{NH}_3(\text{OFm})_2$  and  $t\text{-Pt}(4\text{-pic})\text{NH}_3(\text{OAc})_2$ , showed minimal losses in cytotoxic efficacy and outperformed cisplatin after pre-incubation with serum. The same trends were seen when monitoring the effects of protein binding on cellular uptake and DNA platination. The rate of protein binding/drug deactivation was shown to be directly related to the stability of the leaving group ( $\text{OAc} > \text{OFm} > \text{Cl}$ ). Thus, our results suggest that utilization of the 'carboxylate strategy' substantially enhances the cellular efficacy of TPA compounds over cisplatin by allowing for an optimal balance between cytotoxic and metabolic efficiency.

## **Introduction**

The platinum based chemotherapeutic, cisplatin, is among the most commonly used anticancer drug for the treatment of testicular, head and neck, ovarian, small cell lung, and colorectal carcinomas.<sup>4-5</sup> The cytotoxicity of cisplatin results mainly from the formation of DNA crosslinks resulting in the inhibition of DNA synthesis and replication.<sup>6-7</sup> However, the clinical effectiveness of cisplatin is limited due to inherent cellular resistance and dose-limiting side effects due to high levels of protein binding.<sup>8</sup> One common feature among current clinical platinum therapeutics is the bis, *cis* orientation of the labile leaving groups. The *trans* isomer of cisplatin,  $\text{trans-}[\text{PtCl}_2(\text{NH}_3)_2]$  is much less toxic than the *cis* counterparts, presumably due to its inability to form 1,2-intrastrand cross links between the N7 atoms of adjacent guanines in double strand DNA.<sup>9-10</sup>

Although transplatin itself is clinically inactive, substitution of one of the  $\text{NH}_3$  groups with a planar heterocyclic ligand such as pyridine, thiazole, quinoline, isoquinoline, etc., yields a class of platinum chemotherapeutics, called transplanaramines (TPA's). These TPA compounds possess substantially enhanced cytotoxicity profiles as compared to the "parent" *trans*- $[\text{PtCl}_2(\text{NH}_3)_2]$ , with  $\text{IC}_{50}$  values in the 1-10 $\mu\text{M}$  range across numerous tumor cell lines. Most interestingly, TPA compounds usually exhibit no cross resistance with cisplatin or oxaliplatin and thus demonstrate a unique cytotoxicity profile across the NCI tumor panel.<sup>2</sup> Although these TPA compounds are relatively active, they are poorly water soluble and still possess high levels of protein binding due to the lability of the chloride leaving group.

The most common modification to the TPA structures to address these issues is through replacing the chlorides with a more stable group of carboxylate ligands. The use of carboxylates as leaving groups for TPA's was first introduced to address the low aqueous solubility of TPA's, but in preliminary studies showed that the 'carboxylate' strategy could also be employed to improve the pharmacokinetic properties of mono-nuclear trans-platinum compounds.<sup>11</sup> These carboxylate derivatives have shown similar cytotoxicities to their parent chlorides.<sup>12-13</sup> The use of carboxylate ligands also results in increased cellular accumulation even in cisplatin and oxaliplatin-resistant cell lines.<sup>12-13</sup> In attempts to optimize drug design, previous studies in our group have shown that the use of formate as leaving group gives enhanced cytotoxicity in comparison to acetate.<sup>1</sup>

In order to evaluate the *in vivo* properties of these TPA compounds, it is first necessary to understand the three major factors affecting the clinical success of any type of platinum-based cancer therapy. These factors include the rate of cellular

uptake, the frequency and the type of DNA adducts formed and metabolic deactivation. Although DNA is the proposed target for a majority of platinum chemotherapeutics, the first step in evaluating the clinical efficacy is to understand the metabolic interactions that occur following administration. One of the most plausible targets responsible for metabolic deactivation of platinum compounds is blood serum. Serum is the liquid portion of blood, containing all serum proteins, at a concentration of 70 g/L.<sup>14</sup> Among these proteins include globulin and serum albumin. Interactions of platinum anti-tumor compounds with sulfur containing amino acids in proteins have been shown to cause severe nephrotoxicity in patients and are responsible for a large portion of the toxic side effects associated with platinum based treatments.<sup>15</sup> It is mainly accepted that once bound to plasma proteins, platinum compounds are 'deactivated' and eliminated from the body.

The development of oxaliplatin and carboplatin has shown the ability of using the carboxylate strategy to avoid these high levels of protein binding.<sup>16-17</sup> Although this strategy has been used to improve the pharmacokinetic profile of cisplatin, and spurred the development of carboplatin and oxaliplatin, the use of the *cis* leaving group geometry still limits the treatment of these compounds in tumors which are currently "platin" resistant. By extending the carboxylate strategy to TPA compounds it may be possible to avoid high levels of protein binding while concomitantly treating tumor types untreatable with current clinical platinum chemotherapeutics.

## **Results and Discussion**

### NMR Spectroscopy



It has previously been seen that modifying the leaving group ligand in a series of TPA compounds can greatly influence the rate of hydrolysis.<sup>11</sup> To evaluate this change in hydrolysis rate and its effect on thiol binding, NMR binding studies of TPA's with N-Acetyl-Methionine (NAM) were performed. (Figure 2.1) The reaction of a series of a series of TPA's with acetate and formate leaving groups was monitored by  $^1\text{H}$  and  $^{195}\text{Pt}$  NMR spectroscopy. As seen in (Table 2.1), the reaction of  $t\text{-Pt}(4\text{-pic})\text{NH}_3(\text{OFm})_2$  with NAM was followed by monitoring the H1 proton of 4-picoline and the CH proton of the formate leaving group. Initial spectra at  $t = 0$  show peaks at approximately  $\delta = 8.25\text{ppm}$  for the H1 of 4-picoline. The spectrum acquired at  $t = 4\text{hrs}$  of a 1:2  $t\text{-Pt}(4\text{-pic})\text{NH}_3(\text{OFm})_2$ :NAM molar ratio reaction shows a shift of the H1 of 4-picoline from  $\delta = 8.25\text{ppm}$  to  $8.67\text{ppm}$ . (Figure 2.2) After 4 hours, the peaks remained relatively unchanged, and  $^{195}\text{Pt}$  NMR was used to probe the resulting platinum coordination sphere. The  $^{195}\text{Pt}$  NMR spectra showed only one peak at  $\delta = -3340\text{ ppm}$ , consistent with a *trans*-bis thiol coordination to the platinum atom.<sup>18-19</sup> Similar results were seen with the reaction of  $t\text{-Pt}(\text{Isoquin})\text{NH}_3(\text{OFm})_2$  with NAM, indicating the dependence of protein binding on the formate leaving group and not the carrier ligand. (Table 2.1) The binding rates ( $t_{1/2}$ ) of each reaction were calculated and found to be  $2.6 \pm 0.2\text{ hrs}$  for  $t\text{-Pt}(\text{Isoquin})\text{NH}_3(\text{OFm})_2$  and  $2.3 \pm 0.1\text{ hrs}$  for  $t\text{-Pt}(4\text{-pic})\text{NH}_3(\text{OFm})_2$ . (Table 2.1)

The same conditions were used to probe the binding rate of  $t\text{-Pt}(4\text{-pic})\text{NH}_3(\text{OAc})_2$  with NAM. Initial spectra at  $t = 0$  show peaks at approximately  $\delta = 8.30\text{ppm}$  for the H1 of 4-picoline. (Figure 2.3) Due to the slower rate of reactivity for the acetate ligand, the reaction was able to be monitored by both  $^1\text{H}$  and  $^{195}\text{Pt}$  NMR. The resulting  $^{195}\text{Pt}$  NMR spectra showed only one peak at  $t = 0\text{hrs}$ ,  $\delta = -1445\text{ ppm}$ . After 4hrs, a second peak at

$\delta = -2860$  ppm was observed. (Figure 2.4) This peak represents the displacement of one acetate group by NAM, with a coordination sphere of Pt[N<sub>2</sub>OS]. After 24hrs, the peak seen at  $\delta = -2860$  ppm disappeared and was replaced with a peak at  $\delta = -3325$  ppm, consistent with a *trans*-bis thiol coordination of Pt[N<sub>2</sub>S<sub>2</sub>]. (Table 2.1) <sup>1</sup>H NMR spectra of the H1 of the 4-picoline revealed peaks at  $\delta = 8.30$ , 8.55, and 8.70 ppm, indicating initial compound, mono-NAM and bis-NAM species respectively. (Figure 2.3) Similar results were seen with the reaction of *t*-Pt(Isoquin)NH<sub>3</sub>(OAc)<sub>2</sub> with NAM. The binding rates ( $t_{1/2}$ ) of each reaction were calculated and found to be  $10.1 \pm 1.0$  hrs for *t*-Pt(4-pic)NH<sub>3</sub>(OAc)<sub>2</sub> and  $10.7 \pm 0.8$  hrs for *t*-Pt(Iso)NH<sub>3</sub>(OAc)<sub>2</sub>. (Table 2.1)

By utilizing small molecules such as NAM as a model for drug-protein binding, it is possible to understand the contribution of the carboxylate ligand to metabolic deactivation and therefore predict the binding to larger serum proteins such as human serum albumin. These results show the ability of employing the carboxylate strategy as a way to manipulate high levels of drug-protein binding with TPA compounds. These modifications have previously been shown to play a vital role in determining the cytotoxicity and cellular uptake of TPA compounds.<sup>20</sup> Therefore, the general [PtN<sub>2</sub>O<sub>2</sub>] motif could allow researchers the capability of “fine-tuning” a balance between biological and metabolic activity of these compounds.

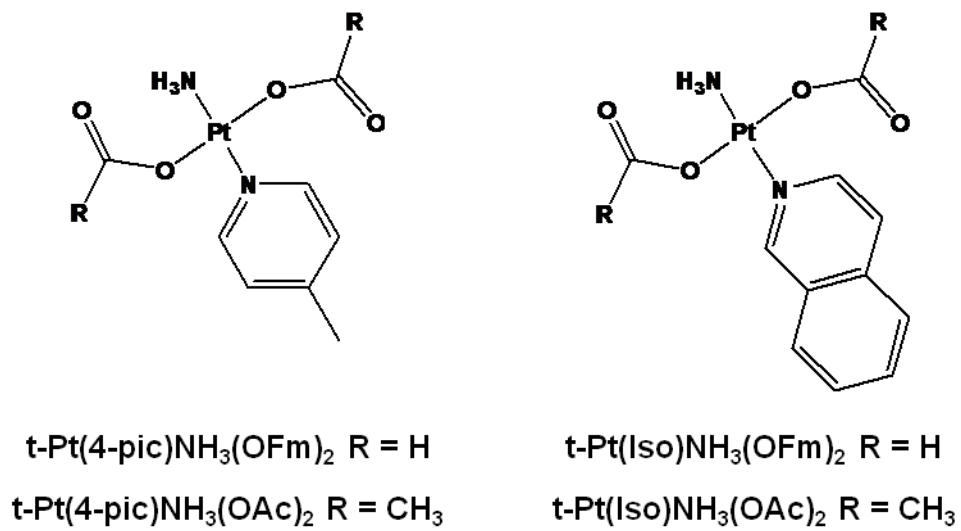


**Figure 2.1** Structures of *trans*-platinum planar amine (TPA) carboxylate compounds studied.

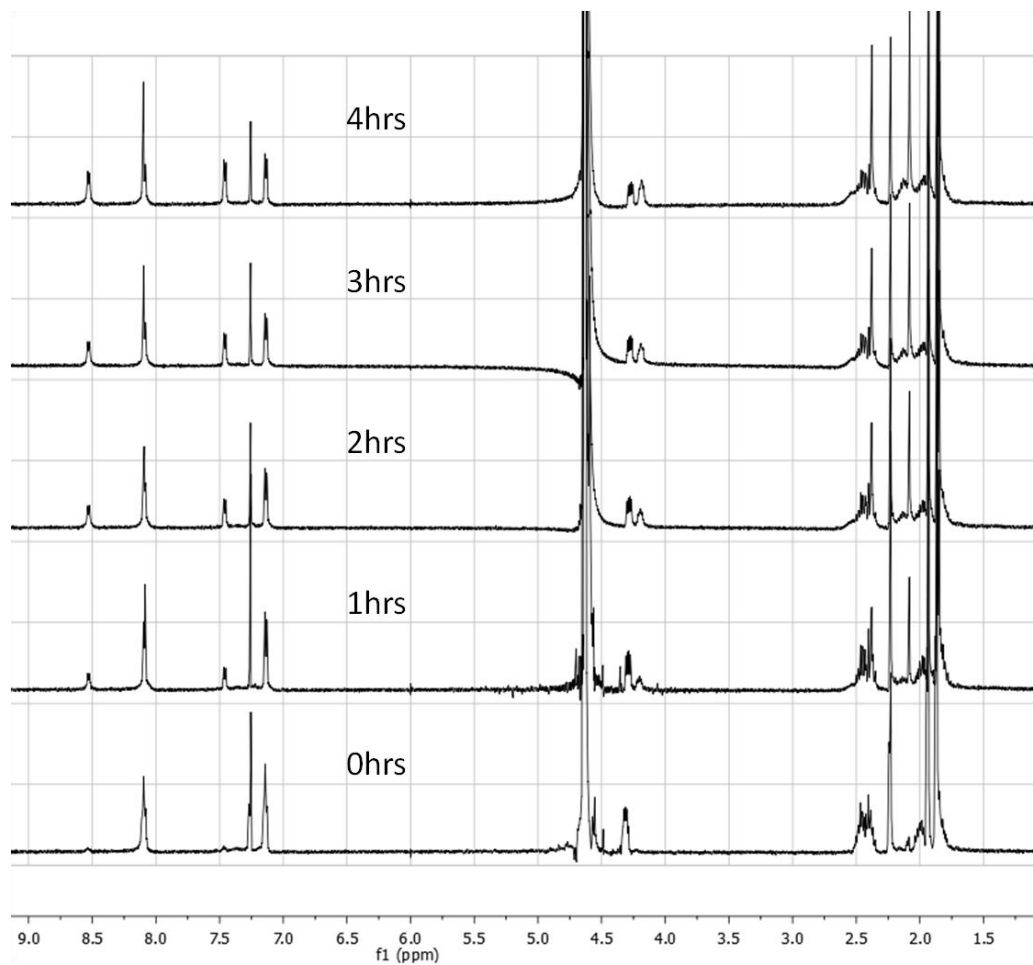


**Figure 2.2** NMR Spectra of  $t\text{-Pt}(4\text{-pic})\text{NH}_3\text{OFm}$  reaction with N-Acetyl Methionine

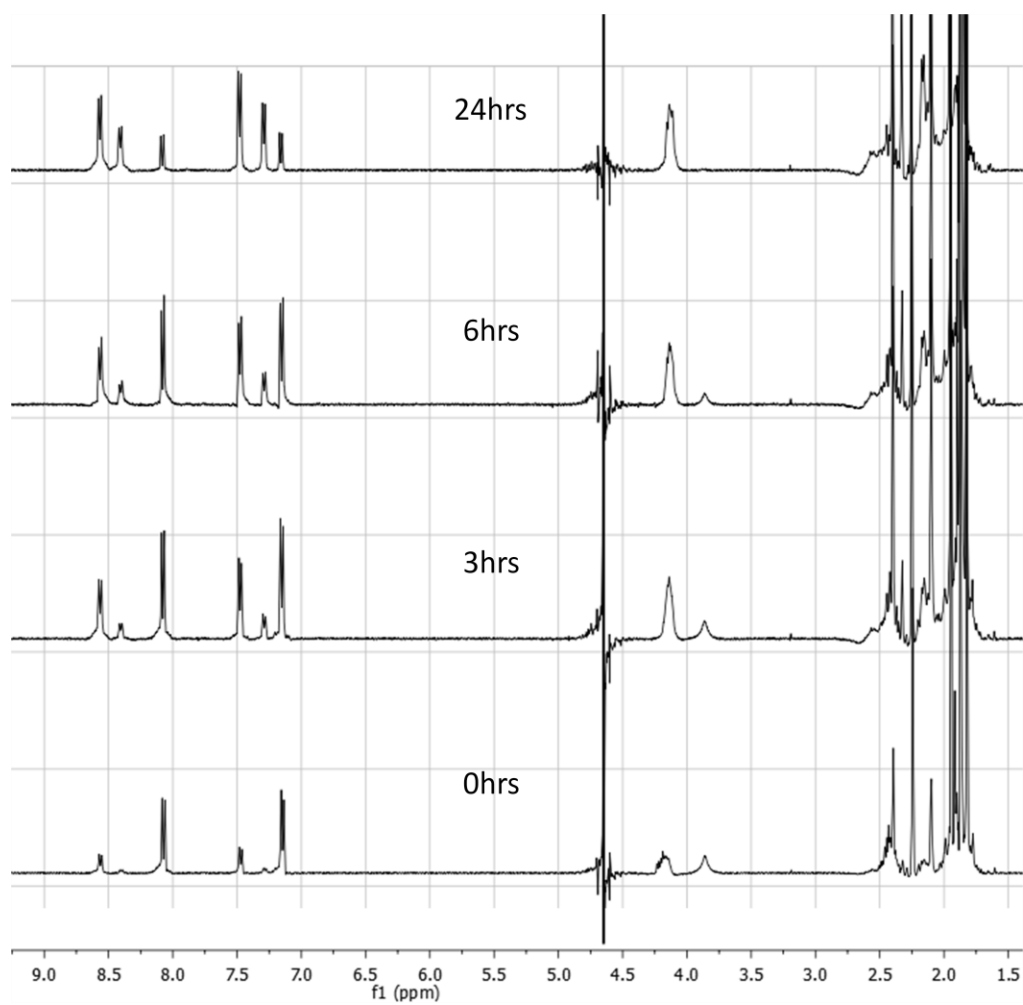


**Figure 2.3** NMR Spectra of t-Pt(4-pic)NH<sub>3</sub>OAc reaction with N-Acetyl Methionine

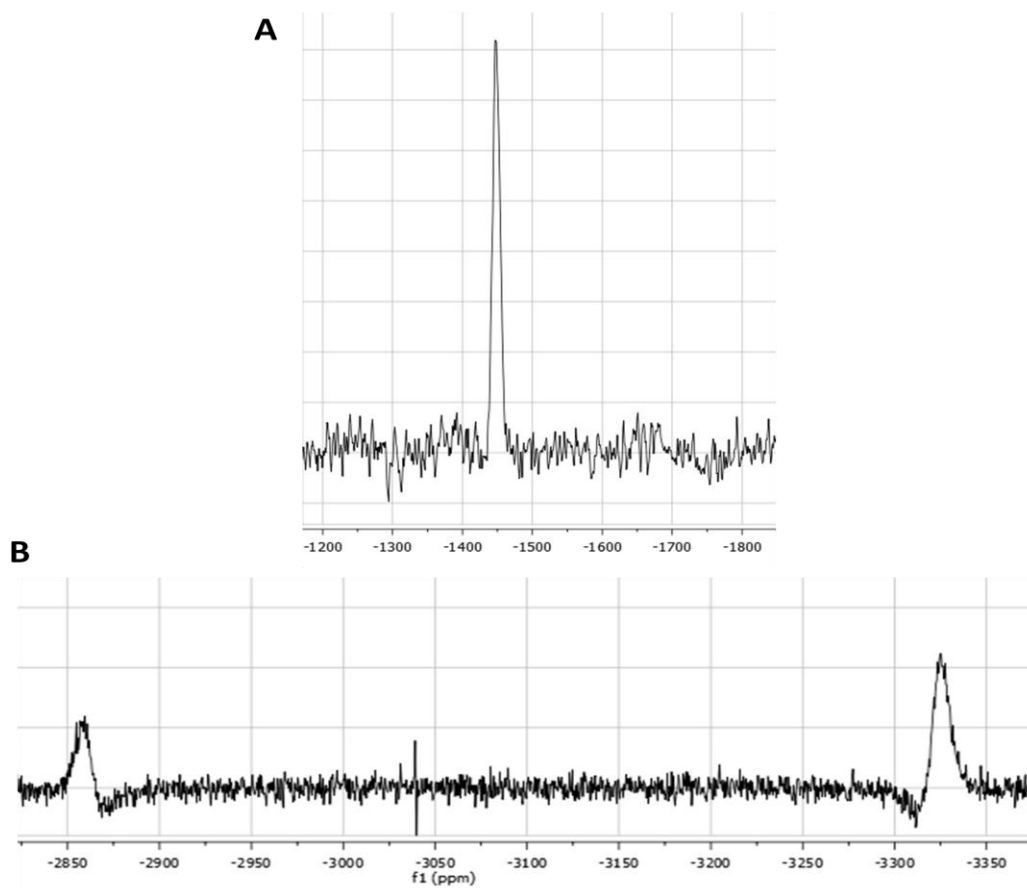


**Figure 2.4**  $^{195}\text{Pt}$  NMR Spectra of  $t\text{-Pt(4-pic)NH}_3\text{OAc}$  reaction with N-Acetyl Methionine after 0hrs (A) and 4hrs (B)

| Compound  | Methionine Binding NMR Data |                       |                        |                       | Methionine Binding Rate<br>( $t_{1/2}$ Hrs) |
|---|-----------------------------|-----------------------|------------------------|-----------------------|---|
|   | t-Pt(OCOR <sub>2</sub> )    |                       | t-Pt(Met) <sub>2</sub> |                       |   |
|   | $\delta(H1)$<br>(ppm)       | $\delta(Pt)$<br>(ppm) | $\delta(H1)$<br>(ppm)  | $\delta(Pt)$<br>(ppm) |   |
| <b>t-Pt(4pic)NH<sub>3</sub>(OFm)<sub>2</sub></b><br>R=Formate                 | 8.25                        | -1450                 | 8.67                   | -3340                 | <b>2.3 ± 0.1</b>                            |
| <b>t-Pt(Isoquin)NH<sub>3</sub>(OFm)<sub>2</sub></b><br>R=Formate              | 9.3                         | -1455                 | 9.7                    | -3335                 | <b>2.6 ± 0.2</b>                            |
| <b>t-Pt(4pic)NH<sub>3</sub>(OAc)<sub>2</sub></b><br>R=Acetate <sup>1</sup>    | 8.30                        | -1445                 | 8.70                   | -3325                 | <b>10.1 ± 1.0</b>                           |
| <b>t-Pt(Isoquin)NH<sub>3</sub>(OAc)<sub>2</sub></b><br>R=Acetate <sup>1</sup> | 9.3                         | -1455                 | 9.8                    | -3335                 | <b>10.7 ± 0.8</b>                           |

(1) The reaction of t-Pt(4pic)NH<sub>3</sub>(OAc)<sub>2</sub> and t-Pt(Isoquin)NH<sub>3</sub>(OAc)<sub>2</sub> with methionine was sufficiently slow such that the mono-methionine product [Pt(N<sub>2</sub>OS)] was observed.  $\delta^{195}\text{Pt}$  (ppm) = -2860 and  $\delta^{195}\text{Pt}$  (ppm) = -2895 respectively.

**Table 2.1** Effects of ligand substitution on methionine binding: Reaction of each TPA compound with N-Acetyl Methionine was monitored by <sup>1</sup>H and <sup>195</sup>Pt NMR spectroscopy.

### Human Serum Albumin Binding

To evaluate the effect of leaving group stability on protein binding, cisplatin,  $t\text{-Pt}(4\text{-pic})\text{NH}_3(\text{OFm})_2$  and  $t\text{-Pt}(4\text{-pic})\text{NH}_3(\text{OAc})_2$  were incubated with human serum albumin and allowed to react for selected time points. The extent of drug-protein binding was analyzed by ICP-OES. Analysis of platinum content by ICP-OES shows a decrease in free drug availability over time for all three compounds. (Figure 2.5) This time dependent decrease in free drug availability represents a displacement of the platinum-chloride or platinum-carboxylate bond and the formation of the covalent platinum-protein adduct. As seen with the small molecule binding studies, the rate of protein binding is directly related to the stability/lability of the leaving group. Within 30 minutes of incubation, approximately 25% of cisplatin was bound to serum albumin, while only 5% of both  $t\text{-Pt}(4\text{-pic})\text{NH}_3(\text{OFm})_2$  and  $t\text{-Pt}(4\text{-pic})\text{NH}_3(\text{OAc})_2$  were protein bound. After 24hrs of protein exposure, approximately 85% of  $t\text{-Pt}(4\text{-pic})\text{NH}_3(\text{OAc})_2$ , and 50% of  $t\text{-Pt}(4\text{-pic})\text{NH}_3(\text{OFm})_2$  remain unbound to serum albumin, while only 20% of administered cisplatin remains in solution. These studies show the ability to manipulate high levels of protein binding by modifying the stability of the carboxylate ligand.



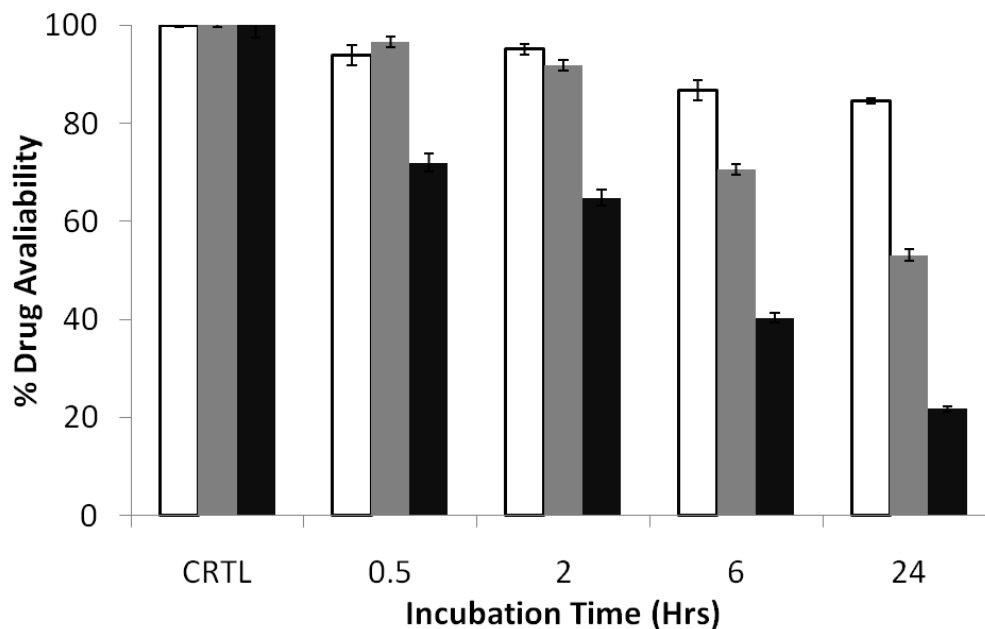


**Figure 2.5** Effects of ligand substitution on HSA protein binding: Binding of  $t\text{-Pt}(4\text{pic})\text{NH}_3(\text{OAc})_2$  (white),  $t\text{-Pt}(4\text{pic})\text{NH}_3(\text{OFm})_2$  (grey), and Cisplatin (black) to human serum albumin over time. Compounds were incubated with albumin (3:1) (drug:protein) and platinum content was observed by ICP-OES.

### Effects of Protein Binding on Drug Cytotoxicity

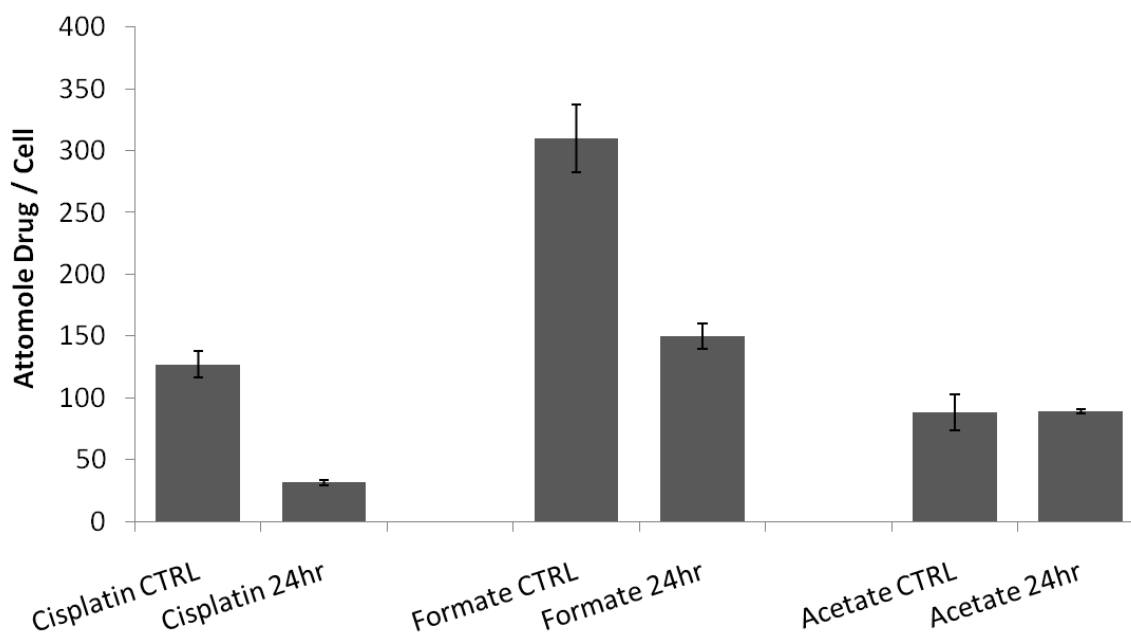
To further understand the translatability of utilizing the carboxylate strategy to improve the drug deactivation profile of TPA's, cytotoxicity assays were performed before and after incubation of TPA's with whole serum in A2780 ovarian carcinoma cell lines. Cisplatin,  $t\text{-Pt}(4\text{-pic})\text{NH}_3(\text{OFm})_2$  and  $t\text{-Pt}(4\text{-pic})\text{NH}_3(\text{OAc})_2$  were incubated with whole serum for 0hr and 24hr and drug cytotoxicity was then examined. Cisplatin shows a complete loss of cytotoxicity upon incubation with serum for 24hrs, with an observed  $\text{IC}_{50}$  increase of >30 fold. (Table 2.2) Cellular treatment with  $t\text{-Pt}(4\text{-pic})\text{NH}_3(\text{OFm})_2$  and  $t\text{-Pt}(4\text{-pic})\text{NH}_3(\text{OAc})_2$  after 24hr incubation with whole serum show only a 3-fold and 2-fold increase in  $\text{IC}_{50}$  value respectively. (Table 2.2) Although less cytotoxic in the control, once administered, a majority of the cytotoxic action of cisplatin is lost within a very short time due to interactions with serum proteins in the blood stream. In contrast, the cytotoxicity of  $t\text{-Pt}(4\text{-pic})\text{NH}_3(\text{OFm})_2$  and  $t\text{-Pt}(4\text{-pic})\text{NH}_3(\text{OAc})_2$  is retained after serum incubation. The rate of drug deactivation is directly related to the rate of hydrolysis, as the  $-\text{OFm}$  ligand is more labile than the  $-\text{OAc}$  ligand, which are both more stable than  $-\text{Cl}$ . Utilizing the bis-*trans*-geometry of the carboxylate groups provides little driving force for ligand substitution. This finding shows a class of drugs with significantly longer plasma half lives and decreased drug deactivation over current clinical platinum based chemotherapeutics.

| Compound   | IC <sub>50</sub> (uM)<br>Control | IC <sub>50</sub> (uM)<br>24hr Serum Incubation | Fold Increase in IC <sub>50</sub> |
|--|----------------------------------|--|-----------------------------------|
| Cisplatin  | 0.5                              | >15  | >30                               |
| t-Pt(4-pic)NH <sub>3</sub> ( <i>OFm</i> ) <sub>2</sub> | 5                                | 12   | 2.4                               |
| t-Pt(4-pic)NH <sub>3</sub> ( <i>OAc</i> ) <sub>2</sub> | 13                               | 28   | 2.1                               |

**Table 2.2** Effects of serum binding on efficacy of trans-platinum compounds in A2780 ovarian carcinoma cells. Platinum compounds were incubated with whole serum for 24hrs and compared to control. Cellular growth inhibition was then measured by MTT after treatment.

### Effects of Protein Binding on Cellular Accumulation

Since the rate of cellular uptake and total accumulation correlates to the cytotoxic effect of platinum drugs, cellular accumulation of each platinum compound, before and after whole serum treatment, was examined. Treatment of A2780 cells with 10 $\mu$ M cisplatin produced an increase in cellular platinum levels reaching approximately 130 attomole Pt/cell after 24hrs. In contrast, cells treated with cisplatin, after a 24hr incubation period with whole serum prior to treatment, showed a drug accumulation of 30 attomole Pt/cell. (Figure 2.6) Cellular treatment with 10 $\mu$ M t-Pt(4-pic)NH<sub>3</sub>(OFm)<sub>2</sub> also shows a decrease in overall platinum accumulation after serum incubation, 310 attomole Pt/cell in the control and 150 attomole Pt/cell after 24hr serum treatment. Serum pretreatment with 10 $\mu$ M t-Pt(4-pic)NH<sub>3</sub>(OAc)<sub>2</sub> shows no significant decrease in overall platinum content as compared to the control; 90 attomole Pt/cell in both the control after 24hr serum incubation. (Figure 2.6) While the serum pretreatment of t-Pt(4-pic)NH<sub>3</sub>(OFm)<sub>2</sub> results in a decrease in cellular uptake, the overall decrease in cellular uptake is only 2-fold, as compared to a 4-fold decrease for cisplatin. Once again the same trend is seen, where an increase in leaving group lability, Cl > OFm > OAc, results in increased protein binding and thus, a decrease in cellular uptake. By minimizing interactions with serum proteins, TPA compounds have the ability to maintain high levels of cellular uptake and thus a greater level of cytotoxicity over metabolic deactivation.

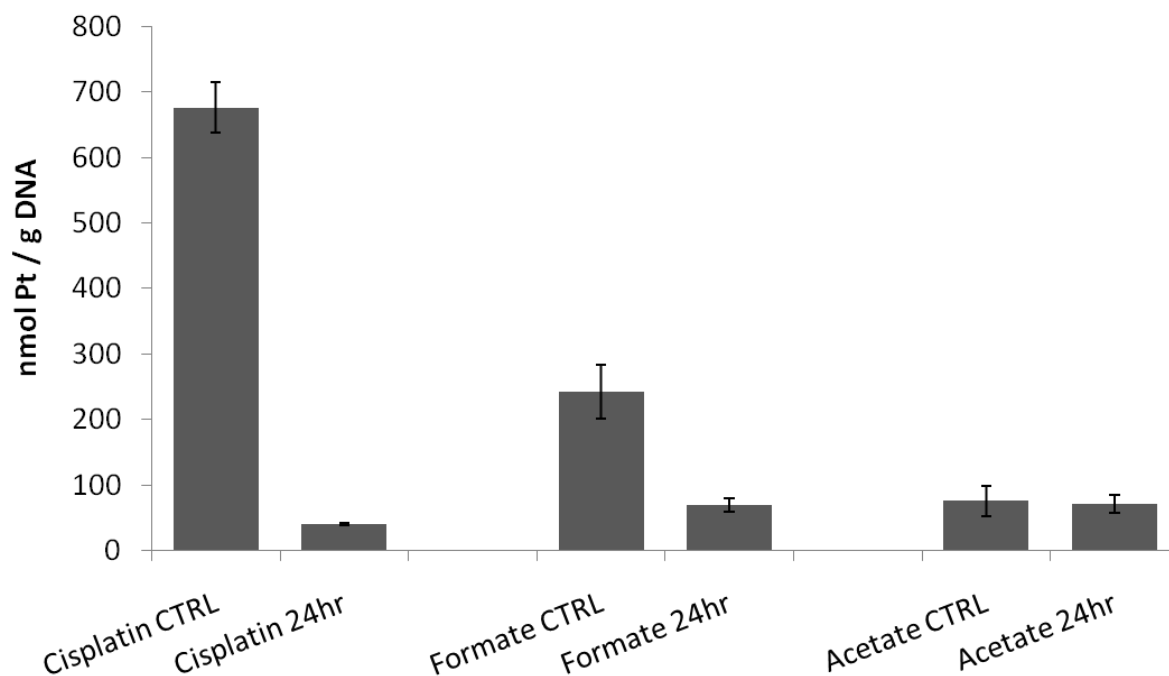


| Compound                                      | Pt Conc. (Attomol/Cell) Control | Pt Conc. (Attomol/Cell) 24hr Serum Incubation | Fold Decrease in Platinum Uptake |
|---|---------------------------------|---|----------------------------------|
| Cisplatin                                     | 130                             | 30  | 4.3                              |
| t-Pt(4-pic)NH <sub>3</sub> (OFm) <sub>2</sub> | 310                             | 150   | 2.1                              |
| t-Pt(4-pic)NH <sub>3</sub> (OAc) <sub>2</sub> | 90                              | 90  | N/A                              |

**Figure 2.6** Influence of protein binding on platinum cellular uptake in A2780 ovarian carcinoma cells. A2780 Cells were treated with 10 $\mu$ M cisplatin, t-Pt(4-pic)NH<sub>3</sub>(OFm)<sub>2</sub> and t-Pt(4-pic)NH<sub>3</sub>(OAc)<sub>2</sub> before and after serum pretreatment for 24hrs. After 24hr cellular treatment of each compound, cells were removed from the plate and analysis of platinum content was performed on a Varian ICP-MS. Values are the average (+/- S.E.M.) of three independent experiments.

### Effects of Protein Binding on DNA Platination

The cytotoxicity of platinum chemotherapeutics is mainly accepted to be modulated by the frequency and type of platinum-DNA adducts formed during drug treatment. Upon treatment, TPA compounds promote DNA strand breaks, interstrand cross-links and ultimately trigger the apoptosis cascade, resulting in programmed cell death.<sup>1</sup> To examine the role of protein binding on the levels of DNA platination, A2780 cells were treated for 24hrs with 10 $\mu$ M cisplatin, t-Pt(4-pic)NH<sub>3</sub>(OFm)<sub>2</sub> and t-Pt(4-pic)NH<sub>3</sub>(OAc)<sub>2</sub> before and after serum pretreatment. DNA platination levels after 24 hours of continuous cisplatin treatment reached approximately 675 nmole Pt/g DNA, while platinum levels of cisplatin pretreated with whole serum remained less than 40 nmole Pt/g DNA. (Figure 2.7) The same trend in DNA adduct formation, albeit at a lesser extent, was seen with t-Pt(4-pic)NH<sub>3</sub>(OFm)<sub>2</sub>, with platinum levels reaching 245 nmole Pt/g DNA in the control and 70 nmole Pt/g DNA after pretreatment with serum. (Figure 2.7) In contrast, DNA platination levels after 24 hours of continuous t-Pt(4-pic)NH<sub>3</sub>(OAc)<sub>2</sub> treatment remained constant in both the control and after 24hrs of serum pretreatment, with levels reaching approximately 70 nmole Pt/g DNA. While initial platination levels of both t-Pt(4-pic)NH<sub>3</sub>(OFm)<sub>2</sub> and t-Pt(4-pic)NH<sub>3</sub>(OAc)<sub>2</sub> are lower than seen with cisplatin, after 24hrs of serum pretreatment, both t-Pt(4-pic)NH<sub>3</sub>(OFm)<sub>2</sub> and t-Pt(4-pic)NH<sub>3</sub>(OAc)<sub>2</sub> outperform cisplatin and retain a large portion of their cytotoxic profile.



| Compound                                      | Pt Conc. (nmol Pt / g DNA) Control | Pt Conc. (nmol Pt / g DNA) 24hr Serum Incubation | Fold Decrease in DNA Binding |
|---|------------------------------------|--|------------------------------|
| Cisplatin                                     | 675                                | 40   | 16.9                         |
| t-Pt(4-pic)NH <sub>3</sub> (OFm) <sub>2</sub> | 245                                | 70   | 3.5                          |
| t-Pt(4-pic)NH <sub>3</sub> (OAc) <sub>2</sub> | 75                                 | 72   | N/A                          |

**Figure 2.7** Influence of protein binding on DNA platinumation in A2780 ovarian carcinoma cells. A2780 Cells were treated with 10 $\mu$ M cisplatin, t-Pt(4-pic)NH<sub>3</sub>(OFm)<sub>2</sub> and t-Pt(4-pic)NH<sub>3</sub>(OAc)<sub>2</sub> before and after serum pretreatment for 24hrs. After 24hrs of drug exposure, cells were removed from the plate and washed with PBS. Cellular DNA was then extracted and analysis of platinum content was performed on a Varian ICP-MS. Values are the average (+/- S.E.M.) of three independent experiments.

## **Conclusion**

The development of novel cytotoxic transplatin compounds provides for promising treatment of clinical “platin” drug resistant tumors. By understanding the balance between cytotoxic activity and metabolic deactivation it is possible to defer many of the toxic side effects associated with chemotherapeutics, and thus provide for substantial increases in mean tolerated dosages. Here, we evaluate the ability of using carboxylate ligands to modulate the reactivity of TPA compounds towards sulfur containing proteins. We have found that by increasing the stability of the leaving group leads to decreased protein binding and thus allows for increase cytotoxic activity after pre-incubation with serum proteins. The acetate ligand was shown to be the most stable, followed by the formate and chloride, respectively. Although the stability of the acetate group ultimately provides for the least reactivity towards proteins, this enhanced stability also provides for decreases in DNA binding and therefore a slightly less potent  $IC_{50}$  is seen when compared with the formate derivative. These results show the importance of understand the balance between cytotoxicity and metabolic deactivation. The use of carboxylates in this process ultimately provides the means to “fine-tune” the reactivity of trans-platinum compounds and therefore provides a balance between the cytotoxic and pharmacokinetic profiles.

## **Methods**

### **Materials**



All compounds were synthesized according to methods reported previously.<sup>1,11,20</sup> Albumin from human, 99% and N-Acetyl Methionine was purchased from Sigma. Fetal Bovine Serum (FBS) was purchased from Atlanta Biologicals.

### NMR Spectroscopy

A stock solution of both deuterated (DPBS) and normal (PBS) phosphate-buffered saline ([phosphate] = 150 mM, pH 7.35 at 37° C, [NaCl] = 120 mM, [KCl] = 2.7 mM) was prepared for all reaction solutions to mimic physiological conditions. Platinum compounds were incubated with N-Acetyl-Methionine at a reaction ratio of 1:2 (Platinum Complex : N-Acetyl-Methionine) at 37°C. <sup>1</sup>H NMR and <sup>195</sup>Pt NMR spectra were recorded at various time points up to 24hrs. <sup>1</sup>H NMR and <sup>195</sup>Pt NMR spectra were recorded on a Varian Mercury series 300 MHz NMR spectrometer using a 5 mm probe for <sup>1</sup>H and a 10 mm broad-band probe for <sup>195</sup>Pt. <sup>1</sup>H spectra were referenced to sodium 3-(trimethylsilyl)-propionate (TSP) at  $\delta = 0$  ppm, and <sup>195</sup>Pt spectra were referenced to Na<sub>2</sub>[PtCl<sub>6</sub>]. The scanning frequency for <sup>195</sup>Pt nuclei was set at 64.32 MHz.

### Human Serum Albumin Binding

For HSA binding, 50 $\mu$ L of 1.8mM solutions of each complex were prepared in PBS, pH 7.4 and added to 50 $\mu$ L of 0.6 mM HSA such that the final drug concentration was 0.9 mM. (3:1; Drug:HSA) The reactions were incubated at 37 °C for 0, 0.5, 2, 6, and 24 hours. Unreacted drug was removed by centrifugation through a Millipore

Microcon YM-10 (10,000 kDa) membrane filter at 14,000xg for 30 min. The centrifuge cup was upturned in a second eppendorf and centrifuged at 1000xg for 3 min to isolate the protein-bound drug. The digestion procedure followed published methods.<sup>21</sup> Analysis of platinum content for both the protein-bound and unreacted samples was performed on a Varian ICP-OES.

### Cellular Growth Inhibition

The MTT assay was used to determine growth inhibition potency of platinum drugs before and after incubation with FBS.<sup>22</sup> A2780 cells were seeded in 96-well plates at 6,500 cells/well in 200 $\mu$ L RPMI 1640 media supplemented with 10% FBS and 1% Penicillin:Streptomycin and allowed to attach overnight. Media was removed and 200 $\mu$ L of each compound was added after serial dilution in quadruplicate wells and exposed to cells for 72h. For time dependent media incubation studies 500 $\mu$ M of each Pt compound was incubated in FBS (1:10 v/v) for 24hrs before cellular treatment. Samples were diluted to treatment concentrations with fresh media and exposed to cells for 72hrs. After 72hrs, drug solution was removed and plates were washed with PBS. 100 $\mu$ L of 5mg/mL MTT solution was added and solution was incubated with cells for 3h at 37°C. After incubation, MTT solution was removed and 100 $\mu$ L of DMSO was added. Quantification of cell growth in treated and control wells was then assessed by measurement of absorbance at 562nm. IC<sub>50</sub> values were determined graphically.

### Cellular Uptake of Drug Complexes

A2780 cells were plated in 10cm dishes at 2 million cells/dish and allowed to attach overnight. Cells were then treated with 10 $\mu$ M of each drug for 24hrs before and after serum incubation. After 24hrs, drug solution was removed and plates were washed 3x with PBS. Cells were then removed from the dish with trypsin and centrifuged for 5min at 1000xg. Media was removed, cell pellet was washed three times with PBS, cells were counted and resuspended in 250 $\mu$ L of ddH<sub>2</sub>O. Samples were digested following published methods.<sup>21</sup> Analysis of Pt content was performed on a Varian ICP-MS. Standards and blank were prepared similarly.

#### Quantification of DNA-Drug Adducts

A2780 cells were plated in 10cm dishes at 2 million cells/dish and allowed to attach overnight. Cells were then treated with 10 $\mu$ M of each drug for 24hrs before and after serum incubation. After 24hrs, drug solution was removed and plates were washed 3x with PBS. Cells were then removed from the dish with trypsin and centrifuged for 5min at 1000xg. Media was removed, cell pellet was washed three times with PBS and suspended in 250 $\mu$ L of ddH<sub>2</sub>O. DNA was extracted using a DNeasy blood and tissue kit (Qiagen) according to the manufacturer's protocol. Extent of DNA platination was measured on a Varian ICP-MS.

#### Acknowledgements

This work was supported by a grant NIH RO1CA78754 to NF.

### List of References

1. Aris, S.M., Gewirtz, D.A., Ryan, J.J., Knott, K.M. & Farrell, N.P. Promotion of DNA strand breaks, interstrand cross-links and apoptotic cell death in A2780 human ovarian cancer cells by transplatinum planar amine complexes. *Biochemical Pharmacology* **73**, 1749-1757 (2007).
2. Fojo, T., *et al.* Identification of non-cross-resistant platinum compounds with novel cytotoxicity profiles using the NCI anticancer drug screen and clustered image map visualizations. *Crit Rev Oncol Hematol* **53**, 25-34 (2005).
3. Kelland, L.R., *et al.* A Novel Trans-Platinum Coordination Complex Possessing in-Vitro and in-Vivo Antitumor-Activity. *Cancer Res* **54**, 5618-5622 (1994).
4. Rosenberg, B., Van Camp, L. & Krigas, T. Inhibition of Cell Division in *Escherichia coli* by Electrolysis Products from a Platinum Electrode. *Nature* **205**, 698-699 (1965).
5. Alderden, R.A., Hall, M.D. & Hambley, T.W. The Discovery and Development of Cisplatin. *Journal of Chemical Education* **83**, 728-null (2006).
6. Jamieson, E.R. & Lippard, S.J. Structure, Recognition, and Processing of Cisplatin–DNA Adducts. *Chemical Reviews* **99**, 2467-2498 (1999).
7. Wong, E. & Giandomenico, C.M. Current Status of Platinum-Based Antitumor Drugs. *Chemical Reviews* **99**, 2451-2466 (1999).
8. Safirstein, R., *et al.* Cisplatin Nephrotoxicity. *Am J Kidney Dis*, 356-367 (1986).
9. Brabec, V., Nepelchova, K., Kasparkova, J. & Farrell, N. Steric control of DNA interstrand cross-link sites of trans platinum complexes: specificity can be dictated by planar nonleaving groups. *J Biol Inorg Chem* **5**, 364-368 (2000).

10. Wang, D. & Lippard, S.J. Cellular processing of platinum anticancer drugs. *Nat Rev Drug Discov* **4**, 307-320 (2005).
11. Bulluss, G.H., *et al.* trans-Platinum Planar Amine Compounds with [N<sub>2</sub>O<sub>2</sub>] Ligand Donor Sets: Effects of Carboxylate Leaving Groups and Steric Hindrance on Chemical and Biological Properties. *Inorganic Chemistry* **45**, 5733-5735 (2006).
12. Ma, E.S., *et al.* Enhancement of aqueous solubility and stability employing a trans acetate axis in trans planar amine platinum compounds while maintaining the biological profile. *J Med Chem* **48**, 5651-5654 (2005).
13. Quiroga, A.G., Pérez, J.M., Alonso, C., Navarro-Ranninger, C. & Farrell, N. Novel Transplatinum(II) Complexes with [N<sub>2</sub>O<sub>2</sub>] Donor Sets. Cellular Pharmacology and Apoptosis Induction in Pam 212-ras Cells. *Journal of Medicinal Chemistry* **49**, 224-231 (2005).
14. Wang & Guo, Z. The role of sulfur in platinum anticancer chemotherapy. *Anticancer Agents Med Chem* **7**, 19-34 (2007).
15. Safirstein, R., *et al.* Cisplatin nephrotoxicity. *Am J Kidney Dis* **8**, 356-367 (1986).
16. Knox, R.J., Friedlos, F., Lydall, D.A. & Roberts, J.J. Mechanism of Cytotoxicity of Anticancer Platinum Drugs: Evidence That cis-Diamminedichloroplatinum(II) and cis-Diammine-(1,1-cyclobutanedicarboxylato)platinum(II) Differ Only in the Kinetics of Their Interaction with DNA. *Cancer Res* **46**, 1972-1979 (1986).
17. Natarajan, G., Malathi, R. & Holler, E. Increased DNA-binding activity of cis-1,1-cyclobutanedicarboxylatodiammineplatinum(II) (carboplatin) in the presence of

- nucleophiles and human breast cancer MCF-7 cell cytoplasmic extracts: activation theory revisited. *Biochemical Pharmacology* **58**, 1625-1629 (1999).
18. Berners-Price, S.J. & Kuchel, P.W. Reaction of cis- and trans-[PtCl<sub>2</sub>(NH<sub>3</sub>)<sub>2</sub>] with reduced glutathione inside human red blood cells, studied by <sup>1</sup>H and <sup>15</sup>N-{<sup>1</sup>H} DEPT NMR. *Journal of Inorganic Biochemistry* **38**, 327-345 (1990).
  19. Oehlsen, M.E., Qu, Y. & Farrell, N. Reaction of Polynuclear Platinum Antitumor Compounds with Reduced Glutathione Studied by Multinuclear (<sup>1</sup>H, <sup>1</sup>H-<sup>15</sup>N Gradient Heteronuclear Single-Quantum Coherence, and <sup>195</sup>Pt) NMR Spectroscopy. *Inorganic Chemistry* **42**, 5498-5506 (2003).
  20. Aris, S.M., Knott, K.M., Yang, X., Gewirtz, D.A. & Farrell, N.P. Modulation of transplannamine platinum complex reactivity by systematic modification of carrier and leaving groups. *Inorganica Chimica Acta* **362**, 929-934 (2009).
  21. Harris, A.L., *et al.* Synthesis, characterization, and cytotoxicity of a novel highly charged trinuclear platinum compound. Enhancement of cellular uptake with charge. *Inorganic Chemistry* **44**, 9598-9600 (2005).
  22. Cory, A.H., Owen, T.C., Barltrop, J.A. & Cory, J.G. USE OF AN AQUEOUS SOLUBLE TETRAZOLIUM FORMAZAN ASSAY FOR CELL-GROWTH ASSAYS IN CULTURE. *Cancer Communications* **3**, 207-212 (1991).

## Chapter 3: Pharmacokinetic Studies of Polynuclear Platinum Complexes with Plasma and Human Serum Albumin: Implications for Drug Design and Delivery

Brad T. Benedetti, and Nicholas P. Farrell\*

Department of Chemistry and Massey Cancer Center

Virginia Commonwealth University, Richmond, Virginia. USA

Portions published in Dalton Trans., 2007, 4938-4942

### Abstract

The interactions of various polynuclear platinum complexes with mouse plasma, human plasma, and human serum albumin were studied. Some of the compounds examined were the “non-covalent” analogs of the trinuclear BBR3464 as well as the dinuclear compounds differing in only the presence or absence of a central  $-\text{NH}_2^+$  (SET3007 and analogs). The rate and extent of platinum-protein adduct formation was monitored by ICP-OES and evidence for pre-association, presumably through electrostatic and hydrogen-bonding, was obtained by fluorescence spectroscopy and through the use of methionine and cysteine blocked human serum albumin. In the case of those compounds containing Pt-Cl bonds, further reaction took place presumably through displacement by sulfur nucleophiles, while the non-covalent derivatives showed an initial formation of a platinum-protein complex, but no change in complex formation over time. The implications for protein pre-association and plasma stability of polynuclear platinum compounds, both covalent and non-covalent are discussed.

## **Introduction**

There are four main factors which control the pharmacokinetics of compounds in biological systems. These factors include but are not limited to, absorption, distribution, metabolism, and elimination. These four criteria greatly affect the bioavailability and kinetics of drug exposure towards the biological system of interest. Absorption refers to the ability of a drug, following administration, to effectively reach the systemic circulation; either by passing through intestinal cell membranes in the case of orally administered compounds or other natural membranes such as the blood brain barrier.<sup>1</sup> Once in systemic circulation, the process of metabolism begins to decompose the compounds of interest into drug metabolites. If the metabolites of the compound are 'inert' after metabolism, a large portion of the pharmacological effect is thus diminished and the drug administered can no longer be distributed to the site of action. Metabolism can occur by reactions with liver redox enzymes such as cytochrome P450 and through interactions with proteins in the blood stream.<sup>2</sup> Prolonged elimination half-lives can result in reduced tolerability of the administered drug in patients, often warranting removal of compounds of interest from clinical trials. About  $\frac{3}{4}$  of drug candidates do not enter clinical trials due to pharmacokinetics problems in animals. Also, about 40% of molecules that fail in clinical trials do so because of pharmacokinetics problems.<sup>2</sup> Therefore, these points ultimately control the outcome of drugs introduced into the clinics.

One drug which encountered pharmacokinetic problems via metabolic interactions in the clinical setting is the anti-tumor agent BBR3464 (Figure 3.1).



BBR3464, a novel tri-platinum compound, has demonstrated promising activity in cisplatin-resistant, cisplatin-sensitive and p53 mutant tumors. BBR3464 is also forty to eighty fold more potent on a molar dose basis than its predecessor and most commonly used platinum anticancer agent cisplatin, *c*-DDP (Figure 3.1). Although providing promising pre-clinical and Phase I clinical studies, in Phase II studies BBR3464 showed higher plasma protein binding in human than mice and a more rapid degradation of BBR3464 into inactive metabolites. These pharmacokinetic factors, along with reduced activity in gastric and lung cell carcinomas, have discouraged the use of BBR3464 in the clinical setting.<sup>3-7</sup> Therefore, there is a need for the development of novel platinum compounds to circumvent these factors.

Synthesis, characterization, and biological evaluation of a large variety of novel polynuclear platinum anti-cancer drug candidates have taken place since the introduction of BBR3464 into the clinics in the late '90s.<sup>8-12</sup> Polynuclear platinum compounds which employ polyamine linkers of variable chain length represent a new class of anti-tumor agents showing activity profiles different from *c*-DDP.<sup>13-14</sup> These drugs use a 'covalent' mode of DNA binding, similar to *c*-DDP by displacement of the Pt-Cl bond and formation of a coordinate Pt-DNA adduct. Due to the ease of aquatability of the -Cl leaving group, subsequent Pt-protein bond formation is still a prevalent problem, thus diminishing the overall effect of platinum chemotherapeutic compounds. Replacement of the -Cl leaving groups with substitutionally 'inert' NH<sub>3</sub> ligands introduces an entirely novel class of 'non-covalent' polynuclear platinum compounds. (Figure 3.2 (AH44 and TriplatinNC)) The presence of hydrogen-bonding and electrostatic interactions contributes to the unique profile of this group of drugs.

The presence of a charge in the linker, either as the central tetra-amine unit of a trinuclear compound or through a polyamine linker in a dinuclear species, greatly enhances anti-tumor activity for this 'non-covalent' class.<sup>15</sup>

Although DNA is the core target for the vast majority of platinum anti-cancer compounds, the first step in probing the clinical effectiveness of these drugs is to fully understand the metabolic interactions that may occur with these compounds while traveling through the systemic circulation towards their desired site of action. From a solely chemical standpoint, these metals, following aquation, would be expected to act as soft Lewis acids and to form stable complexes with S or N donors found in proteins.<sup>16</sup> Thus, the rate of hydrolysis of the leaving ligand greatly affects the amount of protein binding. Albumin, the most abundant plasma protein and the most likely candidate for drug metabolic interactions, is a 585 amino acid, 66 kDa, single chain protein involved in transportation of numerous drugs and ligands.<sup>17-18</sup> HSA is largely  $\alpha$ -helical and contains 17 disulfide bridges and only one free cysteine, Cys34. This residue, along with Met298 is speculated as the primary binding sites of *c*-DDP.<sup>19</sup> It is mainly accepted, in the case of most Pt-compounds, that once coordinated to S or N donors in plasma proteins or other biomolecules, platinum compounds are effectively 'deactivated' and eliminated from the body; thus never reaching their desired site of action.<sup>20</sup> Severe nephrotoxicity has also been associated with interactions of platinum anti-tumor compounds with thiol groups of proteins.<sup>21-22</sup>

In an effort to improve the therapeutic efficiency, by minimizing interactions with plasma proteins, novel formulations of platinum compounds have been developed [46]. One pathway to minimize metabolic interactions can be through replacement of the

most commonly used  $-Cl$  leaving group with other, more stable ligands. Cell Therapeutics Inc. (CTI) is currently evaluating a derivative of the polynuclear platinum compound BBR3610 and has shown that replacement of the  $-Cl$  ligand with a carboxylate, such as butyrate or capronate, results in much lower plasma binding *in vitro*, while still retaining its cytotoxicity profile *in vivo*.<sup>23</sup> In this sense, it is possible to minimize the extent of protein binding by modifying the labile leaving group attached to the platinum moiety.

A study of the interactions of BBR3464 and other polynuclear platinum drugs (Figure 3.1, 3.2) with plasma proteins such as albumin has not been as thoroughly investigated as have the interactions with glutathione and other biomolecules. As one of the major contributors to Pt-S binding, albumin, and more specifically its interactions with platinum compounds must be investigated and the pharmacokinetics of these potential drug candidates' interactions understood. An understanding of the effects of ligand substitution rates and geometry contribution can also provide new tools to aid in drug discovery and development. The long term goal is therefore to evaluate, understand, and improve the pharmacokinetic profile of platinum chemotherapeutics in an attempt to prevent drug deactivation and diminish toxic side effects thus, facilitating the better development of platinum compounds for the treatment and prevention of cancer.

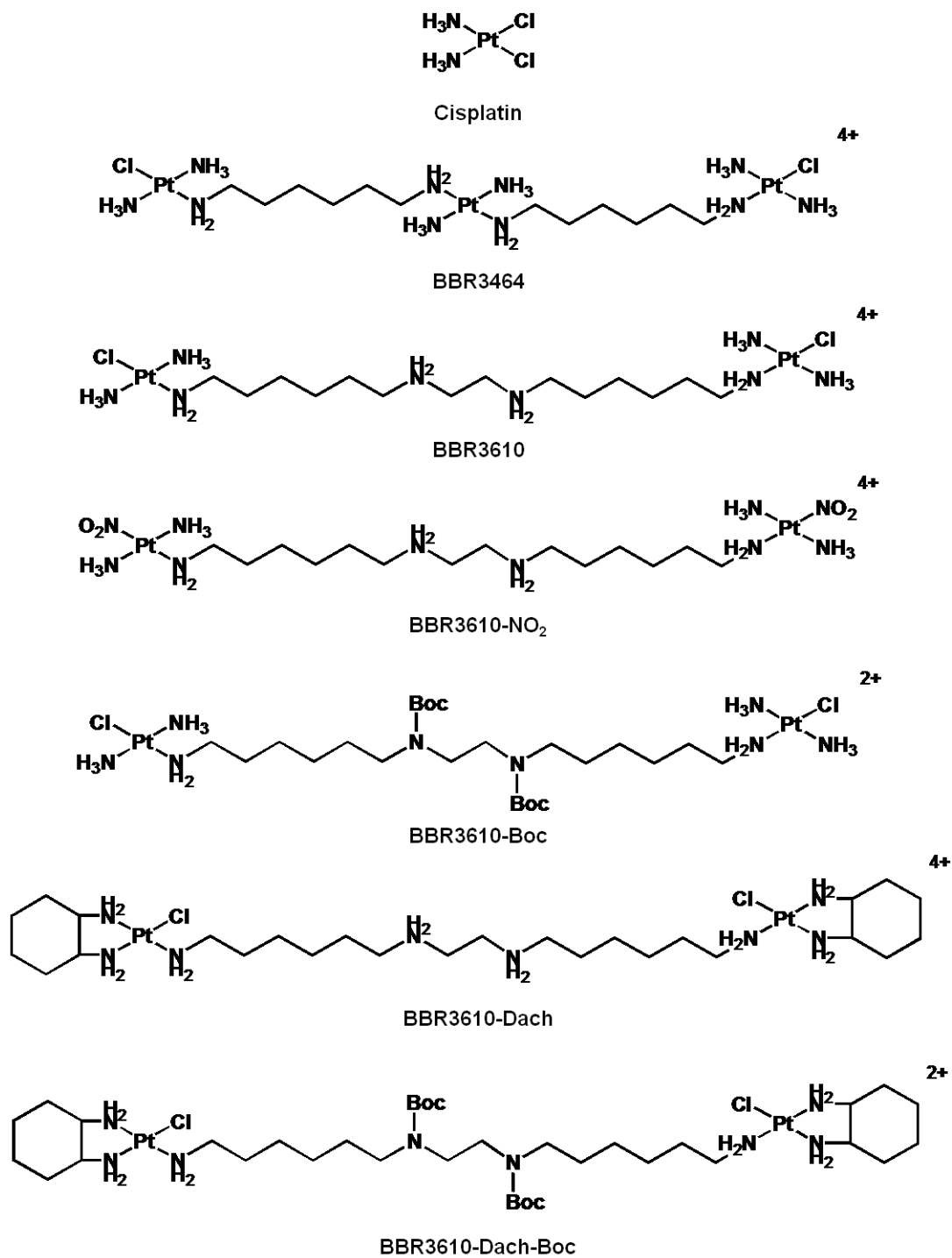


Figure 3.1 Chemical Structures of Cisplatin and Polynuclear Platinum Compounds.

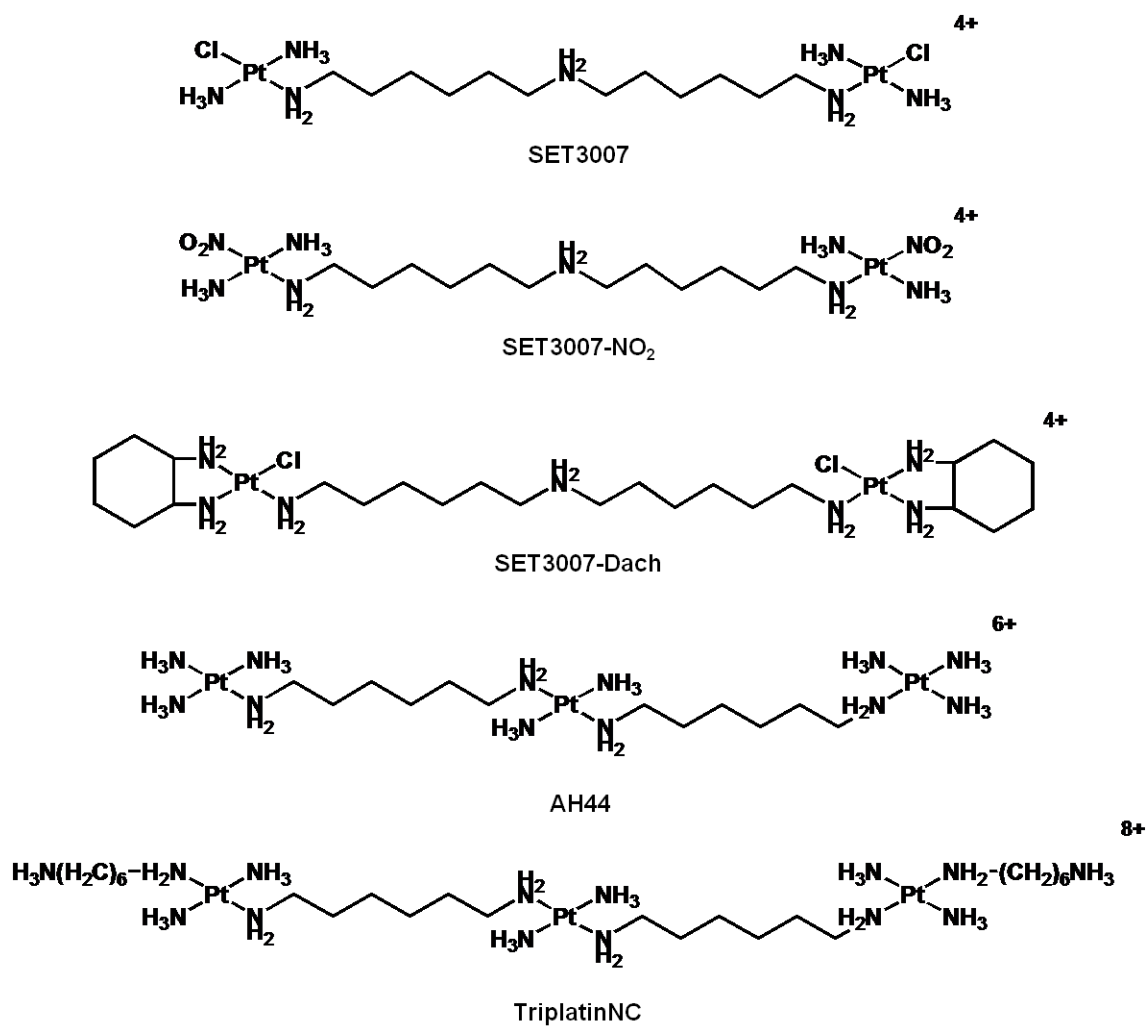
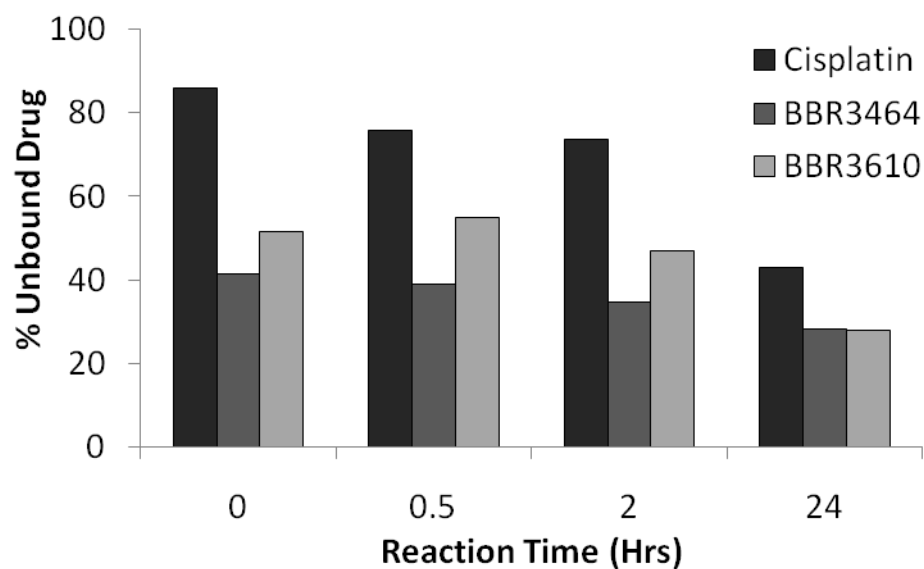


Figure 3.2 Chemical Structures of Selected Polynuclear Platinum Compounds.

## **Results and Discussion**

### **Mouse Plasma Binding with Selected -Cl Polynuclear Platinum Compounds**

Plasma is the liquid portion of blood, approximately 55% of the total volume, not including red or white blood cells, in which all plasma proteins are contained.<sup>20</sup> Among these proteins include fibrinogen, globulins, and human serum albumin (HSA). Due to the discrepancy found between levels of protein binding in mouse plasma and human plasma with BBR3464, it was necessary to first evaluate the binding of selected polynuclear platinum compounds with mouse plasma. Cisplatin, BBR3464 and BBR3610 were incubated with rehydrated mouse plasma for 0-24 hrs and the extent of platinum-protein binding was analyzed by ICP-OES. (Figure 3.3) Binding of Cisplatin, BBR3464 and BBR3610 to plasma proteins was found to increase with time, which can be expected as Pt-Cl bond dissociation occurs and Pt-protein bond formation increases. Percentages noted on all data represent the percentage of “free-drug” available, drug that has not been deactivated due to protein binding. It is worth observation that *c*-DDP shows a much higher free drug percentage at all time points than do BBR3464 and BBR3610. This interaction could be a result of the high charge associated with both BBR3610 and BBR3464. In the early time points, there is an immediate interaction with the protein, much faster than can be accounted for with only Pt-Cl bond displacement. This initial decrease in free drug availability is a combination of both electrostatic charge interactions and covalent Pt-protein bond formation. Due to this high charge, BR3464 shows much higher plasma binding over time than cisplatin.



**Figure 3.3** Effects of mouse plasma binding on drug availability. Cisplatin, BBR3464 and BBR3610 were incubated with mouse plasma for selected time points and platinum content for protein bound and free drug was analyzed by ICP-OES.

### Human Plasma Binding with Selected Polynuclear Platinum Compounds (PPC's)

Further evaluation of a larger group of PPC's was continued by investigating the binding between PPC's and human plasma. Compounds included in this study provided for the analysis of differences in charge and leaving group lability on Pt-protein binding. Cisplatin and BBR3464 were first analyzed to confirm the discrepancy found between binding in mouse plasma and human plasma with BBR3464 in the clinics. At the 0.5hr time point, in mouse plasma and human plasma, the percentage of unbound *c*-DDP was approximately 70%-80%, while the percentage of unbound BBR3464 was 35% in mouse plasma but only 15% in human plasma. Similar observations can be made at subsequent time points. (Figure 3.4) BBR3610 shows a slower rate of protein binding as compared to BBR3464, but after 24hrs the overall amount of free drug available is still less than 10%. Figure 3.5 shows the effects of addition of -Boc and -Dach groups, used to decrease overall charge and mimic oxaliplatin structure respectively, on the rate of drug-protein binding. By adding the -Dach chelate in place of the bis ammonia carrier ligands, the position of the chloride is thus shifted to the -cis position. Although in the -cis position, the amount of protein binding is ultimately unchanged as compared to the parent BBR3610 complex. This trend is also seen with the addition of -Boc alone, and in combination with -Dach (BBR3610-Dach-Boc) Both of these drug derivatives show similar levels of protein binding as BBR3610. Also shown in Figure 3.5 is the effect of ligand substitution of protein binding. Due to decreased hydrolysis rates caused by substitution of -Cl for -NO<sub>2</sub>, protein binding in BBR3610-NO<sub>2</sub> is significantly lower than in the case of BBR3610 at similar time points. Free drug percentage in the case of BBR3610-NO<sub>2</sub>, approximately 30% after 24hrs, shows a significant improvement over



BBR3464, BBR3610 and also cisplatin. Although substitution of  $-Cl$  for  $-NO_2$  has proven to be not clinically relevant, the concept of ligand substitution based on decreasing hydrolysis rates has shown that a decrease in metabolic activity is accessible through ligand substitution. These results were also observed with the SET3007 series. (Figure 3.6) Therefore the driving force behind the extent and rate of drug protein interactions are a direct result of the stability of the leaving group. This result gives support to further investigate the effect of leaving group ligands on the binding on PPC's to plasma proteins.

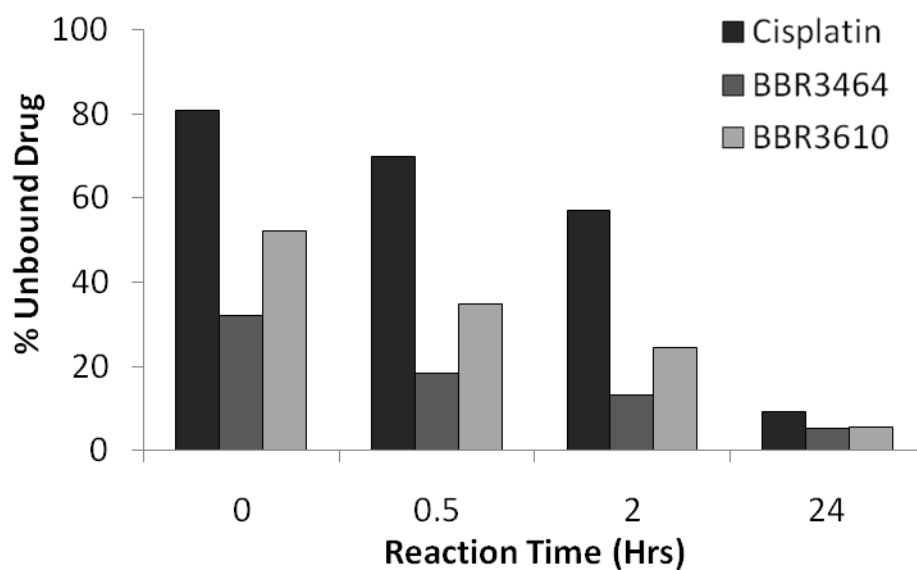


**Figure 3.4** Effects of human plasma binding on drug availability. Cisplatin, BBR3464 and BBR3610 were incubated with human plasma for selected time points and platinum content for protein bound and free drug was analyzed by ICP-OES.

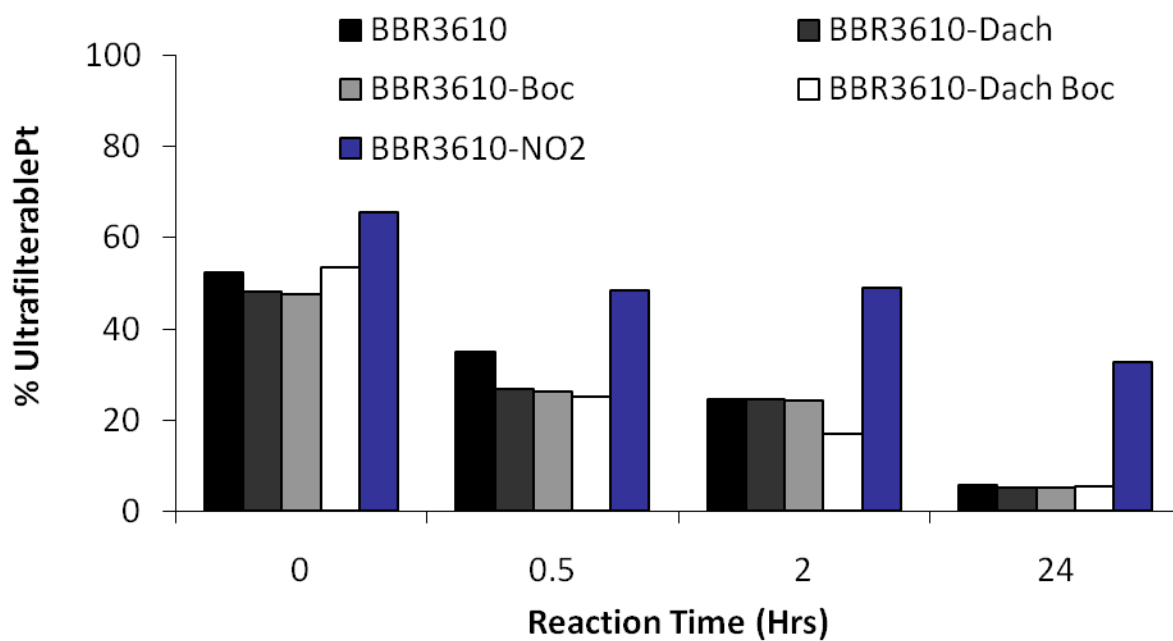


**Figure 3.5** Human Plasma Binding with BBR3610 and derivatives. Compounds were incubated with human plasma for selected time points and platinum content for protein bound and free drug was analyzed by ICP-OES.

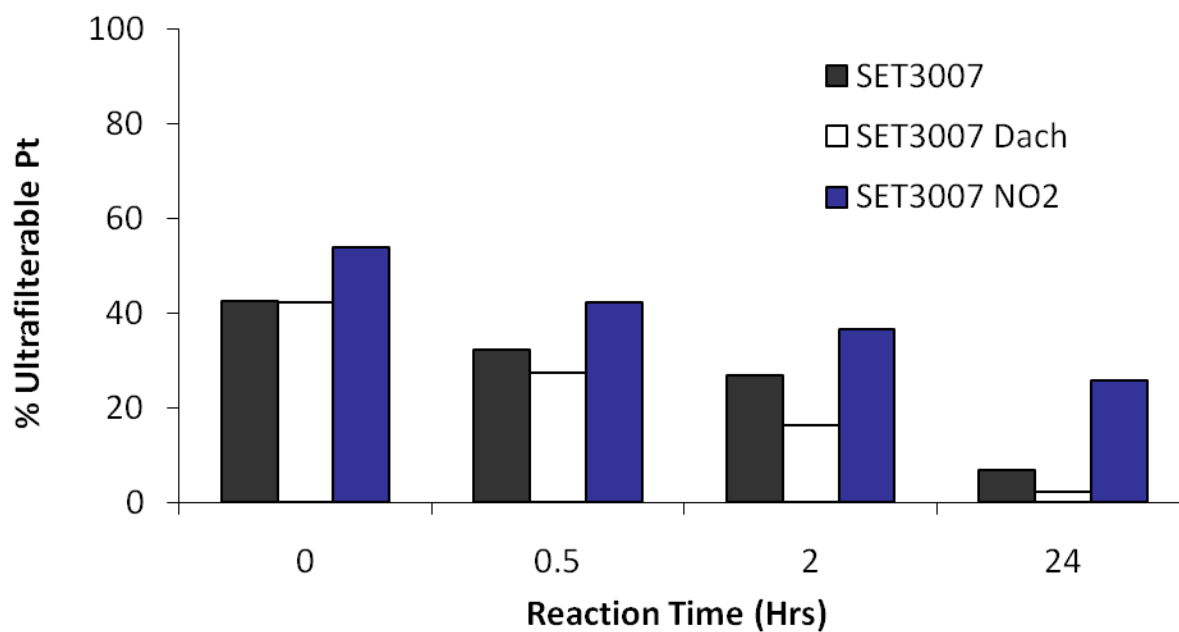


**Figure 3.6** Human Plasma Binding with SET3007 and derivatives. Compounds were incubated with human plasma for selected time points and platinum content for protein bound and free drug was analyzed by ICP-OES.

### Significance of Electrostatic Interactions on Human Serum Albumin Binding

The role of pre-association in dictating the final products of reactions of PPCs with biomolecules has been assisted greatly in the trinuclear case by the synthesis and evaluation of “non-covalent” analogs where the Pt–Cl bonds are displaced by a substitution-inert  $\text{NH}_3$  or a “dangling” amine  $\text{H}_2\text{N}(\text{CH}_2)_6\text{NH}_3^+$ . In order to better investigate these types of interactions, human serum albumin (HSA) was selected as the protein of interest. Human serum albumin is a versatile transport protein and receptor for a variety of ligands and drugs. The primary function of HSA is the transport of fatty acids but since it carries a negative 17 charge, it is also responsible for shuttling a wide variety of metal ions, steroids, and a variety of pharmaceuticals.<sup>24-25</sup> HSA constitutes roughly 60% of the mass of plasma proteins with a concentration of  $\sim 40$  mg/mL. It is highly likely therefore that HSA binding could contribute to these metabolic deactivation reactions, as suggested also for some similar dinuclear complexes.<sup>10</sup> To evaluate and quantitate the binding of PPC's to HSA, BBR3464, BBR3610, Cisplatin, AH44 and TriplatinNC were incubated and the ultrafilterable protein unbound fraction was quantified for selected time points. (Figure 3.7) Analysis by ICP-OES shows a decrease in Pt content immediately upon mixing,  $t = 0$ , for all compounds, excluding cisplatin. This initial decrease in Pt content represents the non-covalent, “pre-association” of the Pt complex with protein. The Pt content corresponding to compounds containing a Pt-Cl bond decreases with time, representing a displacement of the Pt–Cl bond and a formation of the coordinate/covalently bound Pt–protein species (where covalent is used to indicate Pt–amino acid residue formation independent of strict contributions of covalent or coordinate bonding). In contrast, ICP-OES analysis of AH44

and TriplatinNC shows a constant Pt concentration from  $t = 0$  through  $t = 24$  h. Due to the presence of the substitution-inert  $-\text{NH}_3$  group, the initial pre-association is not followed by a covalent Pt-protein interaction. The results for AH44 and TriplatinNC suggest that these non-covalent compounds may “by-pass” the deactivation associated with Pt-S bond formation.

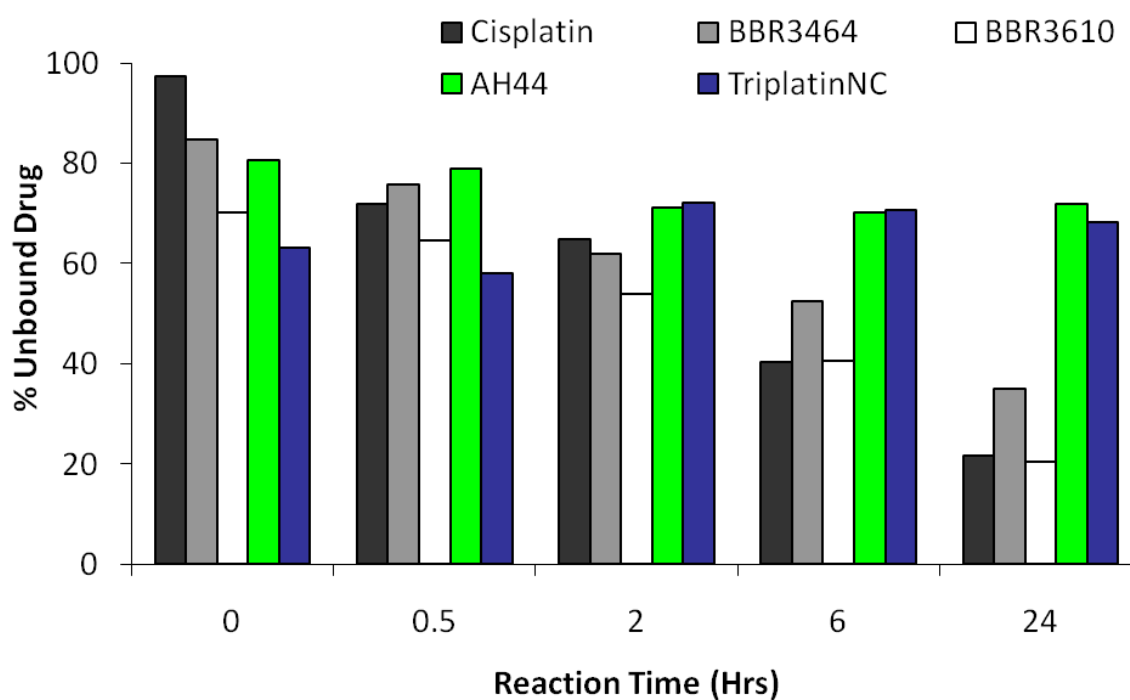


**Figure 3.7** "Pre-Association" Effects and Significance of Electrostatic Interactions on Human Serum Albumin Binding: Compounds were incubated with human serum albumin for selected time points and platinum content for protein bound and free drug was analyzed by ICP-OES.

## HSA Protein Modification and Binding Site Evaluation

Previous studies on the identification of the cisplatin binding site on HSA have been shown to be a combination of both free sulfur containing amino acids, Cys-34 and Met-298.<sup>19,26-27</sup> Although HSA contains 35 cysteine amino acids, 34 are involved in disulfide bridges and only one free cysteine remains. As seen in the Figure 3.8, both Met-298 and Cys-34 are located on the solvent accessible surface of HSA and are valid candidates for the binding of platinum chemotherapeutics. In the case of BBR3464, the addition of a high charge component could cause the drug to specifically or preferentially bind to one amino acid or another. Therefore, in this regard, we examined the role of amino acid blocking and its effect on the binding of BBR3464 to native and modified HSA. BBR3464 was incubated with Cysteine and Methionine blocked HSA and the reaction was monitored by ICP-OES.(Figure 3.9) Cysteine blocked HSA shows equal amounts of free drug after each time point as the native HSA protein. This suggests that Cysteine binding does not play a major role in the binding of BBR3464 to HSA. On the other hand, after the blocking of Methionine residues, Pt-protein bond formation is effectively eliminated. This suggests that Met residues on HSA are the major contributor of Pt deactivation for BBR3464. Also, it is important to note that even after blocking methionine residues on HSA, approximately 20% of administered BBR3464 interacts with the protein. This effect is the pre-association of the positively charged drug, presumably, with negative regions of HSA.



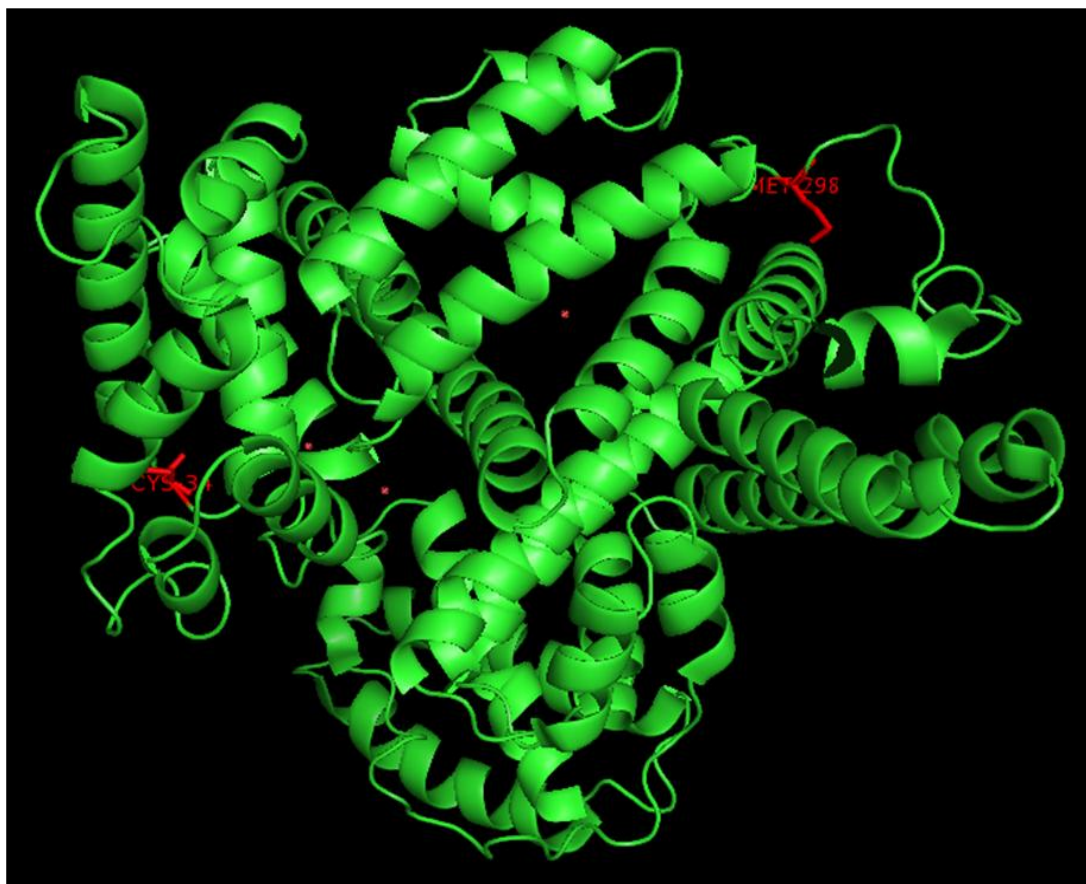


**Figure 3.8** Crystal structure of human serum albumin with Met-298 and Cys-34 highlighted in red. Figure adapted from PDB ID: 1BM0

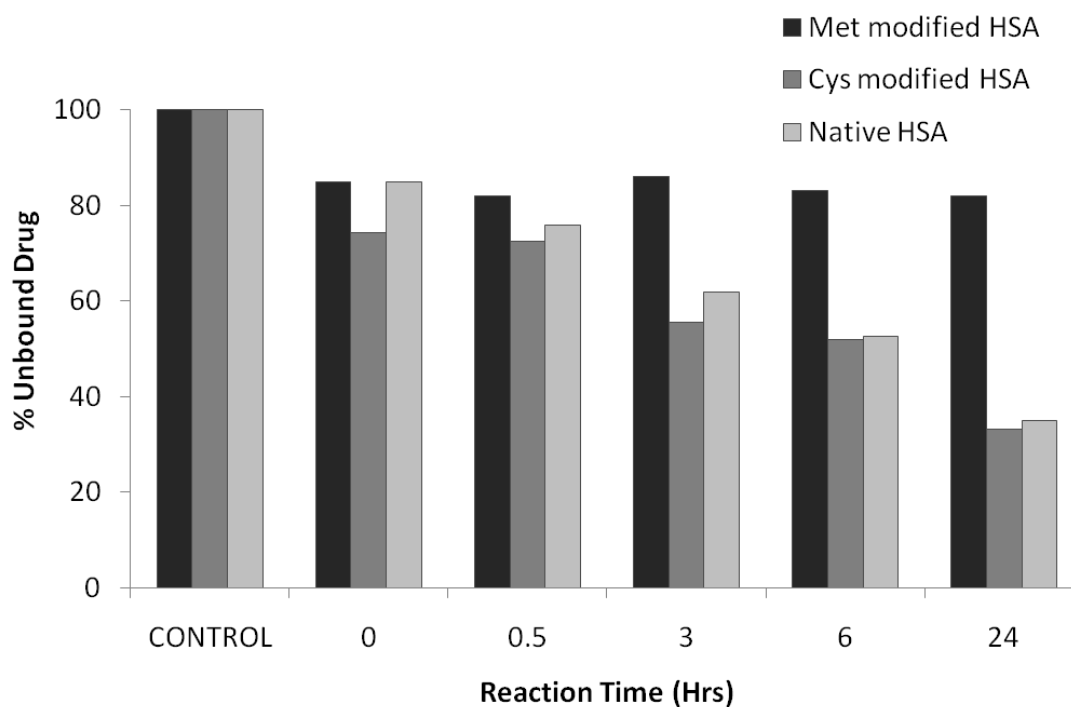


**Figure 3.9** Effects of cysteine and methionine peptide blocking on BBR3464-HSA binding. Compounds were incubated with human serum albumin for selected time points and platinum content for protein bound and free drug was analyzed by ICP-OES.

### Effects of Charge on HSA Global Conformation

As seen in Figure 3.10, the charge density map of HSA shows multiple regions of negative charge, shown in red, where the cationic platinum compounds could first interact and subsequently bind to S-containing amino acids. To understand and examine these changes, fluorescence spectroscopy was utilized. The fluorescence from excitation of HSA at 298nm reflects changes in the microenvironment of the tryptophan 214 residue, serving as a tool to obtain information about conformational changes of the protein.<sup>28</sup> A decrease in fluorescence of the lone tryptophan of HSA is interpreted as a conformational change making the amino acid more accessible to water quenching. The covalent binding and cationic BBR3464, was used to investigate these interactions. Upon incubation with BBR3464, HSA fluorescence was shown to decrease over time with an approximate 16% decrease in overall fluorescence after 72hrs. (Figure 3.11A) The same trend in fluorescence decrease of HSA is also seen in the chemically modified HSA series. Figure 3.11B shows the influence of the charged portion of drug binding on the overall conformation of the methionine blocked protein; with a decrease in fluorescence of approximately 17%. The interaction of BBR3464 with methionine blocked HSA is nearly identical as seen in native HSA, which shows a fluorescence decrease of 16%. Although not covalently bound to methionine blocked HSA, the charge portion of BBR3464 associates with the surface of the protein, causing perturbations in the global HSA structure. The same trend is seen with the interactions of BBR3464 and cysteine blocked HSA, with an overall fluorescence decrease of 14%. (Figure 3.11C) Therefore the decrease in fluorescence represents global changes in the structure of HSA upon BBR3464 electrostatically binding to the surface of albumin.

To this extent, fluorescence spectroscopy provides a means to analyze the effect of charge on the binding between HSA and PPC's, independent on the covalent or non-covalent nature of the final platinum-protein adduct.

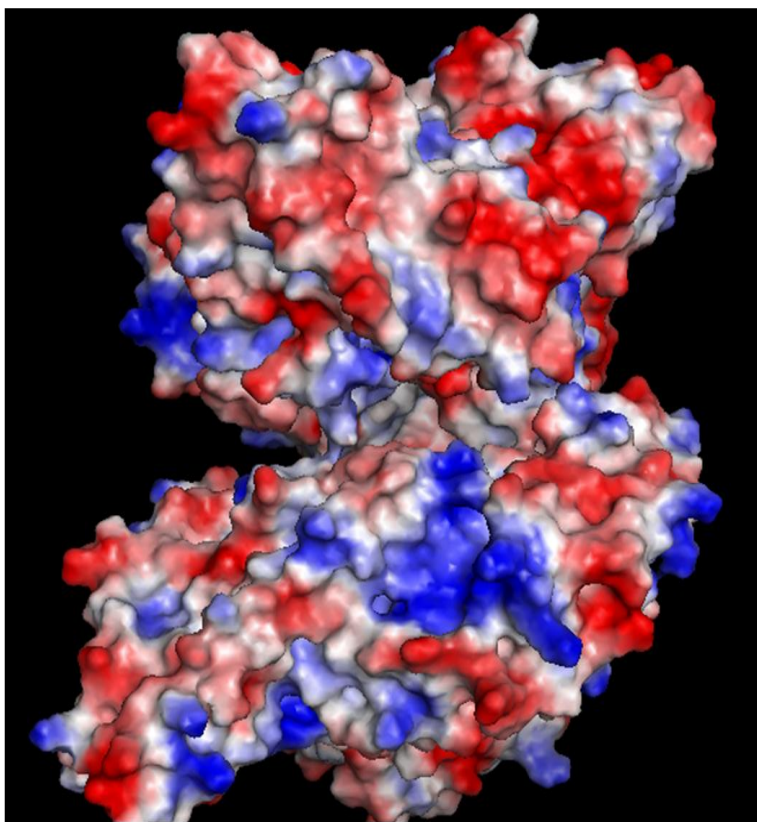


**Figure 3.10** Charge density structure of human serum albumin with positive regions shown in blue and negative regions shown in red. Figure adapted from PDB ID: 1BM0

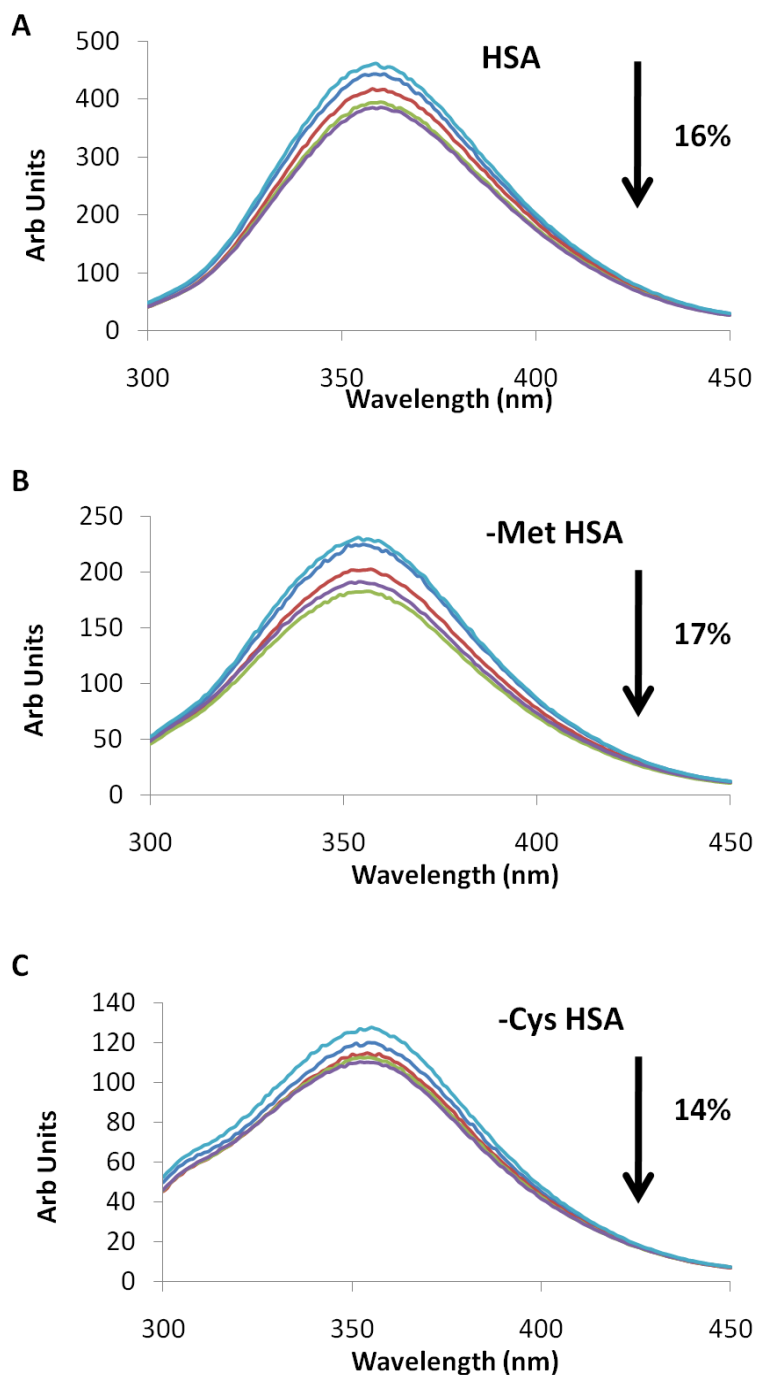


**Figure 3.11** Electrostatic Effects on HSA Global Structure. BBR3464 was incubated with HSA, methionine blocked HSA, and cysteine blocked HSA for 0, 24, 48, and 72hrs. Top spectrum represents protein before addition of BBR3464. Bottom spectrum represents complex formed after 72hr reaction.

## **Conclusion**

In this contribution we examine the reactions of polynuclear platinum compounds with plasma and human serum albumin (HSA). We show for the first time the presence of a pre-associated or “noncovalent” interaction of a platinum drug on the protein, as well as a method to possibly reduce drug protein interactions by ligand substitution. These studies suggest that the non-covalent compounds, AH44 and TriplatinNC may “by-pass” the deactivation associated with Pt–S bond formation. This is especially important for TriplatinNC as this 8+ compound is taken up into cells in a significantly greater concentration than either BBR3464 or AH44, and as a result has demonstrated *in vitro* cytotoxicity equivalent to cisplatin. The “non-covalent” compounds have shown a new mode of DNA binding distinct from intercalation and minor-groove binding. As these reactions with plasma, and especially with HSA, are generally considered responsible for the metabolic deactivation of platinum-based drugs, understanding the biophysical aspects of such interactions may allow for strategies to manipulate their extent with consequent effects on cellular uptake and even therapeutic index.

## **Materials and Methods**

### **Materials**

All platinum compounds were synthesized according to methods reported previously.

<sup>11,29-30</sup> Human plasma was purchased from Innovative Research Inc. Dehydrated citrated mouse plasma and Albumin from human serum, minimum 99%, N-ethylmaleimide, and Iodomethane, were obtained from Sigma-Aldrich (St. Louis, MO).

### Mouse Plasma Binding

Dehydrated citrated mouse plasma was purchased from Sigma Aldrich and reconstituted in accordance with the manufacturer's directions. Complex solutions were prepared in sterilized water and added to mouse plasma such that the final concentration of complex was 0.9 mM. The mixtures were reacted at 37 °C for 0, 0.5, 2 and 24 hours in the dark, then centrifuged through a Microcon YM-10 10,000 kDa membrane filter at 14000 g for 10 min to isolate the ultrafiltrate. The centrifuge cup was upturned in a second eppendorf and then centrifuged at 1000 g for 3 min to isolate the protein-bound fraction. The samples were stored at -20 °C prior to digestion. Analysis was performed on a Varian ICP-OES.

### Human Plasma Binding

Solutions of each drug were prepared in PBS and added to human plasma such that the final concentration of complex was 0.9mM (1:1 v/v). The reactions were incubated at 37 °C for 0, 0.5, 2 and 24 hours. Unreacted drug was removed by centrifugation through a Millipore Microcon YM-10 (10,000 kDa) membrane filter at 14,000xg for 30 min. The centrifuge cup was upturned in a second eppendorf and centrifuged at 1000xg for 3 min to isolate the protein-bound drug. Both ultrafiltrate and protein samples were stored at -20°C immediately following centrifugation. The digestion procedure followed published methods.<sup>29</sup> Analysis of platinum content for both the protein-bound and unreacted samples was performed on a Varian ICP-OES. Protein concentration was determined by the Bradford method with human serum albumin as the standard.<sup>31</sup>



### Human Serum Albumin Protocol

1.8mM solutions of each complex were prepared in phosphate buffer and added to 0.6 mM HSA such that the final concentration of complex was 0.9 mM. (3:1; complex:HSA) The mixture was reacted at 37 °C and 100 $\mu$ L aliquots were removed at t=0, 0.5, 2, 6, and 24 hours. Aliquots were then centrifuged through a Microcon YM-10 10,000 kDa membrane filter as described above.

### HSA Protein Modification and Binding Site Evaluation

Cys-34-blocked HSA was prepared by incubation of albumin solution in 100 mM ammonium bicarbonate, pH 7.9, with 2 mol eq of N-ethylmaleimide for 24 h at ambient temperature in the absence of light. Methionine residues were methylated by reaction with iodomethane. Iodomethane in 500-fold molar excess was added to an HSA solution in 0.1 M citric acid-phosphate buffer, pH 4.0. The solutions were stirred at ambient temperature for 24 h in the dark. Blocking reagents were removed by centrifugation through a 10,000MW membrane filter. Concentrated protein sample was then redissolved in ddH<sub>2</sub>O and lyophilized.

### Fluorescence Binding Studies with Chemically Modified HSA

Fluorescence Binding Studies were performed on Native HSA, Cys-Modified HSA, and Met-Modified HSA in an attempt to determine the influence of amino acid availability on BBR3464 binding. Fluorescence measurements were conducted on a Cary Eclipse Fluorimeter with the excitation and emission wavelengths set at 279 and 310 nm, respectively, with a scan rate 120 of nm min<sup>-1</sup>. The reactions of platinum compounds

were studied at 10:1 (Pt:HSA). An initial concentration for a 10:1 reaction was prepared for each drug. Separate measurements were taken at  $t = 0$  and appropriate time intervals.

### Fluorescence Spectroscopy

Fluorescence measurements were conducted on a Cary Eclipse Fluorimeter with the excitation and emission wavelengths set at 280 and 320 nm, respectively, with a scan rate of 120 nm/min. The reaction of TriplatinNC was studied at reactant ratio of 1:1 (Drug:HSA). Each sample was allowed to react for the stated time at 37°C before the measurement was taken. Separate measurements were taken at  $t = 0$  and appropriate time intervals.

### List of References

1. Castillo-Garit, J.A., Marrero-Ponce, Y., Torrens, F. & García-Domenech, R. Estimation of ADME properties in drug discovery: Predicting Caco-2 cell permeability using atom-based stochastic and non-stochastic linear indices. *Journal of Pharmaceutical Sciences* **97**, 1946-1976 (2008).
2. Silverman, R. *The Organic Chemistry of Drug Design and Drug Action*, (Elsevier Acad. Press, Oxford, 2004).
3. Hensing, T.A., *et al.* Phase II study of BBR 3464 as treatment in patients with sensitive or refractory small cell lung cancer. *Anti-Cancer Drug* **17**, 697-704 (2006).
4. Jodrell, D.I., *et al.* Phase II studies of BBR3464, a novel tri-nuclear platinum complex, in patients with gastric or gastro-oesophageal adenocarcinoma. *Eur J Cancer* **40**, 1872-1877 (2004).
5. Perego, P., *et al.* A novel trinuclear platinum complex overcomes cisplatin resistance in an osteosarcoma cell system. *Mol Pharmacol* **55**, 528-534 (1999).
6. Pratesi, G., *et al.* A novel charged trinuclear platinum complex effective against cisplatin-resistant tumours: hypersensitivity of p53-mutant human tumour xenografts. *Br J Cancer* **80**, 1912-1919 (1999).
7. Sessa, C., *et al.* Clinical and pharmacological phase I study with accelerated titration design of a daily times five schedule of BBR3464, a novel cationic triplatinum complex. *Ann Oncol* **11**, 977-983 (2000).

8. Harris, A.L., *et al.* Synthesis, characterization, and cytotoxicity of a novel highly charged trinuclear platinum compound. Enhancement of cellular uptake with charge. *Inorg Chem* **44**, 9598-9600 (2005).
9. Hegmans, A., *et al.* Amide-based prodrugs of spermidine-bridged dinuclear platinum. Synthesis, DNA binding, and biological activity. *J Med Chem* **51**, 2254-2260 (2008).
10. Kapp, T., Dullin, A. & Gust, R. Mono- and Polynuclear [Alkylamine]platinum(II) Complexes of [1,2-Bis(4-fluorophenyl)ethylenediamine]platinum(II): Synthesis and Investigations on Cytotoxicity, Cellular Distribution, and DNA and Protein Binding. *Journal of Medicinal Chemistry* **49**, 1182-1190 (2006).
11. Qu, Y., *et al.* Synthesis and DNA conformational changes of non-covalent polynuclear platinum complexes. *J Inorg Biochem* **98**, 1591-1598 (2004).
12. Williams, J.W., Qu, Y., Bulluss, G.H., Alvorado, E. & Farrell, N.P. Dinuclear Platinum Complexes with Biological Relevance Based on the 1,2-Diaminocyclohexane Carrier Ligand. *Inorg Chem* **46**, 5820-5822 (2007).
13. Billecke, C., *et al.* Polynuclear platinum anticancer drugs are more potent than cisplatin and induce cell cycle arrest in glioma. *Neuro-Oncology* **8**, 215-226 (2006).
14. Mitchell, C., *et al.* Low-Dose BBR3610 Toxicity in Colon Cancer Cells Is p53-Independent and Enhanced by Inhibition of Epidermal Growth Factor Receptor (ERBB1)-Phosphatidyl Inositol 3 Kinase Signaling. *Mol Pharmacol* **72**, 704-714 (2007).

15. Rauter, H., *et al.* Selective Platination of Biologically Relevant Polyamines. Linear Coordinating Spermidine and Spermine as Amplifying Linkers in Dinuclear Platinum Complexes. *Inorg Chem* **36**, 3919-3927 (1997).
16. Esposito, B.P. & Najjar, R. Interactions of antitumoral platinum-group metallodrugs with albumin. *Coordin Chem Rev* **232**, 137-149 (2002).
17. Carter, D.C. & Ho, J.X. Structure of Serum-Albumin. *Adv Protein Chem* **45**, 153-203 (1994).
18. Peters, T. Serum-Albumin. *Adv Protein Chem* **37**, 161-245 (1985).
19. Ivanov, A.I., *et al.* Cisplatin binding sites on human albumin. *J Biol Chem* **273**, 14721-14730 (1998).
20. Wang & Guo, Z. The role of sulfur in platinum anticancer chemotherapy. *Anticancer Agents Med Chem* **7**, 19-34 (2007).
21. Borch, R.F., Katz, J.C., Lieder, P.H. & Pleasants, M.E. Effect of diethyldithiocarbamate rescue on tumor response to cis-platinum in a rat model. *Proc Natl Acad Sci U S A* **77**, 5441-5444 (1980).
22. Borch, R.F. & Pleasants, M.E. Inhibition of cis-platinum nephrotoxicity by diethyldithiocarbamate rescue in a rat model. *Proc Natl Acad Sci U S A* **76**, 6611-6614 (1979).
23. Gatti, L., *et al.* Novel Bis-platinum Complexes Endowed with an Improved Pharmacological Profile. *Molecular Pharmaceutics* **7**, 207-216 (2009).
24. Curry, S., Mandelkow, H., Brick, P. & Franks, N. Crystal structure of human serum albumin complexed with fatty acid reveals an asymmetric distribution of binding sites. *Nat Struct Biol* **5**, 827-835 (1998).

25. Petitpas, I., Grune, T., Bhattacharya, A.A. & Curry, S. Crystal structures of human serum albumin complexed with monounsaturated and polyunsaturated fatty acids. *J Mol Biol* **314**, 955-960 (2001).
26. Gonias, S.L. & Pizzo, S.V. Complexes of serum albumin and cis-dichlorodiammineplatinum (II). The role of cysteine 34 as a nucleophilic entering group and evidence for reaction between bound platinum and a second macromolecule. *J Biol Chem* **258**, 5764-5769 (1983).
27. Pizzo, S.V., Swaim, M.W., Roche, P.A. & Gonias, S.L. Selectivity and stereospecificity of the reactions of dichlorodiammineplatinum(II) with three purified plasma proteins. *J Inorg Biochem* **33**, 67-76 (1988).
28. Timerbaev, A.R., Hartinger, C.G., Aleksenko, S.S. & Keppler, B.K. Interactions of Antitumor Metallodrugs with Serum Proteins: Advances in Characterization Using Modern Analytical Methodology. *Chemical Reviews* **106**, 2224-2248 (2006).
29. Harris, A.L., *et al.* Synthesis, Characterization, and Cytotoxicity of a Novel Highly Charged Trinuclear Platinum Compound. Enhancement of Cellular Uptake with Charge. *Inorganic Chemistry* **44**, 9598-9600 (2005).
30. Kauffman, G. & Cowan, D. cis- AND trans-DICHLORODIAMMINE-PLATINUM (II). in *Inorganic Syntheses*, Vol. 7 (ed. Kleinberg, J.) 236-238 (Jacob Kleinberg, 1963).
31. Bradford, M.M. A rapid and sensitive method for the quantitation of microgram quantities of protein utilizing the principle of protein-dye binding. *Analytical Biochemistry* **72**, 248-254 (1976).

## Chapter 4: Effects of non-covalent platinum drug-protein interactions on drug efficacy: Use of fluorescent conjugates as probes for drug metabolism

Brad T. Benedetti<sup>1,2</sup>, Erica J. Peterson<sup>2</sup>, Peyman Kabolizadeh<sup>1,2</sup>, Alberto Martinez<sup>1</sup>,

Ralph Kipping<sup>1</sup> and Nicholas P. Farrell<sup>1,2\*</sup>

Department of Chemistry<sup>1</sup> and Massey Cancer Center<sup>2</sup>

Virginia Commonwealth University, Richmond, Virginia. USA

Submitted to Molecular Pharmaceutics, 2011

BSO Experimentation performed by Peyman Kabolizadeh

### **Abstract**

Although the cytotoxic effects of clinical platinum based chemotherapeutics result mainly from damaging drug-DNA adducts, the overall efficacy of these drugs is limited by metabolic deactivation through covalent drug-protein binding. In this study the effects of glutathione, human serum albumin (HSA) and whole serum binding with cisplatin, BBR3464, and TriplatinNC, a “noncovalent” derivative of BBR3464 were investigated. Specifically, we ask whether these interactions can influence the efficacy of TriplatinNC, including cytotoxicity, levels of cellular accumulation, DNA adduct formation, and intracellular distribution. After 48 hours of treatment with buthionine sulphoximine (BSO), the cellular glutathione level was reduced and cisplatin and BBR3464-induced apoptosis was augmented. In contrast, TriplatinNC-induced cytotoxicity was unaltered by inhibiting glutathione synthesis. Treatment of A2780 ovarian carcinoma cells with

HSA bound cisplatin (cisplatin/HSA) and cisplatin pre-incubated with whole serum show dramatic decreases in cytotoxicity, cellular accumulation, and DNA adduct formation compared to treatment with cisplatin alone. Treatment with HSA bound BBR3464 (BBR3464/HSA) and BBR3464 pre-treated with whole serum also show a drastically reduced cytotoxic profile, and significantly less DNA platination. In contrast, TriplatinNC, the HSA bound derivative (TriplatinNC/HSA), and TriplatinNC pre-treated with whole serum retained identical cytotoxic profiles and equal levels of cellular accumulation at all time points. Confocal microscopy of TriplatinNC-NBD, a fluorescent derivative of TriplatinNC, and TriplatinNC-NBD/HSA both show nuclear/nucleolar localization patterns, distinctly different from the lysosomal localization pattern seen with HSA. Cisplatin-NBD, a fluorescent derivative of cisplatin, was shown to accumulate in the nucleus and throughout the cytoplasm while the localization of Cisplatin-NBD/HSA was limited to lysosomal regions of the cytoplasm. The results suggest that TriplatinNC can avoid high levels of metabolic deactivation currently seen with clinical platinum chemotherapeutics, and therefore retain a unique cytotoxic profile after cellular administration.

## **Introduction**

Platinum drugs are among the most commonly used chemotherapeutics for the treatment of testicular, head and neck, ovarian, small cell lung, and colorectal carcinomas<sup>1-3</sup>. The cytotoxicity of cisplatin is accepted to result mainly from the formation of bifunctional DNA crosslinks resulting in the inhibition of DNA synthesis and replication.<sup>4</sup> The DNA-reactive platinum species are considered to be monoquo and



diaquo complexes – in general  $[\text{Pt}(\text{amine})_2(\text{H}_2\text{O})_2]^{2+}$  or  $[\text{Pt}(\text{amine})_2(\text{Cl})(\text{H}_2\text{O})]^+$  - produced upon hydrolysis of the administered drugs, and the chemistry of these species has been well examined.<sup>5</sup> While this concept has been useful in rationalizing some structure-activity relationships, there is increasing understanding that even anions with nominally weak affinity for platinum –  $\text{CO}_3^{2-}$ <sup>6-7</sup>;  $\text{SO}_4^{2-}$ <sup>8</sup>;  $\text{PO}_4^{3-}$  and even  $\text{RCOO}^-$ <sup>9</sup> - become physiologically relevant ligands because of their high concentrations in plasma and cells. Similarly, cellular accumulation of platinum drugs is multifactorial with evidence for both passive and active transporter-mediated processes.<sup>10</sup>

The three major pharmacological factors affecting the clinical success of any type of platinum-based cancer therapy are cellular uptake, the frequency and the type of DNA adducts formed and metabolic deactivation. Metabolic deactivation is also mediated through interactions of the small molecules with biomolecules, specifically sulfur-containing amino acids in proteins, and these interactions may contribute to the toxic side effects associated with platinum based treatments.<sup>11-12</sup> One of the most plausible extracellular non-DNA targets for platinum compounds is blood serum. Serum is the liquid portion of blood, approximately 55% of the total volume, excluding red and white blood cells, containing all plasma proteins at a concentration of 70 g/L.<sup>13</sup> These proteins include fibrinogen, globulins, and human serum albumin (HSA). Albumin, the most abundant serum protein at 30-50g/L and the most likely protein candidate for drug metabolic interactions, is a 585 amino acid, 66 kDa, single chain protein involved in transportation of numerous drugs and ligands<sup>14-15</sup>. It is mainly accepted that once coordinated to plasma proteins, platinum compounds are effectively 'deactivated' and eliminated from the body; thus never reaching their desired site of action<sup>16-17</sup>.

Another important sulfur-containing protein found intracellularly is the tripeptide, glutathione (GSH)<sup>18</sup>. The normal intracellular concentration of GSH ranges from 5 to 10 mM<sup>19</sup>, therefore the binding of platinum-containing drugs to GSH is highly probable. Cells with elevated glutathione (>10mM) are more resistant to cisplatin<sup>20</sup>, indicating its clinical importance. Due to these metabolic consequences resulting in low cellular Pt-DNA binding, it is necessary to fully investigate the interactions of sulfur-containing biomolecules with current clinical and pre-clinical platinum chemotherapeutics.

Polynuclear platinum compounds are a structurally discrete class of drugs whose chemical and biological properties differ significantly from cisplatin.<sup>21-23</sup> BBR3464, the only non-cisplatin-like molecule to enter human clinical trials, and has promising activity in cisplatin-resistant, cisplatin-sensitive and p53 mutant tumors.<sup>24-26</sup> BBR3464 is also forty to eighty fold more potent on a molar basis than cisplatin.<sup>27</sup> Promising pre-clinical, Phase I and Phase II clinical studies of BBR3464 have been offset to some extent by rapid degradation of BBR3464 into inactive metabolites due to enhanced interactions with plasma proteins.<sup>28-29</sup> The production of these inactive metabolites may be replicated by the chemical reactions of BBR3464 with reduced GSH.<sup>18</sup> These pharmacokinetic factors are thought to contribute to reduced activity in gastric and lung cell carcinomas<sup>30-31</sup>. For the development of subsequent generations of platinum derivatives, it is necessary to design platinum compounds which may have the ability to avoid or minimize these metabolic deactivations.

Most platinum chemotherapeutics bind to DNA in a covalent manner by formation of a Pt-DNA adduct. Replacement of the chloride leaving groups of BBR3464 with substitutionally 'inert' ammine ligands or 'dangling' ammines,  $H_2N(CH_2)_6NH_3^+$ , gives

'non-covalent' polynuclear platinum compounds; most notably TriplatinNC, Figure 4.1. Although chemically non-reactive, TriplatinNC binds to DNA through the formation of a 'phosphate clamp', a ligand mode of binding distinct from the "classical" minor-groove binders and intercalators.<sup>32</sup> TriplatinNC has significantly higher cellular accumulation than either BBR3464 or cisplatin, and in some cases equivalent or greater cytotoxicity than cisplatin.<sup>33-34</sup>

Biophysical studies on the interaction of TriplatinNC with albumin have shown the presence of an initial, electrostatic, association with the protein.<sup>35</sup> Previous studies have shown that the interactions of cationic lipids with albumin give approximate binding ratios of 1-2:1 (Lipid:Albumin).<sup>36</sup> Due to its' high charge, TriplatinNC would be expected to associate to albumin and other serum proteins *in vivo*, but in the absence of a substitution-labile leaving group, would not be expected to undergo the same types of deactivation reactions as seen with the covalent platinum analogs.<sup>12,17,35</sup> This protein association, in the absence of deactivation, could provide a promising and novel pharmacokinetic profile not seen in current clinical platinum regimens. This paper addresses the effects of serum protein and glutathione deactivation on platinum drug trafficking and the consequences for compound efficacy, levels of cellular accumulation, DNA adduct formation, and intracellular distribution. The effects of protein association on intracellular localization were examined by confocal microscopy using a new, versatile fluorophore for platinum drugs based on 7-nitro-2,1,3-benzoxadiazole (NBD).

## **Results and Discussion**

### **Importance of Glutathione in TriplatinNC Mediated Cytotoxicity**

One of the main intracellular biomolecules is glutathione (GSH), which has an important role in determination of cellular sensitivity to cytotoxic drugs. (Figure 4.1A) The cellular glutathione level in HCT116 cells was decreased using buthionine sulphoximine (BSO), which inhibits gamma glutamylcysteine synthetase, a rate limiting enzyme in glutathione synthesis.<sup>37-38</sup> As the cellular glutathione level was reduced, cisplatin, and BBR3464-induced apoptosis was augmented, demonstrating their interactions with glutathione. After 48 hours of treatment, BSO alone and BBR3464-induced apoptosis were 1% and 18% (as in control sample), but the combination of BBR3464 and BSO increased apoptosis to 58% (Figure 4.1B). The results showed consistency in testing with cisplatin. BSO increased cisplatin-induced apoptosis from 14% to 45% (Figure 4.1B). In striking contrast to these covalent Pt drugs, TriplatinNC-induced cytotoxicity was completely unaltered by inhibiting glutathione synthesis. (Figure 4.1B)

Since some efflux mechanisms have been shown to be dependent on glutathione<sup>39</sup>, the effects of BSO on the cellular accumulation of platinum drugs was measured. Cellular platinum levels were measured *via* ICP-OES in cells treated with platinum drugs +/- BSO to determine if the increase observed in cytotoxicity is the result of enhanced cellular uptake of platinum drugs. As shown in Figure 4.1C, BSO did not influence cisplatin, BBR3464, or TriplatinNC cellular accumulation. Hence, cellular accumulation does not play a role in the augmentation of Pt-induced cytotoxicity by BSO.

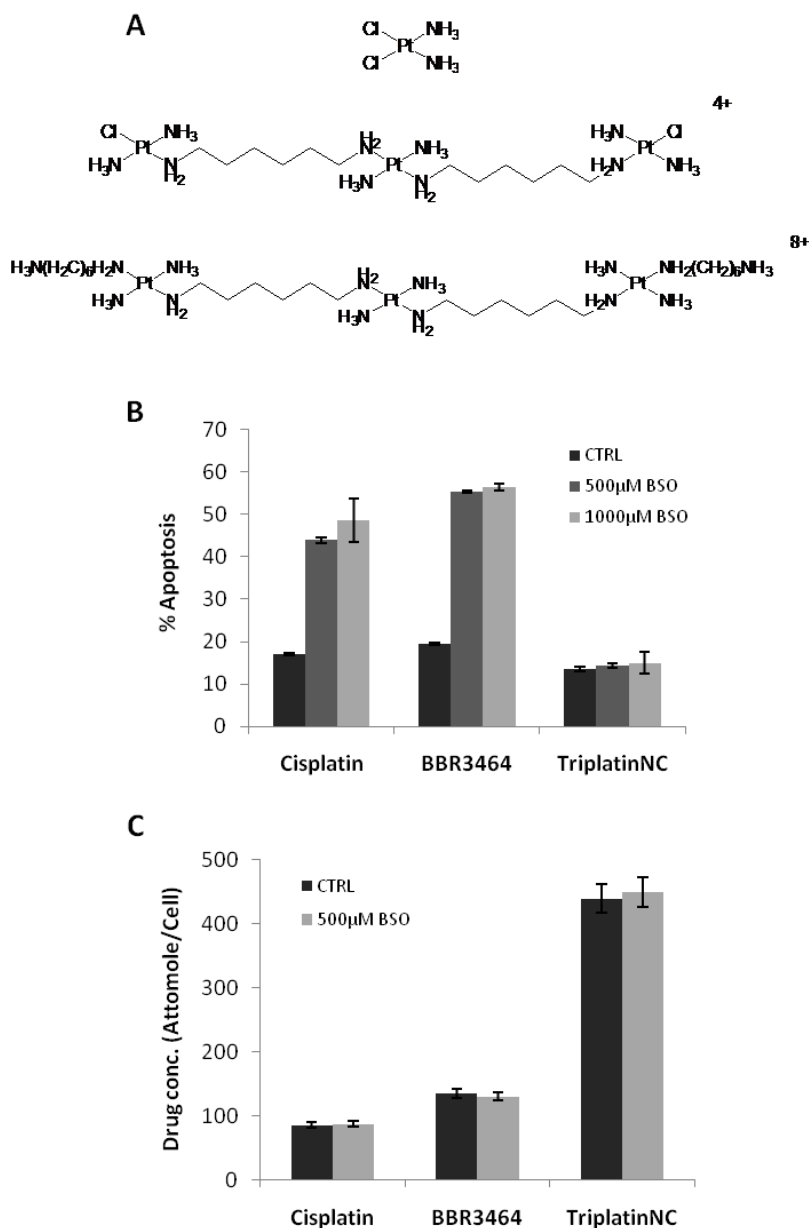


**Figure 4.1** (A) Chemical structures of cisplatin (top), BBR3464 (middle) and TriplatinNC (bottom). (B) Effect of BSO on platinum drug-induced cytotoxicity in HCT116 cells. Sub-diploid cell content was detected by PI-DNA staining. HCT116 cells were cultured with 10 μM cisplatin, 50 μM BBR3464, or 40 μM TriplatinNC for 48h in the absence or presence BSO. Drugs were added to the media after 1h of treatment with BSO. (C) Effect of BSO on platinum drug cellular uptake in HCT116 carcinoma cell lines. HCT116 cells were cultured with 20 μM cisplatin for 16h, 20 μM BBR3464 for 8h, or 20 μM TriplatinNC for 3h in the absence or presence of 500 μM BSO. Drugs were added to the media after 1h of treatment with BSO. Each point represents the average (+/- SEM) of three independent experiments.

### Effects of Protein Binding on Cisplatin, BBR3464, and TriplatinNC

The pharmacokinetic profiles in Phase I clinical trials of BBR3464 and cisplatin have been shown to be vastly different, with protein binding in BBR3464 being much higher than cisplatin at early time points.<sup>27</sup> To evaluate the effect of protein binding on drug deactivation, cisplatin, BBR3464 and TriplatinNC were incubated with human plasma or human serum albumin for selected time points. Analysis of platinum content by ICP-OES shows an increase in protein binding over time for both cisplatin and BBR3464 after incubation with whole serum. This time dependent increase in protein binding represents a displacement of the platinum-chloride bond and the formation of the covalent platinum-protein adduct. (Figure 4.2) In contrast, with the non-covalent compound, TriplatinNC, a 1:1 drug protein complex is immediately formed, representing a rapid association of the positively charged drug, presumably with negative regions of serum proteins.(Figure 4.2) Due to the chemical nature of TriplatinNC, the initial non-covalent binding is not followed by covalent drug–protein adduct formation.

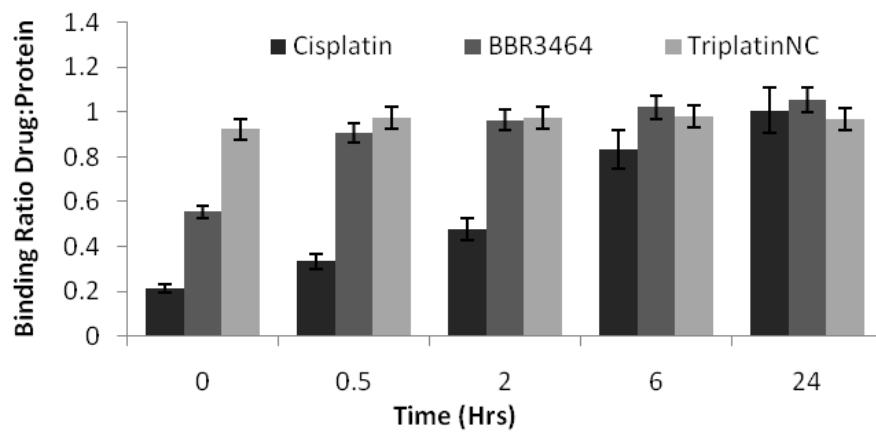


**Figure 4.2** Effects of protein binding on free drug availability of cisplatin, BBR3464, TriplatinNC. Final binding ratio of platinum compounds to human plasma over time.

### Role of Protein Binding on Cytotoxicity of Cisplatin, BBR3464, and TriplatinNC

In theory, once a covalent platinum-protein adduct is formed, the drug “loses” its cytotoxic effect and is rendered inactive.<sup>40</sup> To further understand the differences in binding profile between covalent and ‘non-covalent’ platinum compounds with HSA, cytotoxicity assays were performed on the protein bound derivatives of cisplatin, BBR3464, and TriplatinNC (cisplatin/HSA, BBR3464/HSA, and TriplatinNC/HSA) and compared to the free drug IC<sub>50</sub> values in A2780 ovarian carcinoma cell lines. As seen in Figure 4.3A, A2780 cells treated with cisplatin/HSA show a large decrease in drug efficacy as compared with treatment of cisplatin alone. The same trend can be seen with BBR3464/HSA and BBR3464. (Figure 4.3B) In stark contrast, A2780 cells showed no change in growth inhibition when treated with the complex TriplatinNC/HSA (IC<sub>50</sub>≈3μM) as compared to treatment of the drug alone, TriplatinNC (IC<sub>50</sub>≈3μM). (Figure 4.3C)

Incubation of cisplatin, BBR34364 and TriplatinNC with whole serum provides a physiological approach to studying the effects of protein binding on drug efficacy. Cisplatin and BBR3464 both show a time-dependent decrease in cytotoxicity upon incubation followed by cellular exposure after pretreatment with serum. (Figure 4.3 D, E) For cisplatin and BBR3464, the observed IC<sub>50</sub> values decreased from 0.6μM to >30μM, and 0.2μM to >30μM respectively over a 72 hour period. Cellular treatment with TriplatinNC after 72hr media incubation showed no marked decrease in IC<sub>50</sub> value, remaining approximately 3μM at all timepoints. (Figure 4.3F).



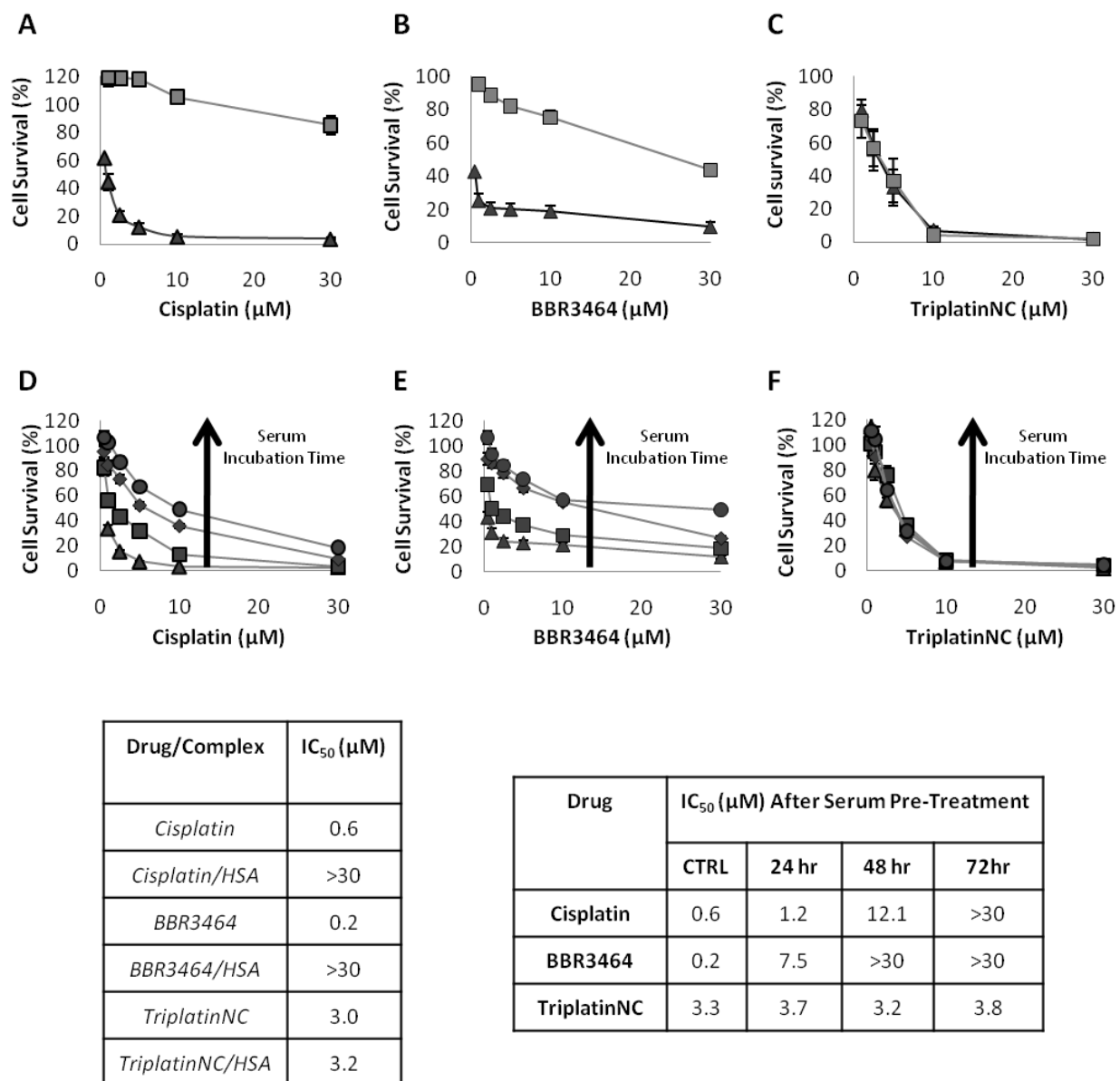


**Figure 4.3** Influence of protein binding on platinum drug efficacy in A2780 ovarian carcinoma cells. (A) Cisplatin cytotoxicity ( $\blacktriangle$ ) in A2780 cells compared with the treatment of cisplatin/HSA ( $\blacksquare$ ). (B) BBR3464 cytotoxicity ( $\blacktriangle$ ) compared with the treatment of BBR3464/HSA ( $\blacksquare$ ). (C) TriplatinNC cytotoxicity ( $\blacktriangle$ ) compared with the treatment of TriplatinNC/HSA ( $\blacksquare$ ). (D-F) Platinum compounds were incubated with serum supplemented media for 0-72hrs. Cellular growth inhibition was then measured after treatment. Efficacy of cisplatin (D), BBR3464 (E), and TriplatinNC (F) following increased serum incubation times (0-72hrs). A2780 cells were cultured in the indicated concentrations of each compound for 72h. Percent growth inhibition was determined by comparing live cell numbers in treated and untreated cultures after 72h, as measured by MTT. Values are the average ( $\pm$  S.E.M.) of three independent experiments.

### Effects of Protein Binding on Cellular Drug Accumulation

Since the rate of cellular uptake and total accumulation correlates to the cytotoxic effect of platinum drugs, cellular accumulation of each platinum compound and its protein bound derivative was examined at  $IC_{90}$  concentrations, Figure 4.4. Treatment of A2780 cells with cisplatin produced an increase in cellular platinum levels in a time dependent manner, reaching approximately 30 attomole Pt/cell after 24hrs. In contrast, cells treated with cisplatin/HSA showed a drug accumulation of 5 attomole Pt/cell or less at all time points. (Figure 4.4A) Cellular treatment with BBR3464 also shows a time dependent increase in drug concentration, reaching approximately 100 attomole Pt/cell after 24hrs. (Figure 4.4B) In contrast to cisplatin/HSA, the protein bound derivative of BBR3464 shows a sporadic increase in platinum concentration over time. Although BBR3464 is covalently bound to albumin, the chemical nature of this binding may cause the tri-nuclear drug to degrade into di-nuclear and mononuclear non-covalent, non-cytotoxic metabolites as seen previously with the treatment of blood cells with BBR3464.<sup>18,29,41</sup> It is reasonable to assume that these di-nuclear and mononuclear metabolites may also enter cells and contribute to the measurement of Pt levels. In contrast, platinum accumulation in cells treated with TriplatinNC and TriplatinNC-HSA was nearly identical at all time points, reaching approximately 400 attomole Pt/cell at the 24hr timepoint. (Figure 4.4C) Note again the enhanced accumulation of charged trinuclear drugs in comparison to cisplatin.

To examine the role of whole serum deactivation on the rate of cellular accumulation levels for cisplatin, BBR3464 and TriplatinNC, intracellular platinum levels were determined after 24 hours of drug exposure, following specified serum incubation

times. Treatment of cisplatin with serum supplemented media shows a time-dependent decrease in cellular platinum uptake following drug exposure for 24 hours. (Figure 4.4D) Treatment of BBR3464 with serum supplemented media shows a constant level of cellular platinum uptake following drug exposure for 24 hours. This platinum accumulation is interpreted to correspond to a mixture of the covalent and non-covalent metabolites of BBR3464, consistent with the metabolic degradation seen after protein binding. (Figure 4.4E) Upon incubation with serum for 24, 48, and 72 hours and subsequent cellular treatment, TriplatinNC cellular accumulation levels remains constant. (Figure 4.4F) A constant  $IC_{50}$  value over time and a consistent rate of cellular drug accumulation shows the ability of TriplatinNC to “by-pass” the typical protein deactivation pathway seen with current platinum chemotherapeutics.

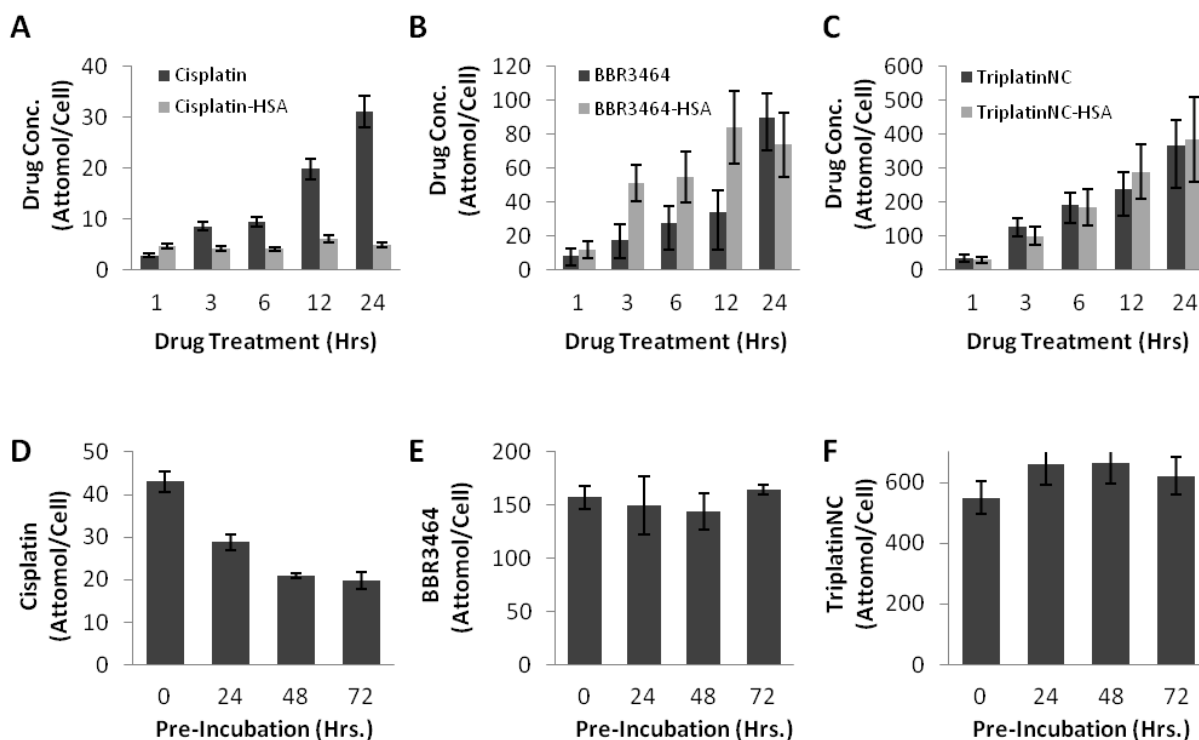


**Figure 4.4** Influence of protein binding on platinum cellular uptake in A2780 ovarian carcinoma cells. A2780 Cells were treated with  $IC_{90}$  concentrations of cisplatin and cisplatin/HSA (A), BBR3464 and BBR3464/HSA (B), TriplatinNC and TriplatinNC/HSA (C) for 0, 3, 6, 12, and 24 hours. For serum incubation studies each platinum drug was pre-incubated with serum for (0-72hrs). A2780 cells were then treated with  $IC_{90}$  concentrations of each compound ((D) Cisplatin, (E) BBR3464, (F) TriplatinNC) for 24hrs. After appropriate incubation times, cells were removed from the plate and washed with PBS. Analysis of platinum content was performed on a Varian ICP-MS. Values are the average (+/- S.E.M.) of three independent experiments.

### Effects of Protein Binding on Levels of DNA Platination

The cytotoxicity of platinum chemotherapeutics is mainly accepted to be modulated by the frequency and type of platinum-DNA adducts formed during drug treatment. To examine the role of protein binding on the amount of DNA platination, A2780 cells were treated for 24hrs with IC<sub>90</sub> concentrations of cisplatin, cisplatin/HSA, BBR3464, and BBR3464/HSA. DNA platination levels after 24 hours of continuous cisplatin treatment reached approximately 225 nmole Pt/g DNA, while platinum levels of cisplatin/HSA remained less than 10 nmole Pt/g DNA. (Figure 4.5A) The same trend in DNA adduct formation was seen with BBR3464 and BBR3464/HSA, with platinum levels reaching 425 and 20 nmole Pt/g DNA respectively. (Figure 4.5B)

DNA platination levels of cisplatin and BBR3464 were also monitored following serum incubation. After incubation with serum proteins for 24, 48, and 72hrs, both cisplatin and BBR3464 DNA platination levels were reduced. Initial levels of DNA platination for cisplatin were approximately 225 nmol platinum / g DNA. After 72hrs of serum treatment prior to cell treatment, DNA platination levels were reduced to 31 nmol platinum / g DNA. (Figure 4.5C) The same trend was seen with serum pre-treatment of BBR3464, where platinum levels decrease from 425 nmol platinum / g DNA to 230 nmol platinum / g DNA. (Figure 4.5D) The decreases in DNA platination seen after protein binding are directly responsible for the reduced activity of both cisplatin and BBR3464.

Due to the non-covalent nature of TriplatinNC-DNA binding<sup>32</sup>, isolation of cellular DNA may disrupt the interaction. To resolve this inherent problem, we have developed a new fluorescent probe for platinum and used fluorescence microscopy as a tool to examine the effects of protein binding on cellular distribution and DNA platination.

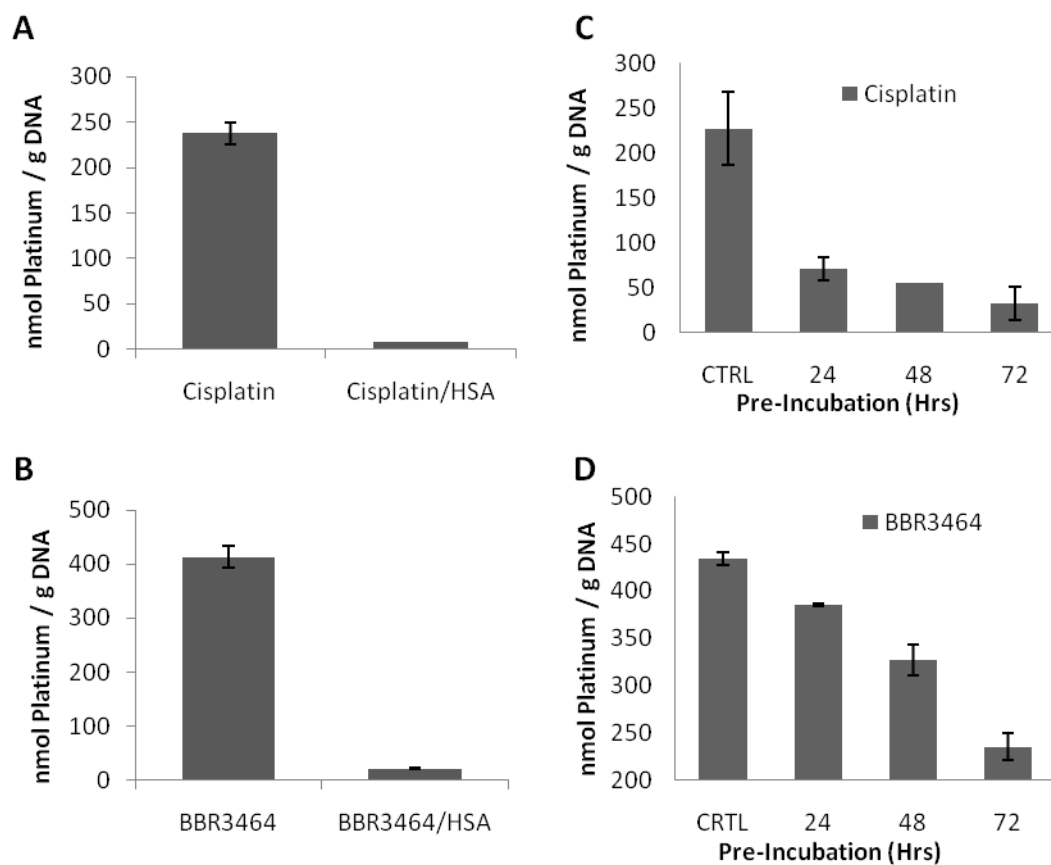


**Figure 4.5** Influence of protein binding on DNA platinumation in A2780 ovarian carcinoma cells. A2780 Cells were treated with  $IC_{90}$  concentrations of cisplatin and cisplatin/HSA (A), BBR3464 and BBR3464/HSA for 24 hours. For serum incubation studies each platinum drug was pre-incubated with serum for (0-72hrs). A2780 cells were then treated with  $IC_{90}$  concentrations of each compound ((C) Cisplatin, (D) BBR3464) for 24hrs. After appropriate incubation times, cells were removed from the plate and washed with PBS. Cellular DNA was then extracted and analysis of platinum content was performed on a Varian ICP-MS. Values are the average (+/- S.E.M.) of three independent experiments.

### Fluorescent Drug Design of TriplatinNC-NBD and Cisplatin-NBD

The use of molecular imaging techniques, such as confocal microscopy, is an important tool in the understanding of platinum drug trafficking and intracellular distribution. To utilize this approach, new fluorescent platinum derivatives were developed using NBD fluorophores. Hambley has summarized recent fluorescent approaches to monitoring platinum trafficking.<sup>42</sup> The advantage of the NBD approach is that rather than use chelates like ethylenediamine and cumbersome chemical modifications, the NBD addition is performed on a primary amine and gives analogs very similar to the “parent drugs”. Previous attempts at “tagging” platinum compounds have yielded cisplatin derivatives in which FITC and Alexa based fluorophores have been utilized. These derivatives tend to mimic the biological properties of the fluorescent “tag” rather than the platinum moiety itself.<sup>42</sup> In the case of TriplatinNC, we conjugated the NBD fluorophore directly to the primary amine on each end of the complex, and for cisplatin, we replace the existing amine group with NBD-ethane-1,2-diamine. TriplatinNC-NBD shows only a 12% increase in molecular weight, retains a high positive charge (6+), and shows similar cytotoxicity to TriplatinNC. (Figure 4.6A) Cisplatin-NBD has a molecular weight increase of 66%, substantially less than seen with FDDP<sup>42</sup>, and also retains a cytotoxic profile in A2780 cells. (Figure 4.6B)

### Role of Albumin in the Cellular Localization of Cisplatin and TriplatinNC

The mechanisms of cellular uptake and distribution of albumin and other serum proteins have been extensively studied and show that serum proteins localize to lysosomal regions of the cytosol.<sup>43</sup> The use of a non-covalent drug, TriplatinNC, affords

a unique handle to examine how macromolecule association affects small platinum molecule biodistribution – in the absence of platinum bond-forming reactions. Confocal microscopy was therefore employed to investigate how internalization and localization of cisplatin and TriplatinNC is affected by albumin. A2780 cells were treated with cisplatin-NBD (15 $\mu$ M) and cisplatin-NBD/HSA (1mg/mL) to investigate the role of covalent protein binding on drug localization. LysoTracker® Red was used as a lysosomal marker to indicate uptake of HSA. (Figure 4.7) Cisplatin-NBD was shown to localize throughout the cytosol and, to a lesser extent, the nucleus. (Figure 4.8A) This distribution is consistent with the fact that less than 10% of cellular cisplatin is found in the nucleus. After treatment of cisplatin-NBD/HSA, the cytosolic and nuclear localization was significantly reduced and limited to lysosomal regions of the cytosol. Co-localization of cisplatin-NBD/HSA and LysoTracker® Red was seen to a greater extent than with the treatment of cisplatin alone, indicating an increase in drug deactivation after protein binding.

HSA (1mg/mL) and TriplatinNC-NBD (15 $\mu$ M) (Protein:Drug, 1:1) were pre-incubated in serum-free media for 2hrs to ensure complex formation. Upon treatment with TriplatinNC-NBD/HSA for 6hrs, punctate cellular localization of LysoTracker® Red was observed in a pattern consistent with lysosomal accumulation while TriplatinNC was shown to localize throughout the cytosol and nucleolus. The uptake of TriplatinNC-NBD alone was shown to be identical to the localization seen upon treatment of the protein bound complex. (Figure 4.8B) The difference in accumulation patterns between TriplatinNC and LysoTracker® Red, and more importantly, the similarity between



TriplatinNC-NBD and TriplatinNC-NBD/HSA localization, show the ability of TriplatinNC to avoid metabolic deactivation associated with serum binding.

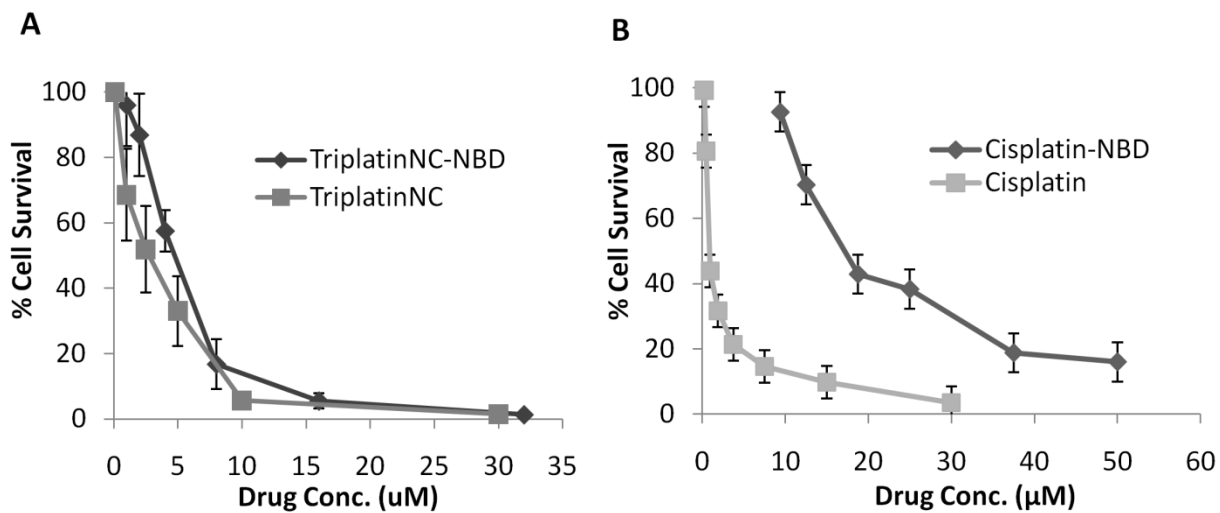


**Figure 4.6** MTT cytotoxicity assay of fluorescent platinum derivatives, TriplatinNC and TriplatinNC-NBD (A) and cisplatin and cisplatin-NBD (B)

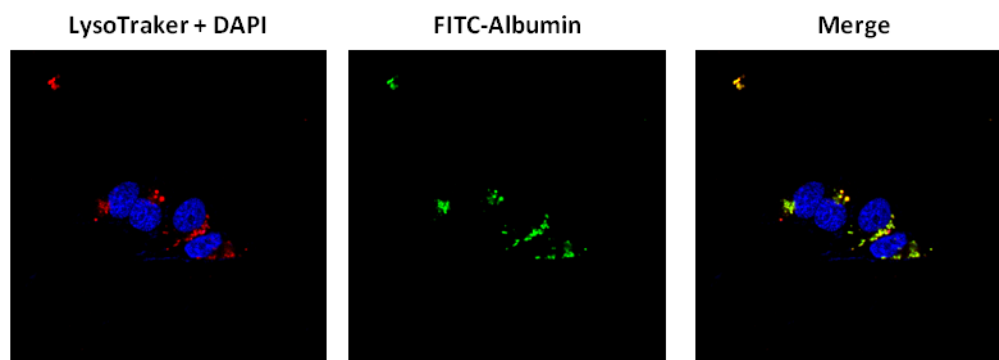


**Figure 4.7** Confocal laser scanning micrographs of A2780 cells. After incubation with FITC-albumin (1mg/mL) for 1hr and with LysoTracker<sup>®</sup> Red (75 nM) for 30 min at 37°C, cells were fixed and observed by confocal laser scanning microscopy. (left) LysoTracker<sup>®</sup> Red (red) + DAPI (blue) (B) FITC-albumin (green), (C) merged (A+B). A2780 Cells were grown on 4-well chamber slides (Lab-TekII Chamber Slide) for 2-3 days until cells reached near-confluency. Cells were then incubated with FITC-albumin (1 mg/mL) for 60 min, and with LysoTracker<sup>®</sup> Red (75 nM) for 30 min at 37°C. After treatment, slides were washed 3x with ice-cold PBS and fixed with 3% paraformaldehyde. Paraformaldehyde was removed and cells were washed again with 3x PBS and allowed to dry. Slides were then mounted with Vectashield mounting media containing DAPI. Fluorescence was observed by confocal laser scanning microscopy (Zeiss LSM 510).

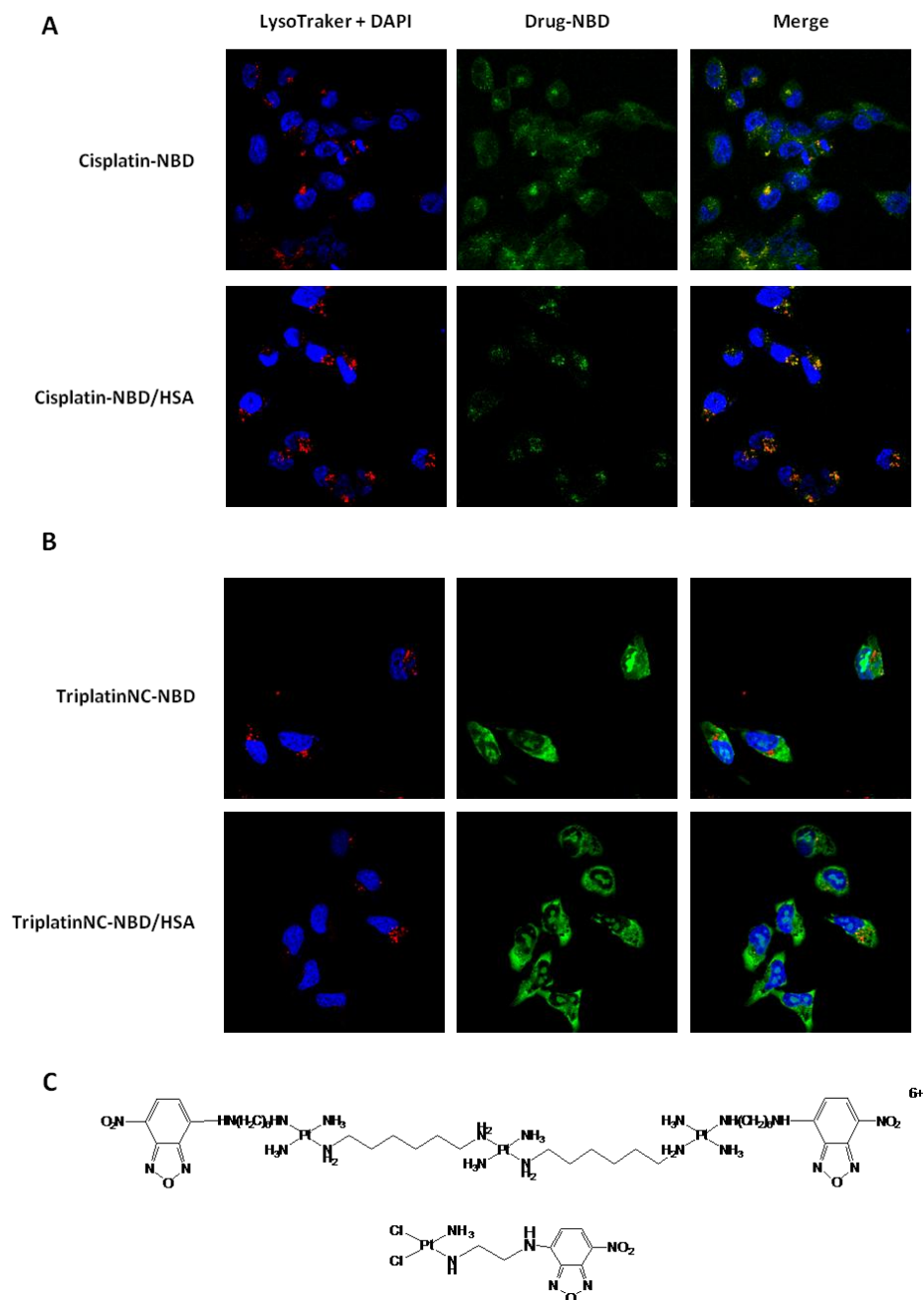


**Figure 4.8** Role of protein binding on the cellular localization and distribution of cisplatin and TriplatinNC. Confocal laser scanning micrographs (A-B) of A2780 cells. (A) (top row) Cisplatin-NBD (15 $\mu$ M) (green) incubated with A2780 cells for 24hrs and LysoTracker Red<sup>®</sup> (75nM) (red) for final 30min of drug incubation. (A) (bottom row) Cisplatin-NBD/HSA (1mg/mL) (green) incubated with A2780 cells for 24hrs and LysoTracker Red<sup>®</sup> (75nM) (red) for final 30min of drug incubation. Orange color represents areas of drug-protein co-localization. (B) (top row) TriplatinNC-NBD (15 $\mu$ M) (green) incubated with A2780 cells for 6hrs and LysoTracker Red<sup>®</sup> (75nM) (red) for final 30min of drug incubation. (B) (bottom row) TriplatinNC-NBD/HSA (1mg/mL) (green) incubated with A2780 cells for 6hrs and LysoTracker Red<sup>®</sup> (75nM) (red) for final 30min of drug incubation. Orange color represents areas of drug-protein co-localization. Slides were mounted with Vectashield mounting media containing DAPI (blue). Fluorescence was observed by confocal laser scanning microscopy (Zeiss LSM 510). (C) Chemical structures of TriplatinNC-NBD (top) and Cisplatin-NBD (bottom).

## **Conclusion**

This study shows, for the first time, a platinum chemotherapeutic with a substantially enhanced and distinctly different pharmacokinetic profile than that of any clinically developed platinum drug. This work has shown the significance of the interaction of TriplatinNC with plasma as well as individual intracellular and extracellular proteins. The non-covalent binding of TriplatinNC to serum proteins allows for an interaction with the protein, but not a deactivation of the platinum compound. The deactivation of cisplatin and BBR3464 upon binding to glutathione, serum or albumin show the major problems associated with the treatment of cancer using the current platinum chemotherapeutic regiment.

The data also allows one to examine the role of albumin as a drug carrier or drug delivery system for TriplatinNC. Albumin is known to function as an important protein in the maintenance of osmotic pressure and also as a transport protein involved in the distribution of hormones, fatty acids and metal ions.<sup>44-45</sup> Once administered, TriplatinNC would be expected to bind to plasma proteins in a non-covalent manner and then be transported to the cellular surface or become actively transported internally through the endocytosis of albumin.<sup>43</sup> The mechanism of uptake of TriplatinNC and the role of albumin in this process was examined by utilizing novel fluorescently labeled derivatives of both cisplatin and TriplatinNC. Further, the non-covalent drug is a unique probe for studying platinum drug molecule-biomolecule interactions in cells. TriplatinNC not only presents a new mode of DNA binding, distinct from any clinical platinum agent, but also allows for the elimination of covalent Pt-protein adduct formation, thus creating a novel pharmacokinetic and cytotoxicity profile worthy of further development.

## **Materials and Methods**

### **Materials**

BBR3464, cisplatin, and TriplatinNC were synthesized according to methods reported previously.<sup>46-48</sup> Synthesis of TriplatinNC-NBD and Cisplatin-NBD is described in the methods section. Human plasma was purchased from Innovative Research Inc. Albumin from human serum, minimum 99%, FITC-Albumin, and Buthionine sulphoximine (BSO) was obtained from Sigma-Aldrich (St. Louis, MO). LysoTracker® Red DND-99 was obtained from Invitrogen and recombinant HSA (rHSA) was a generous gift from Delta Biotechnologies.

### **Synthesis of Cisplatin-2-NBD and TriplatinNC-NBD**

***N-(7-nitro-2,1,3-benzoxadiazol-4-yl)hexane-1,6-diamine***. Ligand was synthesized by a modification of a described procedure.<sup>49</sup> BOC–diaminohexane hydrochloride was dissolved in ddH<sub>2</sub>O and NBD-Cl (5eq) and DIPEA (2eq) was added. After the mixture had been stirred at room temperature overnight the product was extracted with diethyl ether. The organic phase was washed with brine (4x10 mL), dried over Na<sub>2</sub>SO<sub>4</sub> and purified by flash chromatography (CHCl<sub>3</sub>/EtOAc, 90:10). The BOC protecting group of the purified intermediate was removed by using trifluoroacetic acid (1 mL) at room temperature. After the mixture had been stirred overnight, excess TFA was evaporated, and the oily product was treated with diethyl ether to yield the product as orange crystals.

***N-(7-nitro-2,1,3-benzoxadiazol-4-yl)ethane-1,2-diamine (L)***: BOC–diaminoethane (0.79 ml, 4.99 mmol) was dissolved in 20 ml ethanol containing a 10% w/w of Na<sub>2</sub>CO<sub>3</sub>,

and NBD-Cl (0.50 g, 2.51 mmol) was added. The mixture was stirred at room temperature overnight, then 50 ml of water were added and the product was extracted with diethyl ether (3 x 30 ml). The organic phase was washed with brine (3 x 30 ml), dried over Na<sub>2</sub>SO<sub>4</sub> and purified by flash chromatography (CHCl<sub>3</sub>/EtOAc, 70:30). The BOC protecting group of the purified intermediate was removed by using 2 ml of trifluoroacetic acid at room temperature. After the mixture had been stirred overnight, excess TFA was evaporated, and the oily product was treated with diethyl ether to yield the trifluoroacetate salt as orange crystals.

Both ligands were neutralized by dissolving in a mixture of H<sub>2</sub>O/Ethanol 1:1 and addition of 1 equivalent of NaOH. The neutral ligand was then extracted with CH<sub>2</sub>Cl<sub>2</sub>. The organic fractions were dried over K<sub>2</sub>CO<sub>3</sub> and the solvent removed under vacuum. The product was dried under vacuum overnight.

**TriplatinNC-NBD<sub>2</sub>:** BBR3464 Cl<sup>-</sup> salt was treated with 5.97eq of AgNO<sub>3</sub> in ddH<sub>2</sub>O and allowed to stir at room temperature for 4hrs. AgCl was filtered off and to the clear solution was added NBD-diaminohexane (5eq) and DIPEA (5eq). The solution was allowed to stir at 50°C overnight. The solution was then evaporated to dryness and the resulting orange oil was re-dissolved in ddH<sub>2</sub>O and excess NBD-diaminohexane was removed by extraction with EtOAc (5x50 mL). The aqueous layer was removed and the product was redissolved in ddH<sub>2</sub>O and lyophilized. The resulting orange powder was washed with EtOAc, CHCl<sub>3</sub> and diethyl ether to yield TriplatinNC-NBD<sub>2</sub> (1.7mg, 30%)  
<sup>1</sup>H NMR D<sub>2</sub>O δ (ppm): 8.54 (d, 2H); 6.23 (d, 2H); 3.00 (t, 12H); 2.72 (m, 4H); 1.67 (m, 16H); 1.42 (m, 16H).

***Cis-[PtCl<sub>2</sub>((N-NBD)ethane-1,2-diamine)(NH<sub>3</sub>)]:*** The synthesis of this compound was achieved by means of a modification of a patented procedure<sup>50</sup>. K[PtCl<sub>3</sub>(NH<sub>3</sub>)] (30.0 mg, 0.084 mmol) was dissolved in 5 ml of a 15 mM aqueous solution of KCl. A solution of KI (41 mg, 0.248 mmol) in 1 ml of water was prepared. The KI solution was added to the K[PtCl<sub>3</sub>(NH<sub>3</sub>)] solution, followed by a slight excess of the NBD amino ligand L (20.5 mg, 0.091 mmol). The combined solution was stirred in the dark for 5 h at room temperature. A redish precipitate formed which was collected, washed with cold water, cold methanol, and dried under vacuum at room temperature overnight. The product was *Cis*-[PtI<sub>2</sub>((N-NBD)ethane-1,2-diamine)(NH<sub>3</sub>)], confirmed by NMR. The *Cis*-[PtI<sub>2</sub>((N-NBD)ethane-1,2-diamine)(NH<sub>3</sub>)] (40 mg, 0.067 mmol) was suspended in 2 ml of a mixture H<sub>2</sub>O/Acetone 85:15 and 1eq of silver nitrate was added to the suspension. It was then stirred for 24 h in the dark at room temperature. The suspension was filtered and 200 ml of HCl (~12 M) were added to the filtrate. The solution was stirred at room temperature for 2 h, during which time a black precipitate formed. The precipitate was filtered and the solution concentrated to obtain the product as a brownish powder, which was washed with ice cold methanol, ether and dried under vacuum. <sup>1</sup>H NMR D<sub>2</sub>O δ (ppm): 8.45(d, 1H); 6.33 (d, 1H); 3.81 (t, 2H); 3.27 (t, 2H). ESI-MS: m/z: (M+H)<sup>+</sup> 507.22; (M-Cl)<sup>+</sup> 471.23

### Cell System

The colorectal carcinoma cell lines HCT116 were the kind gift of Bert Vogelstein (Johns-Hopkins University, Baltimore, MD). HCT116 and A2780 cells were cultured in RPMI



1640 with 10% fetal bovine serum, 100 U/ml penicillin, 100 µg/ml streptomycin in humidified air with 5% CO<sub>2</sub>.

### Human Plasma Binding

Solutions of each drug were prepared in PBS and added to human plasma such that the final concentration of complex was 0.9mM (1:1 v/v). The reactions were incubated at 37 °C for 0, 0.5, 2 and 24 hours. Unreacted drug was removed by centrifugation through a Millipore Microcon YM-10 (10,000 kDa) membrane filter at 14,000xg for 30 min. The centrifuge cup was upturned in a second eppendorf and centrifuged at 1000xg for 3 min to isolate the protein-bound drug. Both ultrafiltrate and protein samples were stored at -20°C immediately following centrifugation. The digestion procedure followed published methods.<sup>47</sup> Analysis of platinum content for both the protein-bound and unreacted samples was performed on a Varian ICP-OES. Protein concentration was determined by the Bradford method with human serum albumin as the standard.<sup>51</sup>

### Formation of Drug-Albumin Complex

Platinum compounds (Cisplatin, Cisplatin-NBD, BBR3464, and TriplatinNC) were incubated with HSA for 72hrs at 10:1(Drug:Protein). Non-protein bound drug was removed by centrifugation using method described above. The protein was collected, redissolved in 5mL PBS and immediately frozen at -20°C. Pt concentration was determined using ICP-OES by removing a small aliquot of the Pt-protein solution before freezing. Protein concentration was determined by the Bradford method with human serum albumin as the standard.<sup>51</sup>

### BSO Treatment, Propidium Iodide DNA Staining, and Analysis of Apoptosis

HCT116 cells were cultured in 6-well plates at an initial density of  $7.0 \times 10^4$  cells/ml. Different concentrations of drugs were added to each well as indicated. Total cell contents (apoptotic and viable cells) were collected. In experiments using BSO, Pt drug concentrations were adjusted to achieve approximately 15%-20% apoptosis, allowing us to measure enhancement or inhibition. Samples were fixed in an ethanol and fetal bovine serum solution, washed with PBS, and stained with a solution of propidium iodide (PI) and RNase A, as described previously<sup>52</sup>. Samples were then analyzed for subdiploid DNA content on a Becton Dickinson FACScan flow cytometer (BD Biosciences, San Jose, CA). It is noteworthy that this protocol differs significantly from the more common PI-based exclusion, which only differentiates live versus dead cells. Through fixation and RNase A treatment, we were able to detect intact versus fragmented DNA, revealing discrete stages of the cell cycle and the percentage of the population undergoing apoptosis.

### Cellular Growth Inhibition

The MTT assay was used to determine growth inhibition potency of platinum drugs and the corresponding protein bound derivatives.<sup>53</sup> A2780 cells were seeded in 96-well plates at 6,500 cells/well in 200 $\mu$ L of RPMI 1640 media and allowed to attach overnight. Media was removed and 200 $\mu$ L of each compound was added after serial dilution in quadruplicate wells and exposed to cells for 72h. For time dependent media incubation studies 500 $\mu$ M of each Pt compound was incubated in RPMI 1640 media supplemented

with 10% FBS (1:1 v/v) for 0, 24, 48, and 72hrs before cellular treatment. Samples were diluted to treatment concentrations [30 $\mu$ M – 0.25 $\mu$ M] with fresh media after appropriate time points and cells were treated accordingly. Plates were then washed with PBS and 100 $\mu$ L of 5mg/mL MTT solution was added. MTT solution was incubated with cells for 3h at 37°C. After incubation, MTT solution was removed and 100 $\mu$ L of DMSO was added. Quantification of cell growth in treated and control wells was then assessed by measurement of absorbance at 562nm. IC<sub>50</sub> values were determined graphically.

#### Cellular Uptake of Drug and Drug-HSA Complexes

A2780 cells were plated in 10cm dishes at 2 million cells/dish and allowed to attach overnight. Cells were then treated with IC<sub>90</sub> concentrations of each drug and drug-HSA complex, 15  $\mu$ M for TriplatinNC, 4 $\mu$ M for Cisplatin, and 2.5 $\mu$ M for BBR3464, in 15mL media for 0, 3, 6, 12, and 24 hours. After appropriate incubation times, cells were removed from the dish with trypsin and centrifuged for 5min at 1000xg. Media was removed, cell pellet was washed three times with PBS, cells were counted and resuspended in 250 $\mu$ L of ddH<sub>2</sub>O. Samples were then digested following published methods.<sup>47</sup> Analysis of Pt content was performed on a Varian ICP-MS. Standards and blank were prepared similarly.

#### Quantification of DNA-Drug Adducts

A2780 cells were plated in 10cm dishes at 2 million cells/dish and allowed to attach overnight. Cells were then treated with IC<sub>90</sub> concentrations of each drug and drug-HSA

complex, 4 $\mu$ M for Cisplatin, and 2.5 $\mu$ M for BBR3464, in 15mL media for 24 hours. For time dependent media incubation studies 500 $\mu$ M of each Pt compound was incubated in RPMI 1640 media supplemented with 10% FBS (1:1 v/v) for 0, 24, 48, and 72hrs before cellular treatment. After incubation, cells were removed from the dish with trypsin and centrifuged for 5min @ 1000xg. Media was removed and cell pellet was washed three times with PBS and suspended in 200 $\mu$ L of ddH<sub>2</sub>O. DNA was extracted using a DNeasy blood and tissue kit (Qiagen) according to the manufacturer's protocol. Extent of DNA platination was measured on a Varian ICP-MS.

#### Confocal Laser Scanning Microscopy of A2780 Cells

A2780 Cells were grown on 8-well chamber slides (Lab-TekII Chamber Slide) for 2-3 days until cells reached near-confluency. A2780 cells were treated with cisplatin-NBD (15 $\mu$ M) and cisplatin-NBD/HSA (1mg/mL) for 24hrs. LysoTracker® Red (75nM) was added to the slide for the final 30 minutes of drug treatment time. For TriplatinNC-NBD (15 $\mu$ M) and TriplatinNC-NBD/HSA (1mg/mL), and FITC-Albumin (1mg/mL), A2780 cells were treated for 6hrs and LysoTracker® Red (75nM) was added to the slide for the final 30 minutes of drug treatment time. After treatment, slides were washed 3x with ice-cold PBS and fixed with 3% paraformaldehyde. Paraformaldehyde was removed and cells were washed again with 3x PBS and allowed to dry. Slides were then mounted with Vectashield mounting media containing DAPI. Fluorescence was observed by confocal laser scanning microscopy (Zeiss LSM 510).

### List of References

1. O'Dwyer, P., Stevenson, J. & Johnson, S. Clinical pharmacokinetics and administration of established platinum drugs. *Drugs* **59**, 19-27 (2000).
2. Decatris, M.P., Sundar, S. & O'Byrne, K.J. Platinum-based chemotherapy in metastatic breast cancer: current status. *Cancer Treatment Reviews* **30**, 53-81 (2004).
3. Wong, E. & Giandomenico, C.M. Current status of platinum-based antitumor drugs. *Chem Rev* **99**, 2451-2466 (1999).
4. Jamieson, E.R. & Lippard, S.J. Structure, Recognition, and Processing of Cisplatin-DNA Adducts. *Chem Rev* **99**, 2467-2498 (1999).
5. Berners-Price, S.J. & Appleton, T.G. *Platinum-Based Drugs in Cancer Therapy*, (Humana Press, Totowa, NJ, 2000).
6. Centerwall, C.R., Goodisman, J., Kerwood, D.J. & Dabrowiak, J.C. Cisplatin Carbonato Complexes. Implications for Uptake, Antitumor Properties, and Toxicity. *J Am Chem Soc* **127**, 12768-12769 (2005).
7. Centerwall, C.R., *et al.* Modification and Uptake of a Cisplatin Carbonato Complex by Jurkat Cells. *Molecular Pharmacology* **70**, 348-355 (2006).
8. Ruhayel, R.A., *et al.* Determination of the Kinetic Profile of a Dinuclear Platinum Anticancer Complex in the Presence of Sulfate: Introducing a New Tool for the Expedited Analysis of 2D [<sup>1</sup>H, <sup>15</sup>N] HSQC NMR Spectra. *Inorganic Chemistry* **49**, 10815-10819 (2010).

9. Zhang, J., Thomas, D., Davies, M., Berners-Price, S. & Farrell, N. Effects of geometric isomerism in dinuclear platinum antitumor complexes on aquation reactions in the presence of perchlorate, acetate and phosphate. *J Biol Inorg Chem* **10**, 652-666 (2005).
10. Hall, M.D., Okabe, M., Shen, D.-W., Liang, X.-J. & Gottesman, M.M. The Role of Cellular Accumulation in Determining Sensitivity to Platinum-Based Chemotherapy\*. *Annual Review of Pharmacology and Toxicology* **48**, 495-535 (2008).
11. Safirstein, R., *et al.* Cisplatin nephrotoxicity. *Am J Kidney Dis* **8**, 356-367 (1986).
12. Wang & Guo, Z. The role of sulfur in platinum anticancer chemotherapy. *Anticancer Agents Med Chem* **7**, 19-34 (2007).
13. Espósito, B.P. & Najjar, R. Interactions of antitumoral platinum-group metallodrugs with albumin. *Coordination Chemistry Reviews* **232**, 137-149 (2002).
14. Carter, D.C. & Ho, J.X. Structure of Serum Albumin. in *Advances in Protein Chemistry*, Vol. Volume 45 (eds. C.B. Anfinsen, J.T.E.F.M.R. & David, S.E.) 153-176, 176a, 176b, 176c, 176d, 176e, 176f, 176g, 176h, 176i, 176j, 176k, 176l, 177-203 (Academic Press, 1994).
15. Peters Jr, T. Serum Albumin. in *Advances in Protein Chemistry*, Vol. Volume 37 (eds. C.B. Anfinsen, J.T.E. & Frederic, M.R.) 161-245 (Academic Press, 1985).
16. Xiaoyong, W. & Zijian, G. The Role of Sulfur in Platinum Anticancer Chemotherapy. *Anti-Cancer Agents in Medicinal Chemistry* **7**, 19-34 (2007).

17. Timerbaev, A.R., Hartinger, C.G., Aleksenko, S.S. & Keppler, B.K. Interactions of Antitumor Metallo-drugs with Serum Proteins: Advances in Characterization Using Modern Analytical Methodology. *Chemical Reviews* **106**, 2224-2248 (2006).
18. Oehlsen, M.E., Qu, Y. & Farrell, N. Reaction of polynuclear platinum antitumor compounds with reduced glutathione studied by multinuclear ( $^1\text{H}$ ,  $^{15}\text{N}$  gradient heteronuclear single-quantum coherence, and  $^{195}\text{Pt}$ ) NMR spectroscopy. *Inorg Chem* **42**, 5498-5506 (2003).
19. Kosower, N.S. & Kosower, E.M. The glutathione status of cells. *Int Rev Cytol* **54**, 109-160 (1978).
20. Eastman, A.R., V. M. In Biochemical Mechanisms of the Platinum Antitumor Drugs. (ed. McBrien, S.C.H.S., T. F.) 91-119 (Oxford, 1986).
21. Farrell, N., Qu, Y. & Hacker, M.P. Cytotoxicity and antitumor activity of bis(platinum) complexes. A novel class of platinum complexes active in cell lines resistant to both cisplatin and 1,2-diaminocyclohexane complexes. *J Med Chem* **33**, 2179-2184 (1990).
22. Hegmans, A., *et al.* Amide-based prodrugs of spermidine-bridged dinuclear platinum. Synthesis, DNA binding, and biological activity. *J Med Chem* **51**, 2254-2260 (2008).
23. Perego, P., *et al.* The cellular basis of the efficacy of the trinuclear platinum complex BBR 3464 against cisplatin-resistant cells. *J Inorg Biochem* **77**, 59-64 (1999).

24. Manzotti, C., *et al.* BBR 3464: A Novel Triplatinum Complex, Exhibiting a Preclinical Profile of Antitumor Efficacy Different from Cisplatin. *Clinical Cancer Research* **6**, 2626-2634 (2000).
25. Perego, P., *et al.* A novel trinuclear platinum complex overcomes cisplatin resistance in an osteosarcoma cell system. *Mol Pharmacol* **55**, 528-534 (1999).
26. Pratesi, G., *et al.* A novel charged trinuclear platinum complex effective against cisplatin-resistant tumours: hypersensitivity of p53-mutant human tumour xenografts. *Br J Cancer* **80**, 1912-1919 (1999).
27. Sessa, C., *et al.* Clinical and pharmacological phase I study with accelerated titration design of a daily times five schedule of BBR3464, a novel cationic triplatinum complex. *Ann Oncol* **11**, 977-983 (2000).
28. Oehlsen, M.E., Hegmans, A., Qu, Y. & Farrell, N. Effects of geometric isomerism in dinuclear antitumor platinum complexes on their interactions with N-acetyl-L-methionine. *J Biol Inorg Chem* **10**, 433-442 (2005).
29. Vacchina, V., Torti, L., Allievi, C. & Lobinski, R. Sensitive species-specific monitoring of a new triplatinum anti-cancer drug and its potential related compounds in spiked human plasma by cation-exchange HPLC-ICP-MS. *J Anal Atom Spectrom* **18**, 884-890 (2003).
30. Hensing, T.A., *et al.* Phase II study of BBR 3464 as treatment in patients with sensitive or refractory small cell lung cancer. *Anti-Cancer Drugs* **17**(2006).
31. Jodrell, D.I., *et al.* Phase II studies of BBR3464, a novel tri-nuclear platinum complex, in patients with gastric or gastro-oesophageal adenocarcinoma. *European Journal of Cancer* **40**, 1872-1877 (2004).



32. Komeda, S., *et al.* A third mode of DNA binding: Phosphate clamps by a polynuclear platinum complex. *J Am Chem Soc* **128**, 16092-16103 (2006).
33. Harris, A.L., Ryan, J.J. & Farrell, N. Biological consequences of trinuclear platinum complexes: comparison of  $[\{\text{trans-PtCl}(\text{NH}_3)_2\}_2\mu\text{-(trans-Pt}(\text{NH}_3)_2(\text{H}_2\text{N}(\text{CH}_2)_6\text{-NH}_2)_2)]^{4+}$  (BBR 3464) with its noncovalent congeners. *Molecular Pharmacology* **69**, 666-672 (2006).
34. Harris, A.L., *et al.* Synthesis, characterization, and cytotoxicity of a novel highly charged trinuclear platinum compound. Enhancement of cellular uptake with charge. *Inorganic Chemistry* **44**, 9598-9600 (2005).
35. Montero, E.I., *et al.* Pre-association of polynuclear platinum anticancer agents on a protein, human serum albumin. Implications for drug design. *Dalton Transactions*, 4938-4942 (2007).
36. Charbonneau, D., Beaugard, M. & Tajmir-Riahi, H.-A. Structural Analysis of Human Serum Albumin Complexes with Cationic Lipids. *The Journal of Physical Chemistry B* **113**, 1777-1784 (2009).
37. Donenko, F., *et al.* Use of glutathione inhibitors and glutathione transferases to overcome tumor resistance to cytostatics &in vivo&. *Bulletin of Experimental Biology and Medicine* **119**, 206-208 (1995).
38. Drew, R. & Miners, J.O. The effects of buthionine sulfoximine (BSO) on glutathione depletion and xenobiotic biotransformation. *Biochemical Pharmacology* **33**, 2989-2994 (1984).
39. van Brussel, J.P., *et al.* Identification of multidrug resistance-associated protein 1 and glutathione as multidrug resistance mechanisms in human prostate cancer

- cells: chemosensitization with leukotriene D4 antagonists and buthionine sulfoximine. *BJU Int* **93**, 1333-1338 (2004).
40. Moller, C., Tastesen, H.S., Gammelgaard, B., Lambert, I.H. & Sturup, S. Stability, accumulation and cytotoxicity of an albumin-cisplatin adduct. *Metallomics* **2**, 811-818 (2010).
  41. Oehlsen, M.E., Hegmans, A., Yun, Q. & Farrell, N. Effects of geometric isomerism in dinuclear antitumor platinum complexes on their interactions with N-acetyl- L-methionine. *Journal of Biological Inorganic Chemistry* **10**, 433-442 (2005).
  42. Klein, A.V. & Hambley, T.W. Platinum Drug Distribution in Cancer Cells and Tumors. *Chemical Reviews* **109**, 4911-4920 (2009).
  43. Yumoto, R., *et al.* Clathrin-mediated endocytosis of FITC-albumin in alveolar type II epithelial cell line RLE-6TN. *Am J Physiol Lung Cell Mol Physiol* **290**, L946-955 (2006).
  44. Curry, S., Mandelkow, H., Brick, P. & Franks, N. Crystal structure of human serum albumin complexed with fatty acid reveals an asymmetric distribution of binding sites. *Nat Struct Mol Biol* **5**, 827-835 (1998).
  45. Petitpas, I., Grüne, T., Bhattacharya, A.A. & Curry, S. Crystal structures of human serum albumin complexed with monounsaturated and polyunsaturated fatty acids. *Journal of Molecular Biology* **314**, 955-960 (2001).
  46. Qu, Y., *et al.* Synthesis and DNA conformational changes of non-covalent polynuclear platinum complexes. *Journal of Inorganic Biochemistry* **98**, 1591-1598 (2004).

47. Harris, A.L., *et al.* Synthesis, Characterization, and Cytotoxicity of a Novel Highly Charged Trinuclear Platinum Compound. Enhancement of Cellular Uptake with Charge. *Inorganic Chemistry* **44**, 9598-9600 (2005).
48. Kauffman, G. & Cowan, D. cis- AND trans-DICHLORODIAMMINE-PLATINUM (II). in *Inorganic Syntheses*, Vol. 7 (ed. Kleinberg, J.) 236-238 (Jacob Kleinberg, 1963).
49. Schmidinger, H., *et al.* Novel Fluorescent Phosphonic Acid Esters for Discrimination of Lipases and Esterases. *ChemBioChem* **6**, 1776-1781 (2005).
50. Wong, E.S.Y. & Giandomenico, C.M.
51. Bradford, M.M. A rapid and sensitive method for the quantitation of microgram quantities of protein utilizing the principle of protein-dye binding. *Analytical Biochemistry* **72**, 248-254 (1976).
52. Yeatman, C.F., 2nd, *et al.* Combined stimulation with the T helper cell type 2 cytokines interleukin (IL)-4 and IL-10 induces mouse mast cell apoptosis. *J Exp Med* **192**, 1093-1103 (2000).
53. Cory, A., Owen, T., Barltrop, J. & Cory, J. Use of an aqueous soluble tetrazolium/formazan assay for cell growth assays in culture. *Cancer Communications* **3**, 207-212 (1991).

## Chapter 5: Design, Synthesis, and Anticancer Activity of Fluorescent-Based Dual Function *trans*-Platinum-NBD Complexes

Brad T. Benedetti, Alberto Martinez, and Nicholas P. Farrell\*

Department of Chemistry and Massey Cancer Center

Virginia Commonwealth University, Richmond, Virginia. USA

Synthesis and Fluorescence Titration Experiments performed by Dr. Alberto Martinez

### **Introduction**

Platinum drugs continue playing a prominent role in the treatment of cancer and are administered in around 50% of diagnosed patients.<sup>1-3</sup> Cisplatin remains the most used inorganic antitumor drug to date. The cytotoxicity of cisplatin is accepted to result mainly from the formation of bifunctional 1,2-intrastrand DNA crosslinks with purine bases, resulting in the inhibition of DNA synthesis and replication.<sup>4</sup> Unfortunately the success of cisplatin based chemotherapeutics is limited due to eventual acquired drug resistance and a limited range of tumor types that are treatable with the current regime. Therefore, the present research motivation is to find new platinum based drugs which exert a uniquely distinct mode of DNA binding.

Although the *trans* isomer of cisplatin, transplatin, remains clinically inactive, platinum compounds possessing a *trans* geometry became a new alternative when Farrell et al. reported the first examples of *trans* compounds with a higher potency than the respective *cis* isomers.<sup>5-7</sup> It is now well established that the substitution in the inactive transplatin of one NH<sub>3</sub> group by different families of amines, 'activates' these

compounds, producing cytotoxicity values higher than their *cis* counterparts and, in many cases, equivalent to that of cisplatin.<sup>5-6</sup> Two of the most common strategies in the synthesis of such compounds are the replacement of one  $\text{NH}_3$  by a planar ligand, typically a heterocyclic amine or aliphatic primary amine. Because the structure of the DNA adducts determines repair, protein recognition and other crucial cellular processes, it is widely accepted that the distinct platinum-DNA adducts that are formed when *trans* compounds interact with DNA are key for their potential therapeutic effectiveness. One possible explanation for the cytotoxic activity, especially for *trans*-platinum compounds containing heterocyclic derivatives, is the enhanced intercalation or pi-stacking seen between nucleobases on DNA and the aromatic heterocyclic amines on the platinum compound. This interaction provides for a pseudo bi-functional adduct, similar to the cisplatin-DNA adducts.<sup>5</sup>

The idea of a platinum compound that possesses a dual-mode of DNA binding has been slightly explored through the use of DNA intercalators conjugated to cisplatin.<sup>8-10</sup> Although somewhat successful, the design of these compounds has relied on the use aromatic intercalators such as anthraquinone and other cytotoxic aromatic moieties.<sup>11</sup> After conjugation to platinum, these compounds show cytotoxicity profiles nearly identical to that of the intercalator and therefore provide no clinical benefit over the use of the intercalator alone. The synthetic possibilities offered by platinum complexes allow the incorporation of not only DNA intercalators, but also different fluorophore groups that can be used for imaging studies to gain understanding and knowledge of the cellular distribution and action of these drugs. This strategy is a relatively non-invasive procedure that has been successfully exploited in the case of

several cisplatin-like compounds,<sup>12-13</sup> but with very little research devoted to *trans*-platinum complexes. By employing the use of both a fluorescent probe and a DNA intercalator conjugated to a platinum compound, cellular imaging studies can be incorporated to aid in the understanding of drug action.

In this work we report the anticancer activity and primary insights into the mechanism of action of a series of novel water-soluble *trans*-platinum complexes (Figure 5.1) that incorporate an amino ligand composed of an aliphatic carbon chain and a planar fluorophore intercalator, NBD (4-Chloro-7-nitrobenzofurazan). Interestingly, all three compounds are composed of individual components that are inactive when used separately. We also report for the first time the imaging of cellular processing of a *trans*-platin analogue by means of fluorescence microscopy. This is especially significant due to the antitumor potency the compounds exhibit when compared to cisplatin.

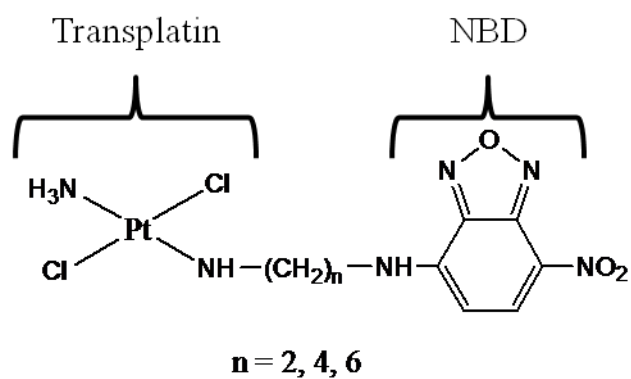


**Figure 5.1** General Chemical Structure of Trans-NBD Compounds

## **Results and Discussion**

It is well known that platinum compounds, including those with *trans* geometry, target DNA and form bifunctional adducts by covalently binding with guanine and adenine nucleobases. The intra- or inter-strand nature of the adducts formed strongly depends on the nature of the complex.<sup>2,14-16</sup> The rationale for the choice of NBD as fluorophore is in addition justified by its ability to intercalate between the nucleobases of DNA, a consequence of its high similarity with adenine.<sup>17</sup> This fact, therefore, allows all compounds the potential capability of a dual mode of action in which the platinum atom interacts covalently with the nucleobases while the NBD moiety intercalates with DNA. This strategy has been used by several groups,<sup>18</sup> but we now include an aliphatic chain between the platinum atom and the intercalator that will allow for the modulation of the lipophilicity/hydrophilicity of the drug and also make the compound flexible enough to allow the NBD molecule to properly intercalate in between the “preferred” nucleobases.

### **DNA Intercalation of Trans-NBD Compounds**

A key factor in the design of the Trans-NBD series that should drastically influence the cytotoxic behavior is the ability of the NBD moiety to intercalate strongly with DNA and therefore allow for the formation of uniquely distinct DNA-platinum adducts. The un-conjugated NBD moiety has previously been shown to intercalate between nucleobases of DNA.<sup>17</sup> Therefore it was necessary to understand the influence of a platinum center on its ability to bind DNA. NBD displays a strong emission transition in the range between 530 and 550 nm that is quenched by the addition of a solution of DNA, indicating that intercalation of the NBD fluorophore with



adjacent DNA nucleotides. The results can be cast in the shape of the Scatchard equation and the strength of the intercalation can be efficiently quantified and compared to that of the known intercalator, ethidium bromide (Table 5.1).

Ethidium bromide is a cationic dye that is widely used as a probe for native DNA. The ethidium ion displays a dramatic increase in fluorescence when it intercalates into DNA.<sup>19</sup> As seen in Table 5.1, all Trans-NBD complexes show a decrease in fluorescence when titrated against DNA, indicating the intercalation of the NBD moiety between adjacent DNA nucleobases. The binding strength is similar in all compounds and ligands, and is shown to be stronger than that of ethidium bromide. This fact reinforces the proposed design of the Trans-NBD series and provides for a secondary binding mode in addition to the classical covalent platinum-DNA interaction. The covalent-intercalation, “dual” mode of binding, along with the addition of a “flexible” carbon chain allows the NBD moiety to intercalate between the preferred nucleobases as well as allowing for the modulation of the lipophilicity of the drug.

| Compound         | Binding affinity M <sup>-1</sup>        |
|------------------|---|
| 2-NBD            | $2.37 \times 10^8 \pm 1.33 \times 10^8$ |
| 4-NBD            | $3.96 \times 10^8 \pm 2.53 \times 10^8$ |
| 6-NBD            | $8.30 \times 10^7 \pm 2.20 \times 10^7$ |
| Trans2-NBD       | $7.74 \times 10^8 \pm 5.50 \times 10^8$ |
| Trans4-NBD       | $2.40 \times 10^8 \pm 8.8 \times 10^7$  |
| Trans6-NBD       | $1.39 \times 10^8 \pm 8.4 \times 10^7$  |
| Ethidium Bromide | $1.83 \times 10^7 \pm 2.9 \times 10^6$  |

**Table 5.1** Binding affinities calculated by fluorometric titration using the Scatchard equation for interaction of small molecules with biomolecules. Excitation and emission set at 465 and 535 nm for 2NBD and Trans2NBD; 480 nm and 542 nm for 4NBD and Trans4NBD; 485 nm and 550 nm for 6NBD and Trans6NBD.

### Cytotoxicity of Trans-NBD Compounds

To evaluate the role of both the NBD intercalator and the trans-platinum moiety on the cytotoxicity of each compound,  $IC_{50}$  values for all three Trans-NBD compounds and linkers (platinum-free primary amine ligand with the NBD moiety) was determined in four tumor cell lines. Table 5.2 All complexes are significantly more cytotoxic than the NBD-linker alone. In addition, transplatin is known to be inactive in all four cell lines at similar concentrations.<sup>20</sup> Therefore the increased activity observed is a consequence of the combination of both the platinum center and NBD moiety, resulting in a “synergistic” effect of combining both inactive components. Trans4-NBD and Trans6-NBD are more than twice as potent as cisplatin in the A2780 ovarian cell line and, the less sensitive, HCT116 colorectal carcinoma cell line, while both display analogous behavior in PC3 and MDA cell lines. On the other hand, Trans2-NBD shows a similar or lower profile of activity than cisplatin in all four cell lines (Table 5.2). The use of a longer aliphatic chain, as in Trans4-NBD and Trans6-NBD should allow for greater flexibility and in turn create the potential for both intercalation and covalent platinum-DNA adduct formation. Steric effects of the short two carbon chain likely also play a role in limiting the dual mode of binding. Interesting to note, the Trans-NBD compounds show a greater cytotoxicity profile than the published cisplatin-NBD, the *cis* analogue to Trans2-NBD.<sup>21</sup> This is probably due to the decreased water solubility of the *cis* derivative, resulting in a drastic decrease in cellular accumulation and DNA platination.

| Compound   | IC <sub>50</sub> (μM) A2780 | IC <sub>50</sub> (μM) HCT116 | IC <sub>50</sub> (μM) PC3 | IC <sub>50</sub> (μM) MDA-MB-435 |
|------------|-----------------------------|------------------------------|---------------------------|----------------------------------|
| Cisplatin  | 1.36 ± 0.31*                | 9.15 ± 1.32                  | 6.10 ± 1.02               | 11.71 ± 3.55                     |
| 2-NBD      | >50                         | >50                          | >50                       | >50                              |
| 4-NBD      | >50                         | >50                          | >50                       | >50                              |
| 6-NBD      | >50                         | >50                          | >50                       | >50                              |
| Trans2-NBD | 1.21 ± 0.08                 | 12.56 ± 2.34                 | 9.13 ± 2.50               | 19.90 ± 3.95                     |
| Trans4-NBD | 0.64 ± 0.06                 | 6.61 ± 1.49                  | 5.94 ± 0.34               | 11.36 ± 2.04                     |
| Trans6-NBD | 0.69 ± 0.08                 | 2.70 ± 1.00                  | 5.57 ± 0.61               | 14.67 ± 5.09                     |

**Table 5.2** Cytotoxic activity of the Trans-NBD complexes and linkers against A2780 (ovarian cancer cell line), HCT116 (colorectal carcinoma cell line), PC3 (prostate cancer cell line) and MDA-MB-435 (breast adenocarcinoma cell line).

### Cellular Accumulation and DNA Adduct Formation of Trans-NBD Compounds

Since the cellular accumulation and frequency of DNA adduct formation correlate with the cytotoxic effect of most platinum compounds, the level of cellular uptake and DNA platination of the Trans-NBD series was studied after 24 hour treatment with 10  $\mu\text{M}$  of each drug. All three Trans-NBD complexes accumulate in a similar extent to cisplatin in the HCT116 cell line, while only Trans6-NBD has a better influx/efflux ratio than cisplatin in the A2780 cell line (Table 5.3). However, none of the Trans-NBD complexes reach DNA more effectively than cisplatin (Table 5.3). Assuming that DNA is the biological target for the activity of these compounds, it is clear that the different type of adducts formed after DNA binding and intercalation result in the formation of lesions than are more toxic than traditional bifunctional 1,2-intrastrand DNA crosslinks formed by cisplatin. It is highly likely that these more toxic crosslinks are triggering cell signaling pathways after platination and different repair mechanisms that are crucial for the overall cytotoxicity of the drugs. More interesting is the comparison of cell accumulation and DNA binding ability within the series of Trans-NBD compounds. It is clear that the complexes that are able to accumulate within the cell and bind DNA at a higher extent (Trans4-NBD and Trans6-NBD) and display a more cytotoxic profile in both, A2780 and HCT116 cancer cell lines. In this sense, the lipophilicity of the drug may be playing an important role. It is reasonable to assume that Trans4-NBD and Trans6-NBD, while both being water soluble, will be more lipophilic than Trans2-NBD as a consequence of the longer carbon chain attached to the NBD fluorophore, and thus more capable of entering the cells by means of passive transport through the cell membrane.<sup>22</sup>

| Compound  | A2780          |                 | HCT116        |                |
|-----------|----------------|-----------------|---------------|----------------|
|           | Cell Uptake*   | DNA binding*    | Cell uptake   | DNA binding    |
| Cisplatin | 129.24 ± 4.33  | 868.73 ± 200.98 | 57.86 ± 4.33  | 160.67 ± 72.60 |
| Trans2NBD | 79.61 ± 17.52  | 171.61 ± 84.25  | 45.24 ± 14.27 | 96.57 ± 11.38  |
| Trans4NBD | 95.79 ± 0.51   | 462.04 ± 78.42  | 53.31 ± 2.36  | 148.44 ± 11.84 |
| Trans6NBD | 163.41 ± 11.73 | 364.01 ± 47.28  | 53.85 ± 1.61  | 151.86 ± 15.39 |

**Table 5.3** Cell accumulation and DNA binding for the Trans-NBD series and cisplatin in A2780 and HCT116 cell lines. All values upon treatment with 10  $\mu$ M drug after 24 hours

### Cellular Localization of Trans-NBD Compounds

Finally, knowledge of the processing and distribution of platinum drugs within living cells is of paramount importance. Information about whether the drugs are able to reach their intended target or if they remain in the cytosol and accumulate in other subcellular compartments that are usually associated with drug resistance and export, can provide insight into the differential behavior of platinum compounds. Due to the fluorescent nature of the NBD intercalator, fluorescent confocal microscopy can be used as a tool to examine and understand drug action and metabolism. As seen in Figure 5.2, fluorescent microscopy images of all Trans-NBD compounds in both HCT116 and A2780 cells, show high levels of drug localization throughout the cytosol and to a lesser extent, inside the nucleus. This is consistent with the fact that only about 10% of the cellular platinum reaches the nucleus of the cells. The decreased fluorescence of the Trans-NBD compounds in the nucleus can also be explained due to quenching upon intercalation of the NBD moiety on nuclear DNA. Increased fluorescence is also observed in the vicinity of the nuclear membrane, likely due to drug accumulation within the compartments of the Golgi, responsible for drug efflux and endosome recycling.<sup>23-24</sup> This pattern of Golgi, endosomal/lysosomal accumulation has been noted before with various types of platinum compounds.<sup>25</sup> The observed cell processing of Trans2-NBD is analogous to that of Trans4-NBD, Trans6-NBD and also for the cisplatin analogue Cisplatin-NBD,<sup>21</sup> therefore, suggesting that the frequency and type of DNA adduct formed play a fundamental role in the overall activity of the Trans-NBD series.

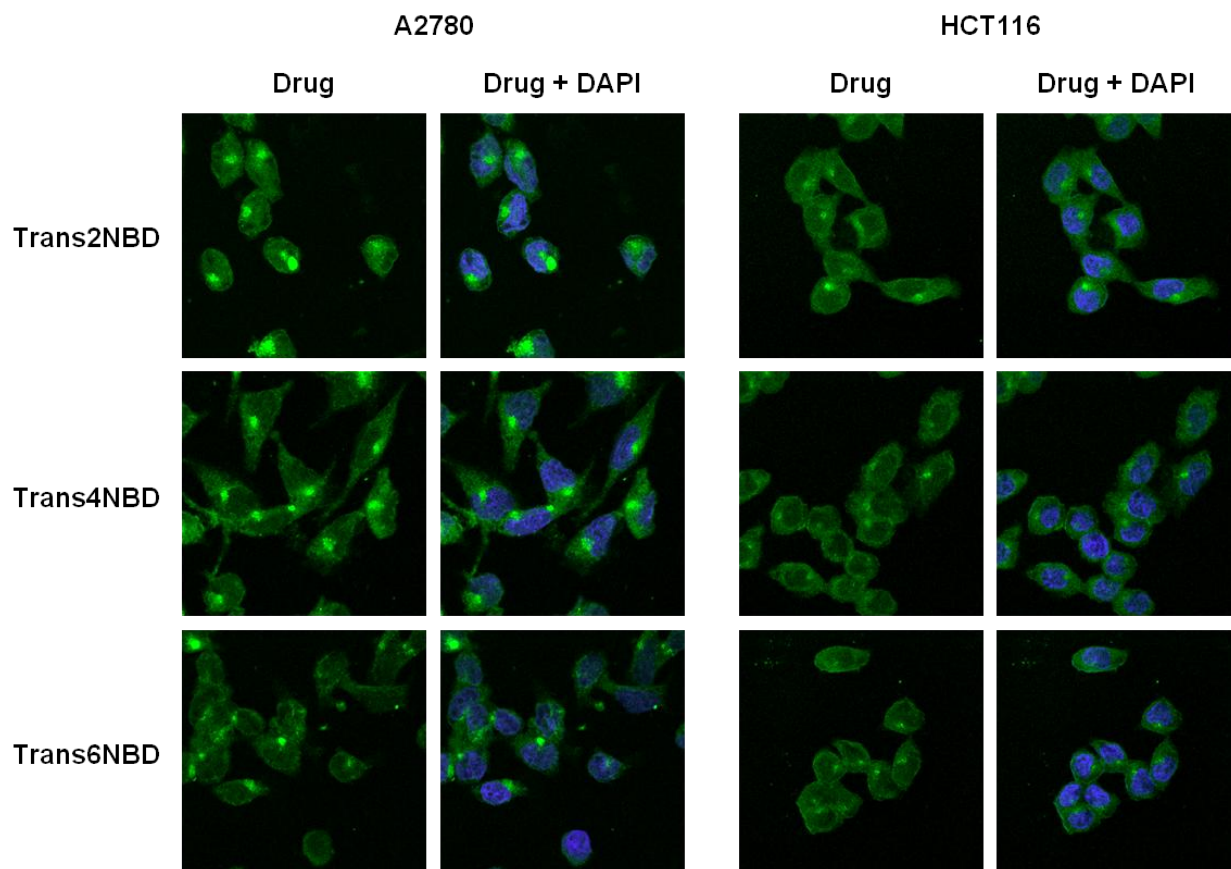


**Figure 5.2** Confocal laser scanning micrographs of A2780 and HCT116 cells. After incubation with Trans-NBD compounds,  $10\mu\text{M}$  for 24hrs at  $37^{\circ}\text{C}$ , cells were fixed and observed by confocal laser scanning microscopy. (left panel) Trans-NBD compounds (green) in A2780 cells + DAPI (blue). (right panel) Trans-NBD compounds (green) in HCT116 cells + DAPI (blue). Cells were grown on 4-well chamber slides (Lab-TekII Chamber Slide) for 2-3 days until cells reached near-confluency. Cells were then incubated with  $10\mu\text{M}$  of each compound for 24hrs. After treatment, slides were fixed with 3% paraformaldehyde and mounted with Vectashield mounting media containing DAPI. Fluorescence was observed by confocal laser scanning microscopy (Zeiss LSM 510).



## **Conclusion**

In conclusion, we have synthesized a new series of *trans* platinum compounds more than twice as potent than cisplatin in the ovarian carcinoma cell line, A2780, and colorectal carcinoma cell line, HCT116. The results of cell uptake and DNA binding suggest that the higher cytotoxicity observed compared to cisplatin is not a consequence of increased cellular accumulation, but of a different and more efficient binding mode to DNA, due to an aliphatic amino ligand that incorporates a planar DNA intercalator. It is believed that all complexes bind covalently the nucleobases of DNA and intercalate between DNA base pairs through the NBD moiety. Also, the NBD-DNA intercalations show a stronger affinity than that observed for ethidium bromide. This dual mode of binding likely activates cell signaling pathways and therefore overcomes cisplatin-DNA repair mechanisms. When compared within the series of Trans-NBD complexes, there is a good correlation between, lipophilicity, cell accumulation, DNA binding and cytotoxicity. Fluorescent microscopy shows that the complexes accumulate preferentially in the cytosol, with areas of strong fluorescence close to the nuclear membrane, where the lysosomes and Golgi apparatus are typically located. This dual mode of DNA-binding, covalent and non-covalent, allow for a distinctly different cytotoxicity profile that that of cisplatin and could allow for the development of a new class of platinum based chemotherapeutics able to overcome current platinum drug resistance and expand the range of tumors currently treatable with clinical platinum drugs.

## **Materials and Methods**

### **Synthesis of Ligands and Platinum Complexes**

***N*-(7-nitro-2,1,3-benzoxadiazol-4-yl)ethane-1,2-diamine (2-NBD); *N*-(7-nitro-2,1,3-benzoxadiazol-4-yl)butane-1,4-diamine (4-NBD); *N*-(7-nitro-2,1,3-benzoxadiazol-4-yl)hexane-1,6-diamine (6-NBD):** BOC–diaminoethane/BOC–diaminobutane/BOC–diaminohexane was dissolved in ethanol containing a 10% w/w of Na<sub>2</sub>CO<sub>3</sub>, and NBD-Cl was added. The mixture was stirred at room temperature overnight, then water was added and the product was extracted with diethyl ether. The organic phase was washed with brine, dried over Na<sub>2</sub>SO<sub>4</sub> and purified by flash chromatography (CHCl<sub>3</sub>:EtOAc, 88:12 / 75:25 / 70:30 for 2-NBD, 4-NBD and 6-NBD respectively). The BOC protecting group of the purified intermediate was removed by using trifluoroacetic acid (2 ml) at room temperature. After the mixture had been stirred overnight, excess TFA was evaporated, and the oily product was treated with diethyl ether to yield the trifluoroacetate salt as orange crystals. The compound was neutralized by dissolving it in a mixture H<sub>2</sub>O/Ethanol 1:1 and addition of 1 equivalent of NaOH. The neutral ligand was then extracted with CH<sub>2</sub>Cl<sub>2</sub>. The organic fractions were dried over K<sub>2</sub>CO<sub>3</sub> and the solvent removed under vacuum. The product was dried under vacuum overnight. The absence of TFAcetate was confirmed by <sup>19</sup>F NMR.

***Trans*-[PtCl<sub>2</sub>((*N*-NBD)ethane-1,2-diamine)(NH<sub>3</sub>)] (*Trans*2-NBD):** Cisplatin (26 mg, 0.087 mmol) was suspended in 5 ml of deionized water and one equivalent of AgNO<sub>3</sub> was added. The mixture was stirred at 45°C for 4.5 hours, then cooled to 5°C for 2 hours to allow full precipitation of AgCl. The silver white salt was double filtered through

a nylon membrane with a porous size of 0.45  $\mu$ m. To that pale yellow filtrate, the amino ligand was added (19.34 mg, 0.087 mmol). That solution was stirred at room temperature overnight, then filtered. 1.5 ml of HCl 37% were added and the resulting solution was stirred at 75°C for 5 hours. The orange clear solution was concentrated under vacuum until a precipitate appeared (~ 3 ml) and then cooled to 5°C to complete the precipitation of the final product. The orange powder was filtered, washed with ice-cold water, ice-cold ethanol and ether, then dried under vacuum for 24 hours.  $^1\text{H}$  NMR  $\text{D}_2\text{O}$   $\delta$  (ppm): 8.47(d, 1H); 6.35 (d, 1H); 3.82 (t, 2H); 3.28 (t, 2H).  $^{195}\text{Pt}$  NMR  $\text{D}_2\text{O}$   $\delta$  (ppm): 2148(s)

**Trans-[PtCl<sub>2</sub>((N-NBD)butane-1,4-diamine)(NH<sub>3</sub>)] (Trans4-NBD):** The same procedure as described for Trans2-NBD was followed.  $^1\text{H}$  NMR  $\text{D}_2\text{O}$   $\delta$  (ppm): 8.36(d, 1H); 6.23 (d, 1H); 3.49 (m, 2H); 2.91 (m, 2H); 1.69 (m, 2H).  $^{195}\text{Pt}$  NMR  $\text{D}_2\text{O}$   $\delta$  (ppm): 2158(s)

**Trans-[PtCl<sub>2</sub>((N-NBD)hexane-1,6-diamine)(NH<sub>3</sub>)] (Trans6-NBD):** The same procedure as described for Trans2-NBD was followed.  $^1\text{H}$  NMR  $\text{D}_2\text{O}$   $\delta$  (ppm): 8.36(d, 1H); 6.23 (d, 1H); 3.45 (m, 2H); 2.85 (m, 2H); 1.66 (m, 2H); 1.54 (m, 2H); 1.32 (m, 2H).  $^{195}\text{Pt}$  NMR  $\text{D}_2\text{O}$   $\delta$  (ppm): 2164(s). EA calculated for C<sub>12</sub> H<sub>20</sub> N<sub>6</sub> O<sub>3</sub> Pt Cl<sub>2</sub>: C, 25.63; H, 3.59; N, 14.94. Found: C, 25.63; H, 3.57; N, 14.96.

### Cell System

HCT116 and A2780 cell lines were cultured in RPMI 1640 (Invitrogen), supplemented with 10% calf serum (Atlanta Biologicals) and 1% penicillin/streptomycin (Invitrogen). Cells were maintained in logarithmic growth as a monolayer in T75 culture flasks at 37°C in a humidified atmosphere containing 5% CO<sub>2</sub>.

### Cellular Growth Inhibition

The MTT assay was used to determine growth inhibition potency of platinum drugs.<sup>26</sup> A2780, HCT116, PC3 and MDA-MB-435 cells were seeded in 96-well plates at 6.5k cells/well for A2780, 5k cells/well for HCT116 and MDA-MB-435, and 10k cells/well for PC3 and allowed to attach overnight. RPMI 1640 media was removed and 200µL of each compound was added after serial dilution to treatment concentrations [50µM – 0.78µM] in quadruplicate wells and exposed to cells for 72h. Plates were then washed with PBS and 100µL of 5mg/mL MTT solution was added. MTT solution was incubated with cells for 3h at 37°C. After incubation, MTT solution was removed and 100µL of DMSO was added. Quantification of cell growth in treated and control wells was then assessed by measurement of absorbance at 562nm. IC<sub>50</sub> values were determined by using the standard curve analysis of SigmaPlot.

### Cellular Drug Accumulation and Quantification of DNA-Drug Adducts

A2780 or HCT116 cells were plated in 10cm dishes at 2 million cells/dish and allowed to attach overnight. Cells were then treated with 10µM of each drug for 24hrs. After 24hrs, drug solution was removed and plates were washed 3x with PBS. Cells were then removed from the dish with trypsin and centrifuged for 5min at 1000xg. Media was

removed, cell pellet was washed three times with PBS, cells were counted and resuspended in 250 $\mu$ L of ddH<sub>2</sub>O. Samples were digested following published methods.<sup>27</sup> For DNA analysis experiments, DNA was extracted using a DNeasy blood and tissue kit (Qiagen) according to the manufacturer's protocol. Extent of DNA platination and cellular platinum accumulation was measured on a Varian ICP-MS.

### Fluorescence Spectrophotometric Titration

Excitation and emission wavelengths were set to 465 and 535 nm for the ligand 2-NBD and complex Trans2-NBD; to 480 nm and 542 nm for the ligand 4-NBD and the complex Trans4-NBD and 485 nm and 550 nm for the ligand 6-NBD and the complex Trans6-NBD. Bandwidths were set to 5 nm and 20 nm for the excitation and the emission, respectively. All fluorescence spectra were measured in a Cary Spectrophotometer instrument with an arc xenon lamp. The absorption of the sample at the wavelength of excitation was less than 0.1 in order to obviate inner filter effects. The fluorimetric titration was carried out at room temperature. Fixed amounts (10  $\mu$ l) of a 12.5 mM solution of CT DNA were added to a 0.4  $\mu$ M solution of the metal complex, both in Tris/HCl buffer (5mM Tris/HCl and 50 mM NaClO<sub>4</sub>, pH = 7.39) and emission spectra were monitored until saturation was reached. Binding data were cast into the form of a Scatchard plot of  $r/C_f$  vs.  $r$  using the equation  $r/C_f = K(n-r)$  for ligand-macromolecule interactions with non-cooperative binding sites<sup>28-30</sup>, where  $r$  is the number of moles of Ru complex bound to 1 mol of CT DNA ( $C_b/C_{DNA}$ ),  $n$  is the number of equivalent binding sites, and  $K$  is the affinity of the complex for those sites.  $\alpha$  was calculated according to  $\alpha = (F_f - F)/(F_f - F_b)$ , where  $F_f$  and  $F_b$  are the fluorescence of the

free and fully bound drug at the selected wavelength, and  $F$  is the fluorescence at any given point during the titration.<sup>31</sup>  $K_b$  is obtained from the slope of the plot.

#### Confocal Laser Scanning Microscopy

A2780 and HCT116 cells were grown on 8-well chamber slides (Lab-TekII Chamber Slide) for 2-3 days until cells reached near-confluency. The cells were treated with Trans2-NBD, Trans4-NBD, and Trans6-NBD (10 $\mu$ M) for 24hrs. After treatment, slides were washed 3x with ice-cold PBS and fixed with 3% paraformaldehyde. Paraformaldehyde was removed and cells were washed again with 3x PBS and allowed to dry. Slides were then mounted with Vectashield mounting media containing DAPI. Fluorescence was observed by confocal laser scanning microscopy (Zeiss LSM 510).

### List of References

1. Alderden, R.A., Hall, M.D. & Hambley, T.W. The Discovery and Development of Cisplatin. *Journal of Chemical Education* **83**, 728-null (2006).
2. Farrell, N. *Platinum-Based Drugs in Cancer Therapy*, (Humana Press, 2000).
3. Galanski, M., Jakupec, M.A. & Keppler, B.K. Update of the Preclinical Situation of Anticancer Platinum Complexes: Novel Design Strategies and Innovative Analytical Approaches. *Current Medicinal Chemistry* **12**, 2075-2094 (2005).
4. Jamieson, E.R. & Lippard, S.J. Structure, Recognition, and Processing of Cisplatin-DNA Adducts. *Chem Rev* **99**, 2467-2498 (1999).
5. Aris, S.M. & Farrell, N.P. Towards Antitumor Active trans-Platinum Compounds. *European Journal of Inorganic Chemistry* **2009**, 1293-1302 (2009).
6. Coluccia, M. & Natile, G. Trans-platinum complexes in cancer therapy. *Anticancer Agents Med Chem* **7**, 111-123 (2007).
7. Farrell, N., *et al.* Cytostatic trans-platinum(II) complexes. *Journal of Medicinal Chemistry* **32**, 2240-2241 (1989).
8. Kalayda, G., *et al.* Dinuclear platinum complexes with N, N'-bis(aminoalkyl)-1,4-diaminoanthraquinones as linking ligands. Part II. Cellular processing in A2780 cisplatin-resistant human ovarian carcinoma cells: new insights into the mechanism of resistance. *J Biol Inorg Chem* **9**, 414-422 (2004).
9. Kalayda, G.V., Jansen, B.A.J., Wielaard, P., Tanke, H.J. & Reedijk, J. Dinuclear platinum anticancer complexes with fluorescent N,N'-bis(aminoalkyl)-1,4-diaminoanthraquinones: cellular processing in two cisplatin-resistant cell lines

- reflects the differences in their resistance profiles. *J Biol Inorg Chem* **10**, 305-315 (2005).
10. Klein, A.V. & Hambley, T.W. Platinum Drug Distribution in Cancer Cells and Tumors. *Chemical Reviews* **109**, 4911-4920 (2009).
  11. Alderden, R.A., Mellor, H.R., Modok, S., Hambley, T.W. & Callaghan, R. Cytotoxic efficacy of an anthraquinone linked platinum anticancer drug. *Biochemical Pharmacology* **71**, 1136-1145 (2006).
  12. Kalayda, G., Wagner, C., BuSZ, I., Reedijk, J. & Jaehde, U. Altered localisation of the copper efflux transporters ATP7A and ATP7B associated with cisplatin resistance in human ovarian carcinoma cells. *BMC Cancer* **8**, 175 (2008).
  13. Liang, X.-J., *et al.* Trafficking and localization of platinum complexes in cisplatin-resistant cell lines monitored by fluorescence-labeled platinum. *Journal of Cellular Physiology* **202**, 635-641 (2005).
  14. Farrell, N. *Metal Ions in Biological Systems*, (Marcel Dekker, Inc., New York, 2004).
  15. Radulovic, S., Tesic, Z. & Manic, S. Trans-platinum complexes as anticancer drugs: recent developments and future prospects. *Curr Med Chem* **9**, 1611-1618 (2002).
  16. Weiss, R.B. & Christian, M.C. New Cisplatin Analogues in Development: A Review. *Drugs* **46**, 360-377 (1993).
  17. Thiagarajan, V., Rajendran, A., Satake, H., Nishizawa, S. & Teramae, N. NBD-Based Green Fluorescent Ligands for Typing of Thymine-Related SNPs by Using an Abasic Site-Containing Probe DNA. *ChemBioChem* **11**, 94-100 (2010).



18. Natile, G. & Coluccia, M. Current status of trans-platinum compounds in cancer therapy. *Coordin Chem Rev* **216-217**, 383-410 (2001).
19. Waring, M.J. Complex formation between ethidium bromide and nucleic acids. *Journal of Molecular Biology* **13**, 269-282 (1965).
20. Leng, M., *et al.* Replacement of an NH<sub>3</sub> by an Iminoether in Transplatin Makes an Antitumor Drug from an Inactive Compound. *Mol Pharmacol* **58**, 1525-1535 (2000).
21. Benedetti, B.T., *et al.* Effects of non-covalent platinum drug-protein interactions on drug efficacy: Use of fluorescent conjugates as probes for drug metabolism. in *In Submission* (2011).
22. Andrews, P.A., Velury, S., Mann, S.C. & Howell, S.B. cis-Diamminedichloroplatinum(II) Accumulation in Sensitive and Resistant Human Ovarian Carcinoma Cells. *Cancer Res* **48**, 68-73 (1988).
23. De Matteis, M.A. & Luini, A. Exiting the Golgi complex. *Nat Rev Mol Cell Biol* **9**, 273-284 (2008).
24. Glick, B.S. & Nakano, A. Membrane Traffic Within the Golgi Apparatus. *Annual Review of Cell and Developmental Biology* **25**, 113-132 (2009).
25. Safaei, R., *et al.* Intracellular Localization and Trafficking of Fluorescein-Labeled Cisplatin in Human Ovarian Carcinoma Cells. *Clinical Cancer Research* **11**, 756-767 (2005).
26. Cory, A., Owen, T., Barltrop, J. & Cory, J. Use of an aqueous soluble tetrazolium/formazan assay for cell growth assays in culture. *Cancer Communications* **3**, 207-212 (1991).

27. Harris, A.L., *et al.* Synthesis, characterization, and cytotoxicity of a novel highly charged trinuclear platinum compound. Enhancement of cellular uptake with charge. *Inorganic Chemistry* **44**, 9598-9600 (2005).
28. Cusumano, M., Di Pietro, M.L. & Giannetto, A. Stacking Surface Effect in the DNA Intercalation of Some Polypyridine Platinum(II) Complexes. *Inorg Chem* **38**, 1754-1758 (1999).
29. McGhee, J.D. & von Hippel, P.H. Theoretical aspects of DNA-protein interactions: Co-operative and non-co-operative binding of large ligands to a one-dimensional homogeneous lattice. *Journal of Molecular Biology* **86**, 469-489 (1974).
30. Wei, C., Jia, G., Yuan, J., Feng, Z. & Li, C. A Spectroscopic Study on the Interactions of Porphyrin with G-Quadruplex DNAs†. *Biochemistry* **45**, 6681-6691 (2006).
31. Satyanarayana, S., Dabrowiak, J.C. & Chaires, J.B. Neither .DELTA.- nor .LAMBDA.-tris(phenanthroline)ruthenium(II) binds to DNA by classical intercalation. *Biochemistry* **31**, 9319-9324 (1992).

## Chapter 6: Conclusion

While platinum chemotherapy represents one of the most utilized forms of cancer treatment, all current therapies have innate problems due to inherent tumor resistance and a limited availability of susceptible tumor types. The inherent resistance of these tumors and the toxic side effects associated with platinum chemotherapy are, in part, a result of metabolic deactivation. By understanding the balance between cytotoxic activity and metabolic deactivation it may be possible to defer many of the toxic side effects associated with chemotherapeutics, and thus provide for substantial increases in mean tolerated dosages and increase the number of tumors treatable by platinum drugs. Two possible ways to diminish these types of metabolic interactions have been described in this thesis and are (1) through the use of carboxylates ligands to “fine-tune” the reactivity of trans-platinum compounds and thus balance the cytotoxic and pharmacokinetic profiles and (2) through the introduction of a non-covalent antitumor agent, TriplatinNC, which not only presents a new mode of DNA binding, distinct from any clinical platinum agent, but also allows for the elimination of covalent Pt-protein adduct formation.

While the *cis* platinum geometry has yielded three clinical platinum based drugs, the second factor in the success of any platinum chemotherapeutic is the range of treatable tumor types over that of the current clinical regime. By extending the platinum geometry to include *trans* based platinum derivatives, this work has also attempted to create platinum compounds which are able to treat tumor types other than that of cisplatin and other *cis* based compounds. By developing a series of Trans-NBD

compounds which include a transplatinum DNA binding agent and a DNA intercalator, we have created transplatinum based drugs which show significant improvements in cytotoxic activity over than of cisplatin. The goal is to combine both improvements in metabolic deactivation and novel antitumor profiles thus creating a class of compounds which can outperform the current clinical antitumor platinum drugs and ultimately provide for a promising outlook for the future of cancer chemotherapeutic treatments.

## Appendix A: TriplatinNC, a Nucleolar-Targeting Agent, Disrupts rRNA Transcription Leading to G1 Arrest and p53-independent Apoptosis

Erica J. Peterson<sup>a</sup>, Vijay R. Menon<sup>b</sup>, Peyman Kabolizadeh<sup>c</sup>, Brad T. Benedetti<sup>a</sup>, Ralph Kipping<sup>a</sup>, John J. Ryan<sup>c</sup>, Lawrence F. Povirk<sup>b</sup>, Nicholas P. Farrell<sup>a1</sup>

<sup>a</sup>Departments of Chemistry, <sup>b</sup>Pharmacology/Toxicology, and <sup>c</sup>Biology; Massey Cancer Center, Virginia Commonwealth University, Richmond, VA 23298

Confocal Microscopy Studies performed by Brad T. Benedetti

Submitted to PNAS 2011

### **Abstract**

TriplatinNC is a highly positively charged, (+8) noncovalent derivative of the phase II clinical platinum drug, BBR3464. TriplatinNC exhibits a distinct mode of high affinity DNA interaction, increased levels of cellular accumulation, and a significant cytotoxic profile in mastocytoma, ovarian carcinoma, and cisplatin-resistant ovarian carcinoma cell lines. Here, it is shown, through use of fluorescent-tagging and confocal colocalization experiments that TriplatinNC rapidly localizes to the nucleolar compartment in HCT116 and A2780 cells. Due to its cationic nature, it was considered that TriplatinNC likely interacts with nucleic acid components of the nucleolus, that is, ribosomal DNA, and its transcripts. <sup>32</sup>P-metabolic labeling of HCT116 cells determined that the production rate of 47S rRNA precursor transcripts is drastically reduced as an early event after drug treatment. Subsequently, there is a marked increase in p53

protein at 12hrs, followed by a robust and continuous G1 arrest at 24 and 48hrs. Morphological characteristics of the apoptotic process are apparent within 24hrs, including: reduction in cell size, membrane blebbing, and cytosolic vacuolization. TriplatinNC induces cleavage of mitochondrial-dependent and -independent initiators of apoptosis, procaspase-9 and -8, followed by activation of the effector procaspase-3, and downstream target, Parp-1. Furthermore, utilizing the isogenic HCT116 p53+/+ and p53-/- cell lines, it was determined that these processes, are not dependent upon the presence of p53 protein.

### **Introduction**

The increased proliferative rate of cancer cells relies on a concomitant upregulation of ribosomal biogenesis in order to meet the cellular demands for protein synthesis<sup>1-4</sup>. The biogenesis of ribosomes is a coordinated process that largely takes place in the nucleolar compartment of the cell. The nucleolus is formed around tandem arrays of more than 400 copies of ribosomal RNA (rRNA) genes as they are transcribed, processed, and assembled into ribosomal subunits<sup>5</sup>. Recently, rRNA synthesis has emerged as a shared target of many anticancer agents<sup>6</sup>. The platinum-based drugs, oxaliplatin, and to a lesser extent, cisplatin, inhibit the transcriptional rate of the 47S rRNA precursor transcript, while the antimetabolite, 5-fluorouracil (5-FU), disrupts processing of the precursor into mature 28S, 18S, and 5.8S rRNA transcripts. In each case, the effects are surprisingly early events; observed within hours after cell treatment. This implies that inhibition of rRNA processes may be an early determinant of the antiproliferative activity of these drugs. Of course, the effects of oxaliplatin, cisplatin,

and 5-FU are not limited to rRNA processes. They are nonselective, genotoxic drugs that modify, or incorporate into the total pool of nucleic acid <sup>7-9</sup>. Limiting genotoxic events by drug-targeting only nucleic acid within the nucleolus and specifically, rRNA synthesis, is an interesting challenge for small molecule therapeutics.

Unlike the nucleus and other membrane-bound organelles, there is no evidence of a membrane or membrane-like structure separating the nucleolus from the surrounding nucleoplasm. In theory, any soluble molecule could diffuse in and out of the nucleolar compartment. Because of sequence similarities in nuclear and nucleolar localization signals, it is currently accepted that targeting of a specific molecule to the nucleolus results from its direct or indirect interaction with components of the nucleolus, that is, ribosomal DNA and its transcripts <sup>10</sup>. Positive charge is a major factor in localization and retention of proteins to the nucleolus. Mutagenesis studies of nucleolar proteins, such as nucleolin, fibrillarin, and the viral HIV TAT, determined that clusters of the positively charged amino acids arginine, and lysine serve as nucleolar localization signals <sup>11-12</sup>. Furthermore, poly-arginines and -lysines, containing more than six amino acids, rapidly penetrate cellular membranes and localize specifically to the nucleolar region of cells <sup>13-15</sup>.

TriplatinNC is a highly positively charged, (+8) non-covalent derivative of the phase II clinical platinum drug, BBR3464 <sup>16</sup> (Fig. A.1 A,B). The crystal and molecular structure of TriplatinNC associated with a double-stranded B-DNA dodecamer 5'-d(CGCGAATTCGCG)<sub>2</sub> at 1.2 Å resolution (PDB:2DYW), shows formation of phosphate clamps, involving two modes of DNA binding: "backbone-tracking", by following along the phosphate backbone of one strand, or "groove-spanning", by crossing over the

minor groove to interact with both strands <sup>17</sup>. The phosphate clamp motif is a discrete third mode of DNA binding, distinct from intercalation or minor groove binding. These interactions are mediated through hydrogen bonding, and are analogous to the "arginine fork", an important motif for protein-DNA interactions, where positively charged guanidino groups of arginine, interact with negatively charged oxygens of DNA phosphate <sup>18-20</sup>, (Fig. A.1C). We have extended this analogy with the hypothesis that the charged nature of TriplatinNC, like poly-arginines, may facilitate its localization to the nucleolar compartment within cells.

In this report, we reveal remarkable differences in the cellular localization pattern of TriplatinNC compared to cisplatin. The fluorophore-drug conjugate, TriplatinNC-NBD, but not cisplatin-NBD, rapidly accumulates within the nucleolar region of the cell. As an early event upon cellular treatment with TriplatinNC, there is a resulting decrease in the production rate of 47S rRNA precursor transcripts. Further studies detailed in this report set a timeline of the subsequent morphological, antiproliferative, and apoptotic events.



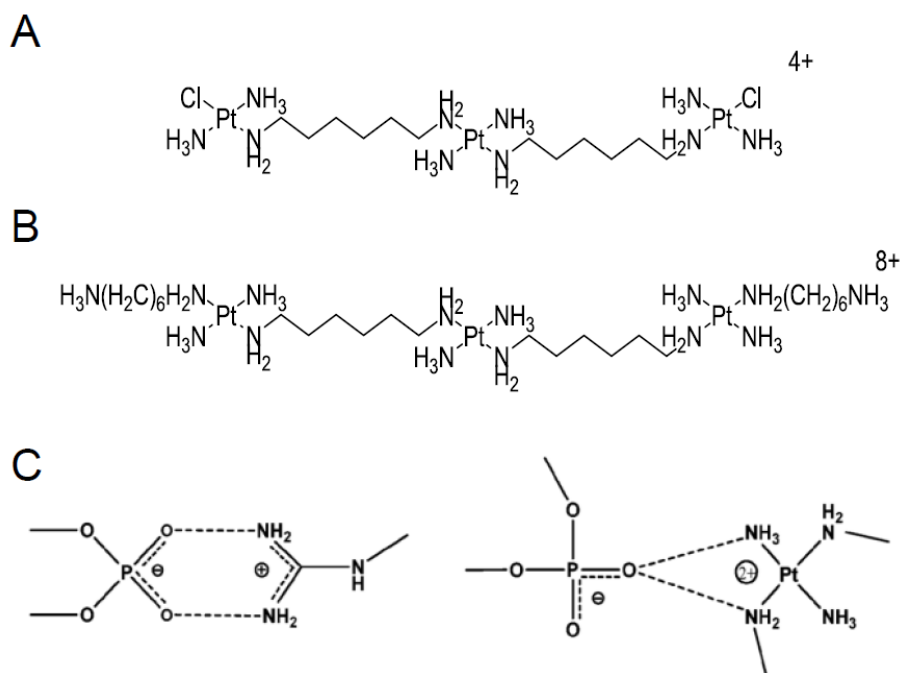


**Figure A.1** Structures of (A) BBR3464 and (B) TriplatinNC. The noncovalent polynuclear compound, TriplatinNC, is a direct structural analog of the Phase II drug BBR3464, where the labile chloride ion is replaced by the amine group,  $\text{NH}_2(\text{CH}_2)_6\text{NH}_2$ . (C) Chemical similarity of "arginine-fork" (left), and "phosphate-clamp" (right) interactions, <http://pubs.rsc.org/en/Content/ArticlePDF/2010/CC/C0CC01254H>

## Results and Discussion

**TriplatinNC rapidly accumulates within the nucleolus.** To determine differences in the cellular localization pattern of TriplatinNC compared to Cisplatin, each compound was labeled with the small fluorophore, 7-nitrobenzoxadiazole (NBD). The resulting drug-NBD conjugates, Cisplatin-NBD and TriplatinNC-NBD (Fig. A.2A), retain charge properties and inhibitory concentration (IC) values comparable to that of the parent compounds (Fig. A.3). Confocal microscopy showed that TriplatinNC-NBD, but not Cisplatin-NBD, rapidly accumulates to punctate regions of the nucleus in HCT116 colon carcinoma and A2780 ovarian carcinoma cell lines (Figure A.2 B,C). In colocalization studies, the distinct nuclear localization patterns of TriplatinNC overlaps the signal of the commonly used nucleolar marker, Fibrillarin, a ribonucleoprotein methyltransferase involved in the first steps of ribosomal RNA (rRNA) processing (Figure A.2D). Due to this unique pattern of localization, and the charged nature of the drug, it was considered that TriplatinNC was likely to interact with ribosomal DNA/RNA within the nucleolus.

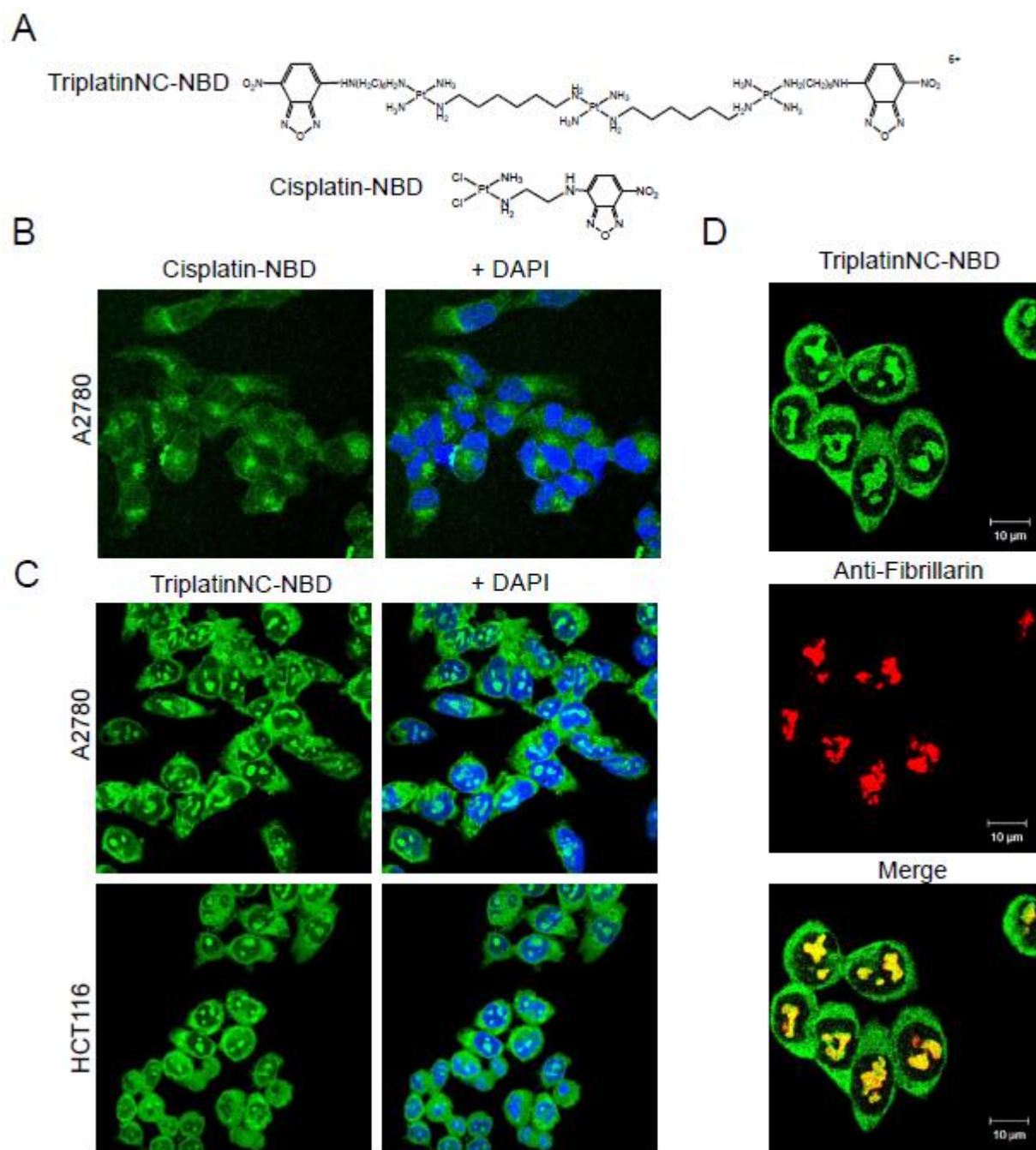


**Figure A.2** Fluorescently-tagged TriplatinNC localizes to the nucleolus. (A.) Structures; Fluorophore conjugates Cisplatin-NBD and TriplatinNC-NBD. (B.) Confocal Microscopy; The cellular distribution of NBD-Cisplatin (green) in A2780 cells after 24hrs incubation in 10 $\mu$ M drug. (C.) NBD-TriplatinNC (green) in A2780 and HCT116 cells after 2hrs incubation with 20 $\mu$ M drug, respectively. The DNA is subsequently stained with DAPI (blue) as reference. (D.) Colocalization (orange) of NBD-TriplatinNC (green) with the nucleolar marker, fibrillarin (red), in HCT116 cells after 4hrs incubation in 20 $\mu$ M drug. Anti-fibrillarin signal was detected using a secondary antibody conjugated to Alexa-fluor 647.

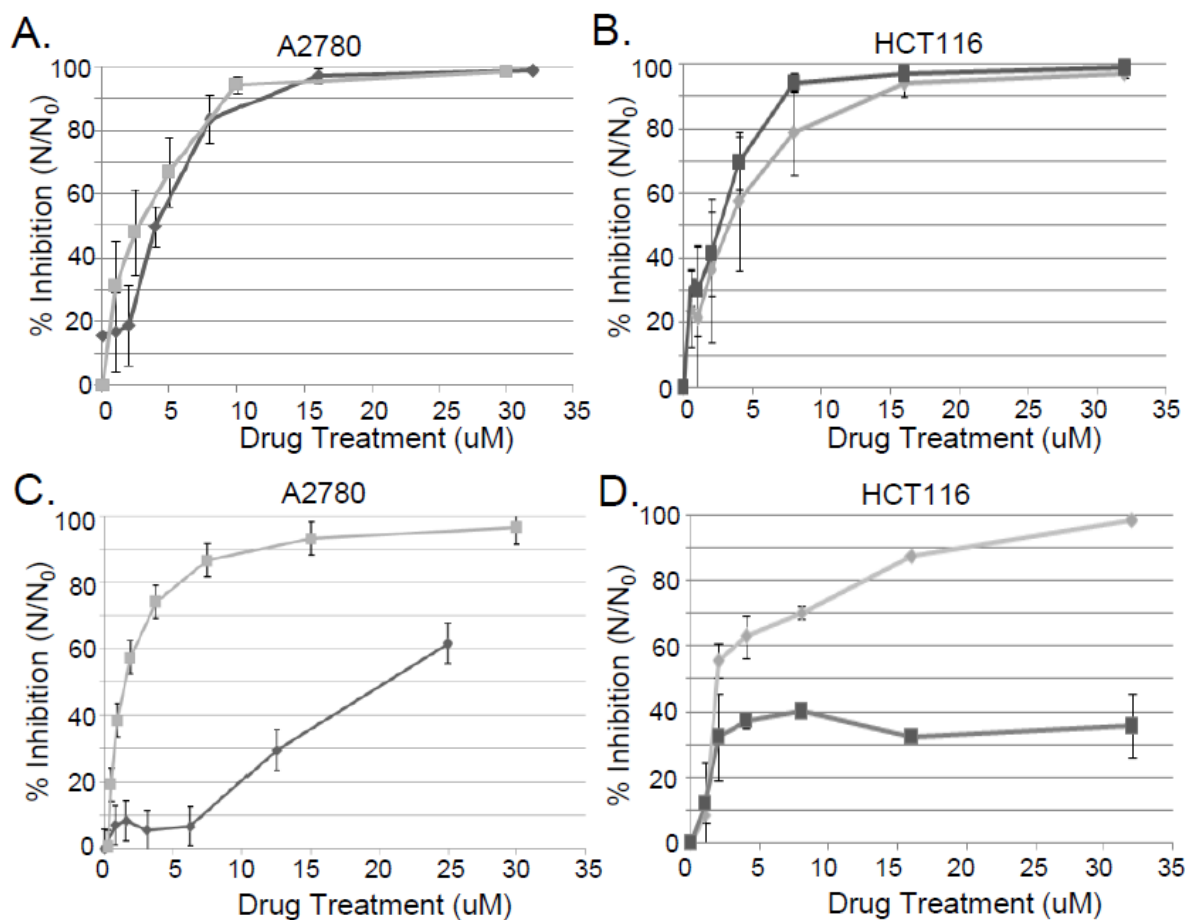


**Figure A.3** MTT Assay; A2780 or HCT116 cells were treated with the indicated concentration of drug for 72hrs. In each graph the drug-NBD derivative is denoted in dark gray and the parent compound in light gray. (A.) A2780 cells treated with TriplatinNC-NBD and TriplatinNC. (B.) HCT116 cells treated with TriplatinNC-NBD and TriplatinNC. (C.) A2780 cells treated with Cisplatin-NBD and Cisplatin. (D.) HCT116 cells treated with Cisplatin-NBD and Cisplatin. Percent Inhibition is calculated as:  $1-(N/N_0)$ , where  $N$ =treated samples and  $N_0$ = untreated control samples. Data are shown as mean  $\pm$  s.d. representative of at least 2 independent experiments.

**As an early event, TriplatinNC disrupts the rate of rRNA transcription.** Initiation of rDNA transcription requires assembly of a specific multiprotein complex that binds to the rDNA promoter containing RNA Polymerase I (Pol I), and two Pol I specific transcription factors, upstream binding protein (UBF), and the promoter selectivity factor complex, SL1<sup>21</sup>. The binding specificity of Pol I at rDNA promoters is conferred by SL1<sup>22</sup>, comprised of the transcription factor TBP (TATA-Box Binding Protein) and several auxiliary TBP-associated factors<sup>23-24</sup>. The ability of TriplatinNC to inhibit the interactions of TBP with DNA was examined *in vitro* using the Electromobility Shift Assay (EMSA). TriplatinNC was found to reduce TBP-DNA complex by 50% using between 0.63 and 1.25 $\mu$ M drug concentrations (Fig. A.4A), which is nearly 100-fold more effective than the similar, less positively charged (+6) platinum agent, AH44 (Fig. A.5). This study suggests the possibility that TriplatinNC may inhibit RNA transcription by displacing DNA-binding proteins required for this process.

To determine whether TriplatinNC affects the rate of rRNA transcription *in vivo*, HCT116 cells were treated with varying drug concentrations for 5.5hrs, and then metabolically labeled according to the scheme depicted in Fig. A.4B. The 47S rRNA precursor transcript is sequentially cleaved to yield the mature 28S, 18S, and 5.8S rRNAs. As cells are pulsed with <sup>32</sup>P-radiolabeled orthophosphate for 30 min. followed by a 3h chase, the abundance of newly formed 47S precursors, 32S intermediate cleavage products, and mature 28S and 18S rRNAs are sufficiently labeled for visualization by autoradiography (6). It was evident that treatment of cells with TriplatinNC inhibits the production rate of 47S rRNA precursor transcripts in a dose dependent manner (Figure A.4B). It does not appear that TriplatinNC affects the rate of 47S rRNA processing, as

the abundance of 32S, 28S, and 18S rRNAs decrease proportionally to that of the precursor.

The transcriptional activity of rRNA genes has been shown to change in accordance with the cell cycle<sup>25</sup>. rRNA transcription levels are highest in S and G<sub>2</sub> phases, nonexistent in mitosis, and rebounding in G<sub>1</sub><sup>26-27</sup>. Therefore, it was important to consider whether the inhibitory effect of TriplatinNC on the rate of rRNA transcription was direct, or if rRNA transcription levels were merely downregulated as an indirect effect of changes within the cell cycle. The latter would be likely if there were an increase in the population of cells in G<sub>1</sub> (when rRNA levels are lower). For this purpose, HCT116 cells treated with TriplatinNC were subjected to cell cycle analysis by flow cytometry (Figure A.6 A, B). In cells treated with 20 $\mu$ M TriplatinNC ([IC<sub>90</sub>]) for 6hrs, there were modest changes that occurred within the cell cycle. The population of cells in G<sub>1</sub> decreases slightly from 37% to 30% compared to untreated control cells, while the population of cells within S+G<sub>2</sub> increases slightly from 63% to 70%. These results imply the disruption of rRNA transcription is an early event of cellular treatment with TriplatinNC, and does not result from changes in the cell cycle.

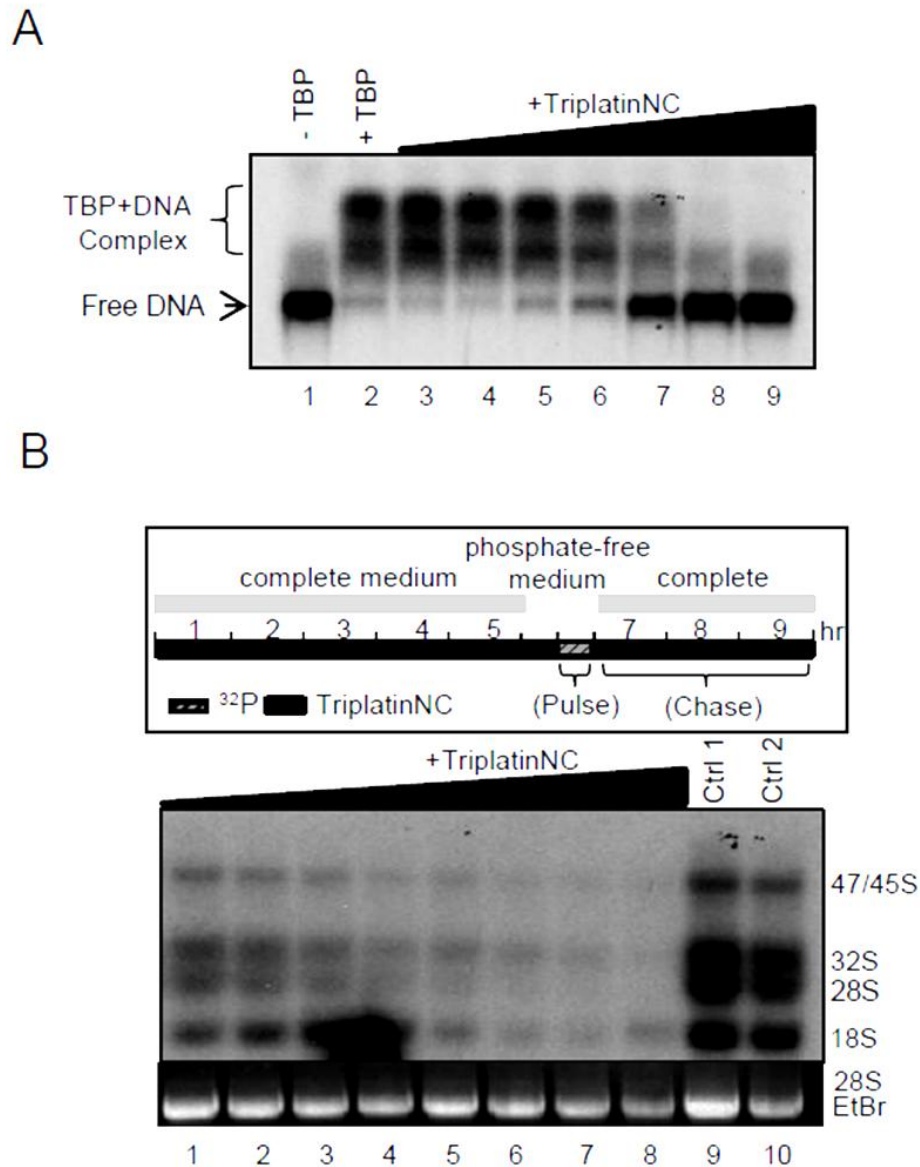


**Figure A.4** TriplatinNC competitively inhibits TBP-DNA interaction and interferes with rRNA transcription. (A.) EMSA; Lanes 3-9; 2nM  $^{32}\text{P}$ -labeled DNA incubated with 0.08, 0.16, 0.31, 0.63, 1.25, 2.5, and 5  $\mu\text{M}$  drug, respectively, followed by 100ng rTBP protein. Lane 2 is the 'TBP/DNA complex' positive control. Lane 1 is the 'free DNA' control containing DNA only. (B.)  $^{32}\text{P}$ -Pulse/Chase Metabolic Labeling; Samples were treated with or without drug according to the experimental outline. Lanes 1-8 were treated with 0.78, 1.6, 3.1, 6.3, 12.5, 25, 50, 100  $\mu\text{M}$  drug, or without drug in lanes 1 and 2. 1.5  $\mu\text{g}$ s total RNA was analyzed for each sample. Ethidium Bromide (EtBr) staining of 28S rRNA was used as a loading control.

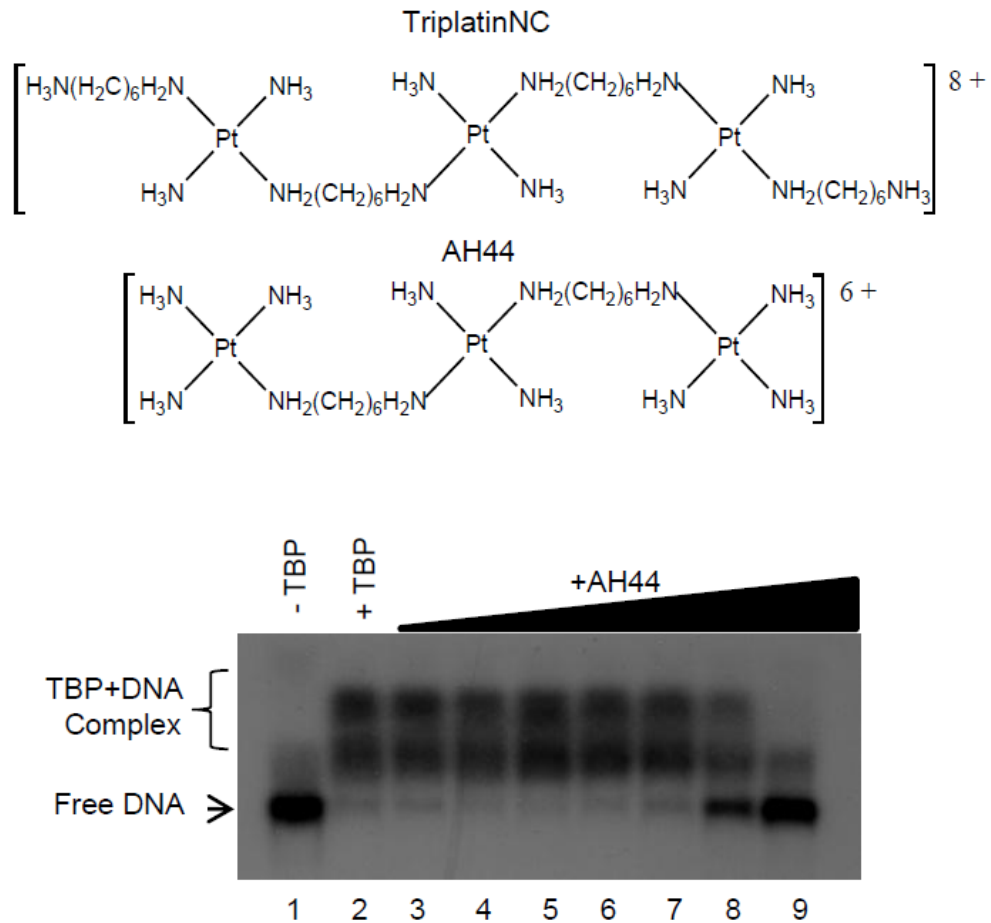


**Figure A.5** A. Structures of *TriplatinNC*<sup>+8</sup> and *AH44*<sup>+6</sup>. B. EMSA; Lanes 3-9; 2nM <sup>32</sup>P-labeled AdML DNA oligo incubated with 0.032, 0.16, 0.8, 4, 20, 100, and 500uM drug, respectively, followed by 100ng rTBP protein. Lane 2 is the 'TBP-DNA complex' positive control. Lane 1 is the 'free DNA' control, containing DNA only.



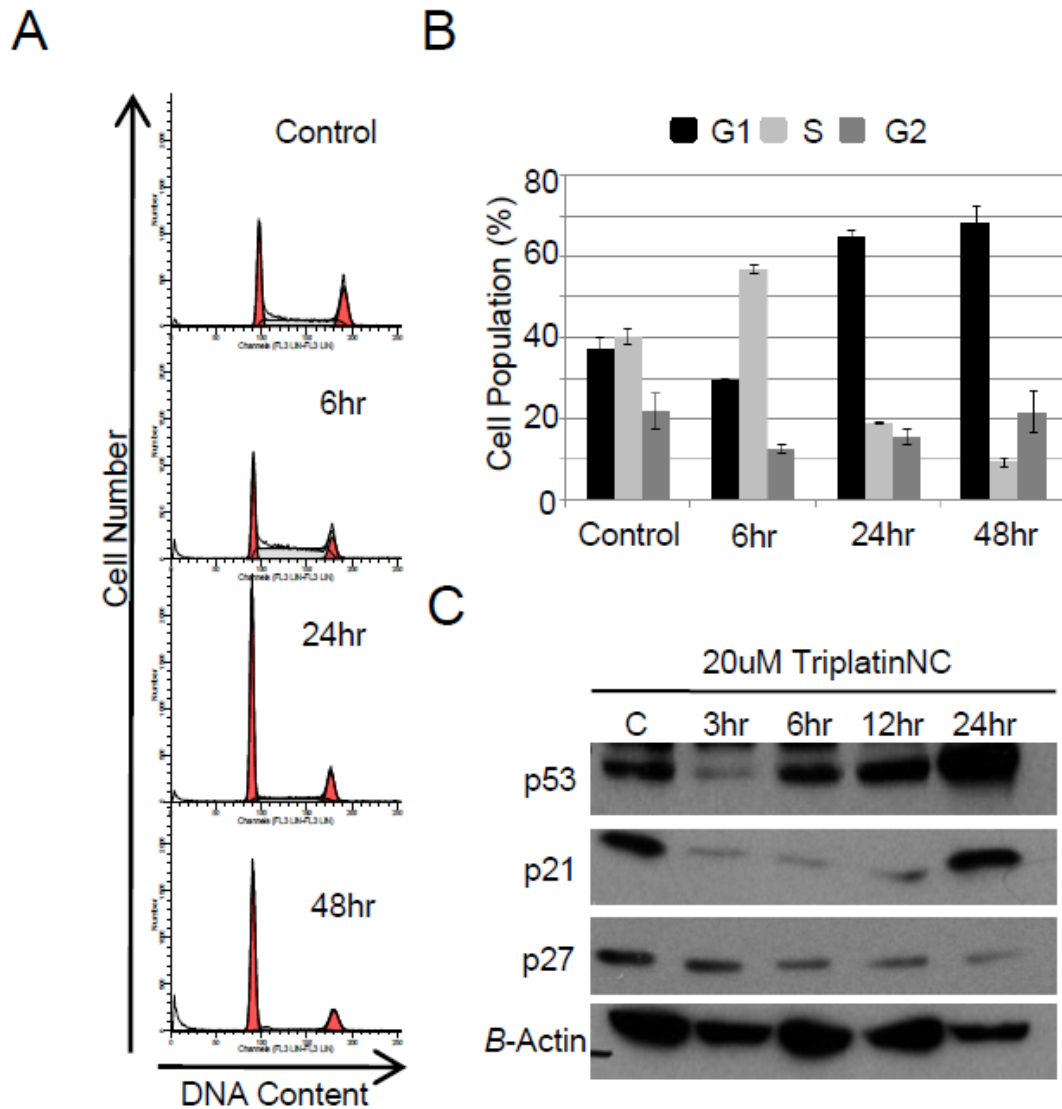


**Figure A.6** TriplatinNC induces G1 cell cycle arrest. (A.) Flow Cytometry; Cell cycle analysis of HCT116 cells treated for 6, 24, and 48hrs with 20 $\mu$ M TriplatinNC (IC90) after RNase B treatment and staining with propidium iodide. (B.) Modfit software analysis of histograms (excluding sub-G<sub>1</sub>). Data points are shown as mean  $\pm$  s.d. of 2 independent experiments with 2 replicates per sample (C.) Western Blot Analysis; Time course analysis of p53, p21, and p27 protein expression after 20 $\mu$ M TriplatinNC for 3, 6, 12, and 24hrs. B-Actin is used as a loading control.

**At 24hrs, TriplatinNC induces a G<sub>1</sub> cell cycle arrest.** Anticancer therapeutics cause proliferative arrest generally through induction of a classical signaling pathway<sup>28</sup>. Central to this pathway is the stabilization of p53 protein by serine/threonine kinases, followed by transactivation of the cyclin-dependent kinase (CDK) inhibitor, p21. Increased protein levels of p21 inhibit CDK activities resulting in cell cycle arrest. This pathway is induced by cisplatin, which has been shown to arrest cells at the G<sub>2</sub>-checkpoint as an attempt to repair DNA damage before cells enter mitosis<sup>29-30</sup>. In agreement with these studies, HCT116 cells treated with 20μM cisplatin ([IC<sub>90</sub>], Fig. S1D) were shown to induce S-phase accumulation at 24hrs, and finally G<sub>2</sub> arrest at 48hrs (Fig. A.7). Treatment of HCT116 cells with 20μM TriplatinNC, on the other hand, induced an earlier arrest in G<sub>1</sub> at 24hrs continuing to 48hrs. The increase in the number of cells in G<sub>1</sub> was mostly at the expense of the proportion of cells undergoing DNA replication in S-phase, which decreased 52% at 24hrs and 77% at 48hrs compared to the control. (Fig. A.6 A,B). As expected, there is a substantial stabilization of p53 protein levels leading into the G<sub>1</sub> arrest at 12 and 24 hrs after treatment with TriplatinNC (Fig. A.6 C). However, p21 expression levels are not concomitantly upregulated in the classical manner. Surprisingly, p21 protein expression levels decreased at 6 and 12 hrs, and increase only to basal level at 24hrs. Furthermore, the protein expression levels of p27, a similar CDK inhibitor with the potential to cause cell cycle arrest<sup>31</sup>, also decreased. These data suggest that the G<sub>1</sub>-arrest induced by TriplatinNC may not depend on classical signaling events. The fact that TriplatinNC induces G<sub>1</sub>-arrest in the HCT116 isogenic cell lines lacking either p53 or p21 (Fig. A.8), furthers this point. It is tempting to speculate that TriplatinNC may disrupt the cell cycle at G<sub>1</sub>, because S-

phase has the highest requirements for rRNA production <sup>32</sup>. The consideration that G<sub>1</sub>-cyclin proteins may be synthesized in insufficient amounts to allow for the transition into S-phase is a subject of continuing research.

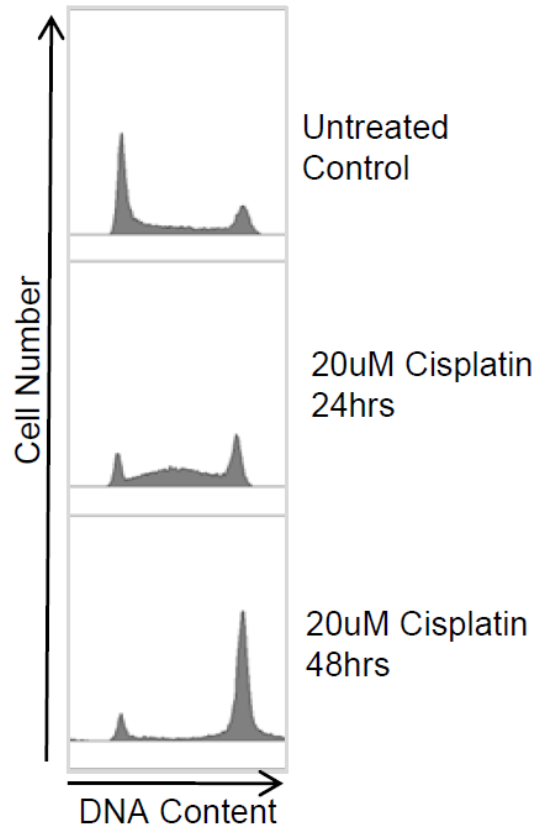


**Figure A.7** Flow Cytometry; Cell cycle analysis of HCT116 cells treated for 0, 24, and 48hrs with 20uM Cisplatin after RNase B treatment and staining with propidium iodide.

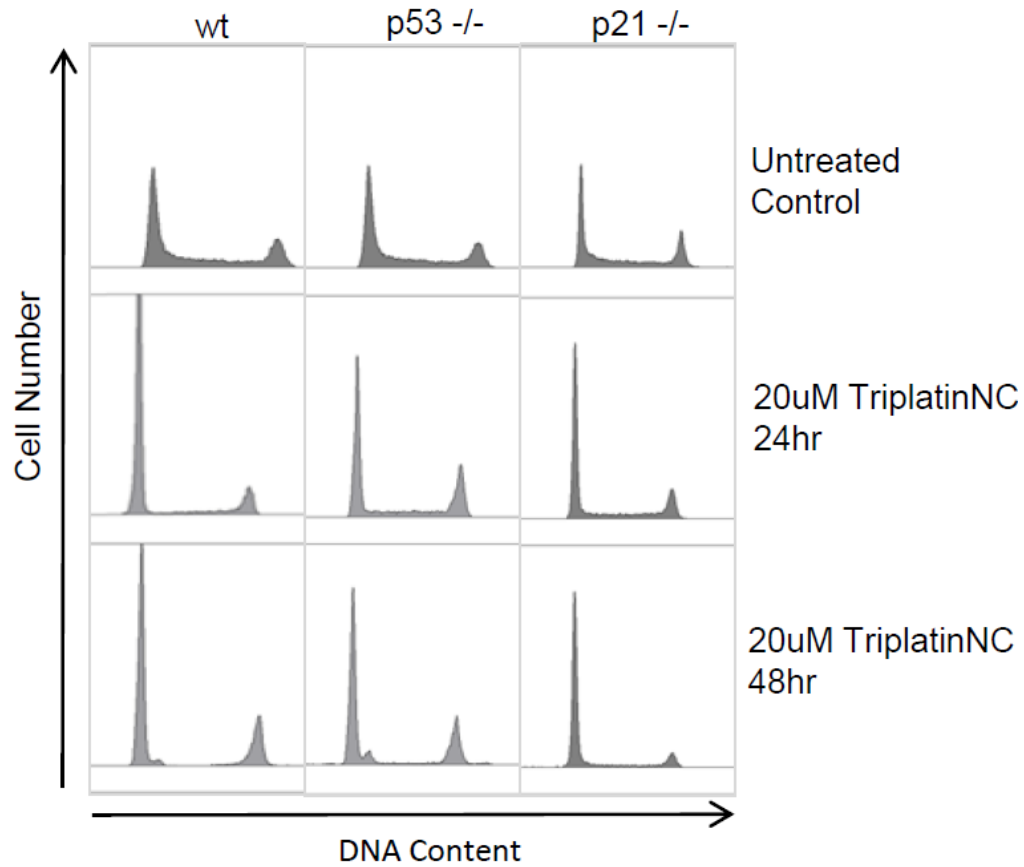


**Figure A.8** Flow Cytometry; Cell cycle analysis of HCT116, HCT116 p53<sup>-/-</sup>, and HCT116 p21<sup>-/-</sup> cells treated for 0, 24, and 48hrs with 20uM TriplatinNC after RNase B treatment and staining with propidium iodide.

**TriplatinNC causes rapid proliferative arrest and cell death independently of p53 status.** In cells undergoing apoptosis, activated cysteine proteases, caspases-3, -6, -7, result in cleavage of cytoskeletal proteins and fragmentation of nuclear DNA. These events result in visible changes to the morphology of the cell including cell shrinkage, chromatin condensation, cytosolic vacuolization, and membrane blebbing<sup>33</sup>. Changes in physiology of HCT116 cells treated with 20 $\mu$ M TriplatinNC-NBD were visualized using confocal microscopy after 2, 10, and 30hrs of treatment (Fig. A.9A). After 10hrs of treatment, cells are much smaller in size and exhibit prolific cytosolic vacuolization. After 30hrs of treatment, blebbing and disintegration of the outer membrane is apparent.

Nearly all cancers harbor genetic defects that directly, or indirectly, inhibit normal proapoptotic, or tumor suppressor functions of p53<sup>28</sup>. For this reason, we asked whether the absence of p53 affects the ability of TriplatinNC to effectively induce proliferative arrest and cell death. HCT116 p53<sup>+/+</sup> and p53<sup>-/-</sup> cells were treated with 20 $\mu$ M cisplatin or TriplatinNC for 12, 24, 48, or 72hrs. Using the MTT assay, it was determined that the ability of cisplatin to inhibit cell growth was significantly limited in the absence of p53 (Fig. A.9B). However, the inhibitory effects of TriplatinNC on cell growth was unaffected by the absence of p53 protein (Fig. A.9C). In support of these results, we asked further whether the absence of p53 affects the ability of TriplatinNC to inhibit colony-formation, or reproductive viability, using the clonogenic survival assay. HCT116 p53<sup>+/+</sup> and HCT116 p53<sup>-/-</sup> cells were treated with 20 $\mu$ M TriplatinNC for 24, 48, and 72hrs (Fig. A.9C, Fig. A.10). The percentage of cells that failed to replicate was determined to be between 63-75% after 24hr, 86-90% after 48hrs, and 85-99% after 72hrs. There was no significant difference in cells with or without p53.

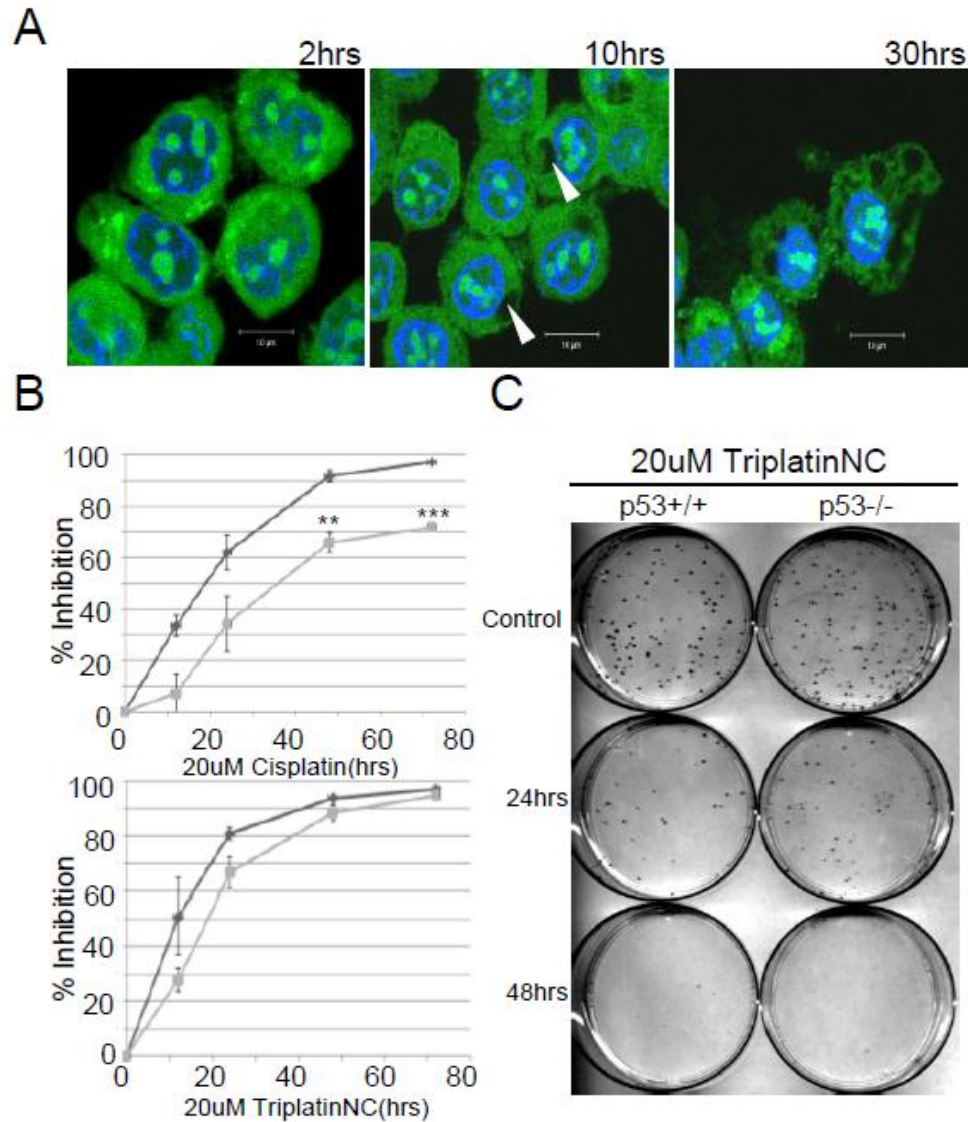


**Figure A.9** TriplatinNC causes rapid proliferative arrest and cell death. (A.) Confocal Microscopy; Morphological effects on HCT116 cells treated with 20 $\mu$ M TriplatinNC for 2, 10, and 30hrs include a reduction in cell size, membrane blebbing, and cytosolic vacuolization (white arrows). (B.) MTT Assay; Comparison of growth inhibition in HCT116 p53+/+ (lt gray) and p53-/- (dk gray) cells treated with 20uM cisplatin or TriplatinNC. Percent Inhibition is calculated as:  $1-(N/N_0)$ , where N=treated samples and  $N_0$ =untreated control samples. Data points are shown as mean  $\pm$  s.d. of 2 independent experiments with 3 replicates per sample. \*\* $p < 0.05$ , \*\*\* $p < 0.005$  (C.) Clonogenic Survival Assay; Comparison of reproductive viability in HCT116 p53+/+ cells and p53-/- cells treated with 20uM TriplatinNC for 24 and 48hrs. Plates are representative of 4 independent experiments with 2 replicates per sample; mean  $\pm$  s.d. of the combined data is shown in Fig. S5.

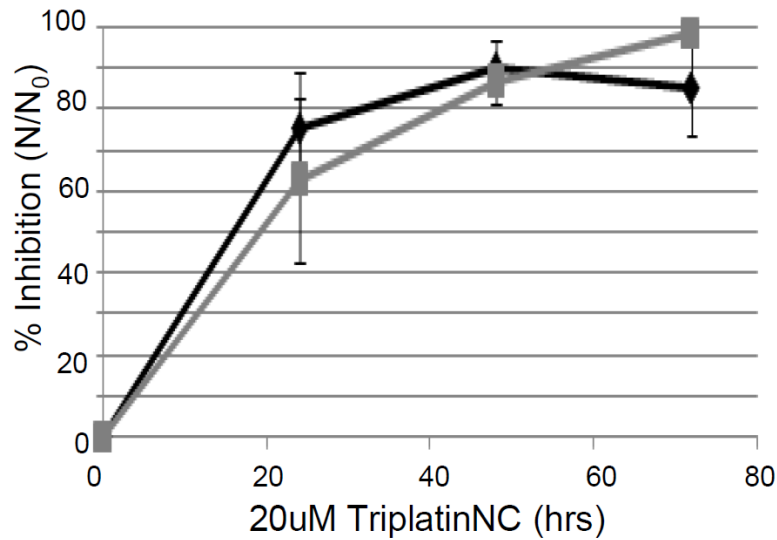


**Figure A.10** Clonogenic Survival Assay; Comparison of colonies formed in HCT116 p53+/+ cells (black) and HCT116 p53-/- cells (gray) treated with 20uM TriplatinNC. Percent Inhibition is calculated as:  $1 - (N/N_0)$ , where  $N$ =treated samples and  $N_0$ = untreated control samples. Data are shown as mean  $\pm$  s.d. representative of 4 independent experiments.



**After 48hrs, TriplatinNC induces a robust apoptotic signaling cascade.** TriplatinNC induces apoptosis in mast cells through activation of the mitochondrial-dependent pathway initiator, procaspase-9, and the downstream effector, procaspase-3<sup>34</sup>. In extension of these studies, it was determined whether TriplatinNC induced accumulation of the activated forms of procaspase-9 and procaspase-3 in p53(+/+) as compared to p53(-/-) HCT116 isogenic colon carcinoma cell lines. Both cells lines show a time-dependent increase in active caspase-9 and caspase-3 after treatment with 20 $\mu$ M TriplatinNC (Fig. A.11A). At 30 or 55hrs after treatment in p53-/- cells, there is less accumulation of active caspase-9 compared to the untreated control than in p53+/+ cells. However, the abundance of active caspase-3 appears to be unaffected by the absence of p53. Therefore, it was asked whether caspase-3 may be activated also by the initiator of the mitochondrial-independent pathway of apoptosis, caspase-8.

Caspase-8, has the ability to activate procaspase-3 through both mitochondrial-dependent and -independent apoptotic pathways. In the mitochondria-dependent pathway, caspase-8 cleaves BID to tBID, which translocates to the mitochondria and causes damage by culminating an efflux of death promoting proteins such as cytochrome-C. These events, in turn, lead to activation of procaspase-9, followed by procaspase-3. In the mitochondrial-independent pathway, caspase-8 instead directly activates procaspase-3, and downstream substrates such as Parp-1, eventually leading to cell death<sup>35</sup>. In HCT116 cells treated with 20 $\mu$ M cisplatin for 48hrs, it was determined that the abundance of active caspase-8 (p18) and downstream target, Parp-1, is severely reduced in cells lacking p53 as compared to the wild-type control (Fig A.11B). However, treatment with 20 $\mu$ M TriplatinNC for 48hrs induced similar

levels of active caspase-8 and Parp-1 in p53+/+ and p53-/- cells (Fig. A.11C). Furthermore, TriplatinNC does not induce the cleavage of BID into tBID (Fig. A.12), therefore, the mitochondrial-dependent and independent pathways are likely activated independent of each other<sup>36</sup>.

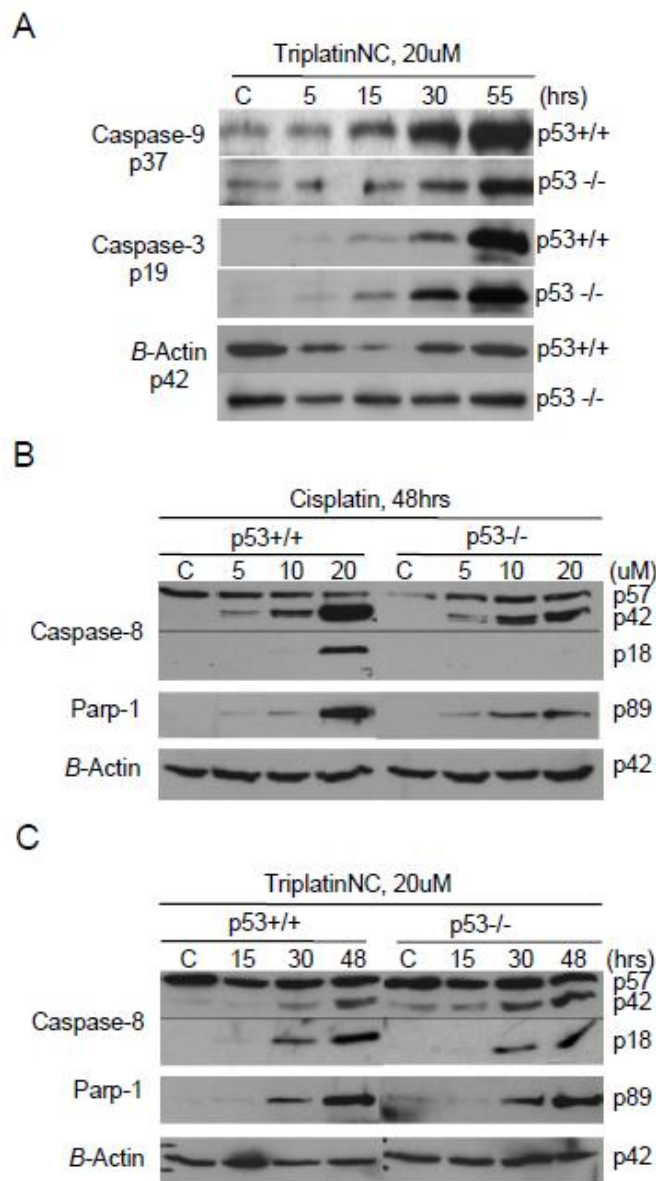


**Figure A.11** *TriplatinNC* induces activation of caspases independent of p53. (A.) Western Blot Analysis; Timecourse analysis of cleaved caspase-9 and -3 protein in HCT116 p53+/+ and p53-/- cells treated with 20μM *TriplatinNC* for 5, 15, 30, and 55hrs. (B., C.) Comparison of cleaved caspase-8 and Parp-1 protein in HCT116 p53+/+ and p53-/- cells treated with 20μM *Cisplatin* or *TriplatinNC* at 48hrs. B-Actin was used as a loading control.

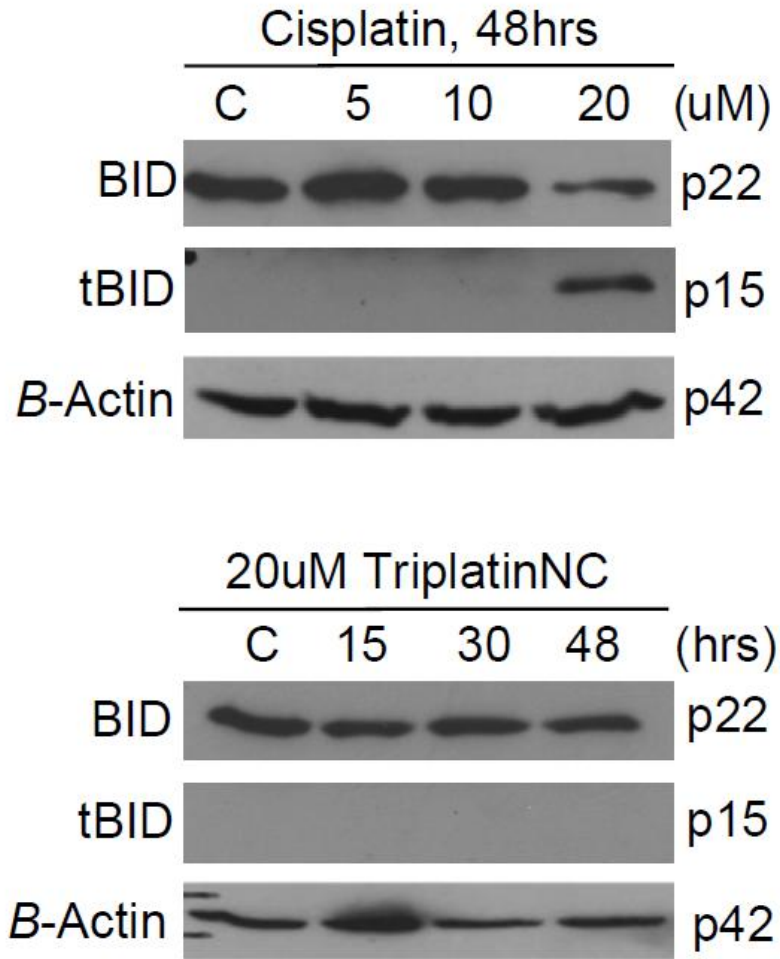


**Figure A.12** Western Blot; Comparison of BID (p22) and the active form, tBID (p15) proteins in HCT116 p53 treated with 20uM Cisplatin or TriplatinNC at 48hrs. B-Actin was used as a loading control.

**Summary.** This study highlights remarkable features and cellular consequences of the noncovalent polynuclear platinum agent, TriplatinNC. Within hours, TriplatinNC accumulates within cells and localizes specifically to the nucleolus. The immediate decrease in rate of rRNA transcription, followed by G1 arrest, is a likely result of unique 'phosphate clamp' DNA binding motif employed by TriplatinNC, which competitively inhibits TBP-DNA interactions. TriplatinNC activates the apoptotic program through mitochondrial-dependent and -independent caspase pathways. TriplatinNC induces morphological changes in cells consistent with the process apoptosis, including shrinkage in cell size, cytosolic vacuolization, and membrane blebbing. Furthermore, TriplatinNC effectively induces proliferative arrest and cell death independent of p53. The activity of TriplatinNC in human cancer cell lines extends to antitumor activity observed *in vivo* using the 2008 human tumor xenograft mouse model. (Fig. A.13 and Table A.1). The results presented here support a basis for selective targeting of rRNA processes as a strategy for p53-independent induction of apoptosis in cancer cells and pave the way for an entirely new class of platinum-based anticancer therapeutics.

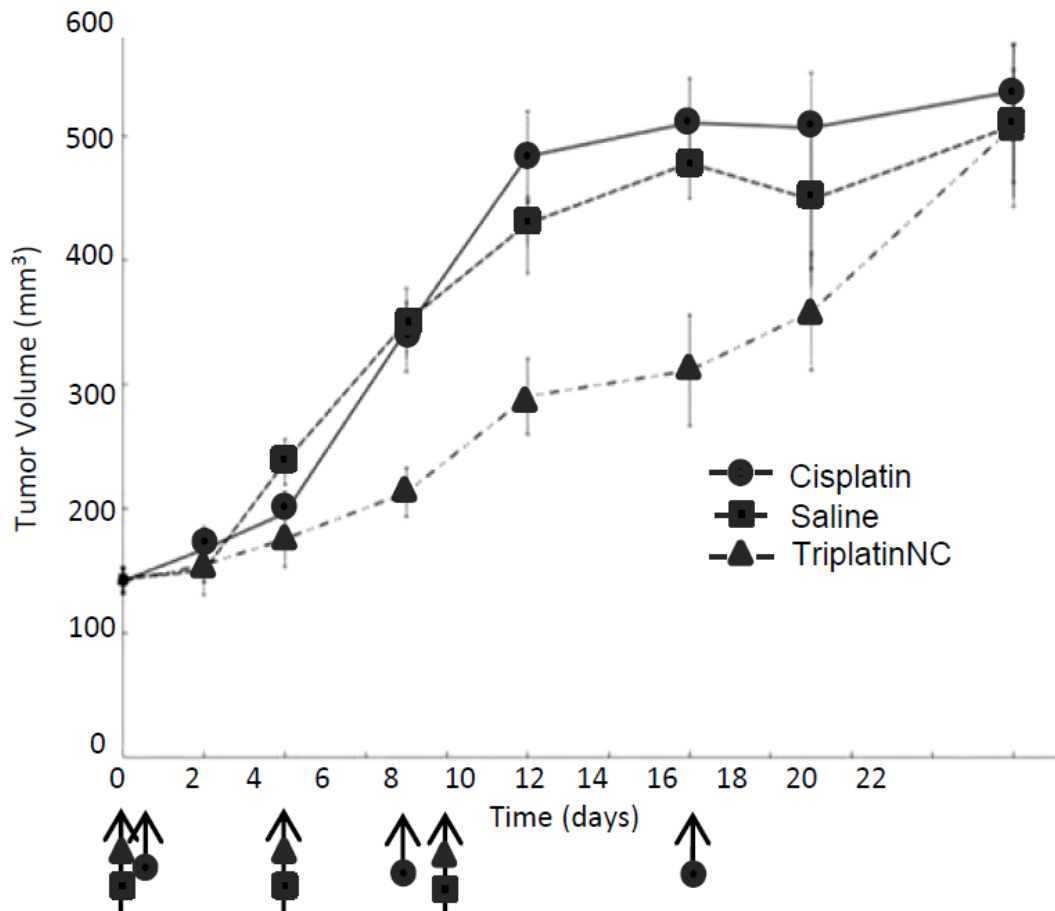


**Figure A.13** 2008 ovarian tumor human xenograft model: Animals were treated on days 0, 4, 8 with either 25mg/kg TriplatinNC by ip injection, saline (0.1ml/10g body weight), or on days 0, 7, 14 with 4mg/kg cisplatin by ip injection.

The effects of TriplatinNC against the 2008 ovarian tumor xenograft mouse model

| Drug        | Dose (mg/kg) | TGI | GDI (a) | GDI (b) | Abs. Growth Delay (to 300%) |
|-------------|--------------|-----|---------|---------|-----------------------------|
| Cisplatin   | 4            | -   | 1.0     | 1.1     | 8.8 days                    |
| TriplatinNC | 25           | 32% | 2.5     | 1.2     | 21.25 days                  |

**Table A.1** Effect of cisplatin and TriplatinNC against the 2008 ovarian tumor xenograft mouse model. Drug efficacy was assessed by measuring the TGI (tumor growth inhibition) on day 10, indicating % decrease in tumor volume in drug treated animals vs. control, GDI (tumor growth delay index) indicating the number of days the tumor takes to reach 3 (a) or 4 (b) times its starting size, and AGD (absolute growth delay), calculated as median time in days to reach 3 times starting tumor volume.

## **Materials and Methods**

**Drug Synthesis.** Cisplatin was synthesized as previously described; [Wong, E.S.Y.; Giandomenico, C.M., Patent No. 09678595]. TriplatinNC and AH44 were synthesized as described previously (16). The synthesis of TriplatinNC-NBD and Cisplatin-NBD are described in the Supplemental Methods section.

**Cell Culture and Drug Treatments.** HCT116, HCT116 p53<sup>-/-</sup>, and A2780 cell lines were cultured in RPMI 1640 (Invitrogen), supplemented with 10% calf serum (Atlanta Biologicals) and 1% penicillin/streptomycin (Invitrogen). Cells were maintained in logarithmic growth as a monolayer in T75 culture flasks at 37°C in a humidified atmosphere containing 5% CO<sub>2</sub>. For drug treatment studies, unless otherwise noted, the molar drug:cell ratio was kept constant by seeding 5x10<sup>4</sup> cells/mL media throughout.

**Confocal Fluorescence Microscopy.** 5x10<sup>4</sup> cells were seeded on chamber slides (Lab-Tek II) in media. 24hrs after seeding, cells were treated with TriplatinNC-NBD or Cisplatin-NBD at the indicated times and concentrations. After removing the media, cells are washed with PBS and mounted as described below. For Immunofluorescence of fibrillarlin, cells were permeabilized with 0.5% Triton-X in PBS for 10 min. and blocked in PBS/Casein for 1hr at room temperature. 1:200 dilution of primary antibody, anti-fibrillarlin (cell signaling, clone C13C3) was added overnight at 4°C, then a 1:500 dilution of secondary antibody anti-rabbit IgG Alexa 647 conjugate (cell signaling) for 3 hrs at room temperature. The antibodies are then fixed with 3% paraformaldehyde for 15 min. at room temperature. All slides were mounted in VectaShield with DAPI (Vector Labs) and viewed using a Zeiss LSM 510 confocal microscope.



**Flow Cytometry.** HCT116 cells were drug treated for 6, 24, and 48hr.  $1 \times 10^6$  cells were suspended in 1ml of propidium iodide solution (3.8mM sodium citrate; 0.05mg/ml propidium iodide; 0.1% Triton X-100) with added RNase B (7000units/ml) and kept in the dark at 4°C. Cells were analyzed by flow cytometry on a CoulterElite XL-MCL (Beckman Coulter). Twenty thousand events were acquired and analyzed using Modfit software.

**Metabolic Labeling and rRNA analysis.**  $2 \times 10^5$  HCT116 cells were grown in 6-well plates in 4ml RPMI/10% FBS media for 24hr. Cells were drug treated for 5h. For phosphate depletion, complete media was replaced with phosphate-free DMEM/10% dialyzed FBS containing drug and incubated for 30 min. before the addition of  $15 \mu\text{Ci/ml}$   $^{32}\text{P}$ -orthophosphate (Perkin Elmer) and further 30 min. incubation. Medium was again changed to RPMI/10% FBS drug-containing medium for 3hr and total RNA was isolated using RNeasy (Qiagen). RNA concentration was determined using a Nanodrop. 1.5ug of total RNA was separated on a 1% agarose-formaldehyde gel. After electrophoresis, 28S rRNA quantities were visualized with Ethidium Bromide as a loading control. Gels were placed on Whatman paper and dried for 2hr at 80°C under vacuum suction. Dried agarose gels were exposed to x-ray film.

**Electromobility Shift Assay.** 2nM end-labeled dsDNA (24mer 5'-GAAGGGGGCTCTAAAAGGGGGTG-3' containing the AdML TATA box.) was incubated for 15 min. at 30°C with or without drug in a final volume of 10 $\mu\text{s}$  reaction buffer (20mM Hepes-KOH, pH7.9, 25mMKCl, 10% glycerol, 0.025% NP-40, 100  $\mu\text{g/ml}$  BSA, 0.5mM DTT, 0.1mM EDTA, and 2mM  $\text{MgCl}_2$ ). Where indicated, 100ng rTBP (Santa Cruz) was added to the reactions and was further incubated for 30 min. The

reactions were separated by electrophoresis in a 6% native polyacrylamide gel in 0.5x TBE buffer (45mM Tris-HCl, 44mM boric acid, and 2mM MgCl<sub>2</sub>). The gel was dried and exposed to x-ray film.

**Growth Inhibition Assay.** Cells were seeded in a 96-well plate at  $5 \times 10^3$  cells/well in 100 $\mu$ l media and allowed 24hrs to attach. Cells were then drug treated for a period of 72hrs. After removal of drug, the cells were treated with 0.5mg/mL MTT reagent [(3,4,5-dimethylthiazol-2-yl)-2,5-diphenyltetrazolium bromide; Sigma] in media for 3hrs at 37°C. The MTT reagent was removed and 100 $\mu$ l of DMSO was added to each well. The plate was then incubated on a shaker at room temperature in the dark. The spectrophotometric reading was taken at 570nm using a microplate reader.

**Clonogenic Survival Assay:**  $2 \times 10^4$  HCT116 +/+ and HCT116-/- cells were seeded in 3ml of medium in a 6-well plate. After 24hrs of incubation, cells were drug treated for a 24hr period. 250 or 2500 cells were seeded into 10cm dishes and allowed to grow for 10-14 days to form colonies. These were then fixed by methanol and stained by 0.1% crystal violet. Colonies consisting of more than 50 cells were counted. Plating efficiency and surviving fraction were determined for each drug.

**Immunoblot Analysis:** Primary antibodies used were p53 (cell signaling, # 9282), p21 (Santa Cruz, clone F-5), p27 (cell signaling, clone SX53G8.5), total caspase-3 (cell-signaling, 9662), total caspase-8 (cell signaling, clone IC12), cleaved caspase-9 (cell signaling, #9501), cleaved Parp (cell signaling, # 9541), and B-Actin (Abcam, ab8226). After drug treatments, both floating and adherent cells were harvested. Cells were washed with ice-cold PBS, repelleted, and, resuspended in SDS lysis buffer (62.5mM

Tris-HCl, pH 7.5, 5% glycerol, 4% SDS, 4% complete protease inhibitor (Roche), 5% BME). After homogenization, proteins were resolved on 7.5-15% polyacrylamide gels, transferred to PVDF membrane, and blocked in 5% non-fat milk at room temperature for 1 hr. The membranes were probed with primary antibodies overnight, followed by secondary anti-rabbit, or anti-mouse antibodies conjugated to horseradish peroxidase (Cell Signaling, Thermo Scientific). Chemiluminescent protein bands were visualized on X-ray film.

**Acknowledgements:** Microscopy was performed at the Virginia Commonwealth University Department of Anatomy and Neurobiology Microscopy Facility, supported, in part, by National Institutes of Health (NIH)-National Institute of Neurological Disorders and Stroke Center Core Grant 5P30NS047463-02.

### List of References

1. White, R.J. RNA polymerases I and III, growth control and cancer. *Nat Rev Mol Cell Biol* **6**, 69-78 (2005).
2. Ruggero, D. & Pandolfi, P.P. Does the ribosome translate cancer? *Nat Rev Cancer* **3**, 179-192 (2003).
3. Thomas, G. An encore for ribosome biogenesis in the control of cell proliferation. *Nat Cell Biol* **2**, E71-E72 (2000).
4. Drygin, D., Rice, W.G. & Grummt, I. The RNA polymerase I transcription machinery: an emerging target for the treatment of cancer. *Annu Rev Pharmacol Toxicol* **50**, 131-156 (2010).
5. Raska, I., Koberna, K., Malínský, J., Fidlerová, H. & Masata, M. The nucleolus and transcription of ribosomal genes. *Biol. Cell* **96**, 579-594 (2004).
6. Burger, K., et al. Chemotherapeutic Drugs Inhibit Ribosome Biogenesis at Various Levels. *Journal of Biological Chemistry* **285**, 12416-12425 (2010).
7. Khyriam, D. & Prasad, S.B. Cisplatin-induced genotoxic effects and endogenous glutathione levels in mice bearing ascites Dalton's lymphoma. *Mutation Research/Fundamental and Molecular Mechanisms of Mutagenesis* **526**, 9-18 (2003).
8. Wang, D. & Lippard, S.J. Cellular processing of platinum anticancer drugs. *Nat Rev Drug Discov* **4**, 307-320 (2005).
9. Longley, D.B., Harkin, D.P. & Johnston, P.G. 5-Fluorouracil: mechanisms of action and clinical strategies. *Nat Rev Cancer* **3**, 330-338 (2003).

10. Carmo-Fonseca, M., Mendes-Soares, L. & Campos, I. To be or not to be in the nucleolus. *Nat Cell Biol* **2**, E107-112 (2000).
11. Emmott, E. & Hiscox, J.A. Nucleolar targeting: the hub of the matter. *EMBO Rep* **10**, 231-238 (2009).
12. Dang, C.V. & Lee, W.M. Nuclear and nucleolar targeting sequences of c-erb-A, c-myb, N-myc, p53, HSP70, and HIV tat proteins. *J Biol Chem* **264**, 18019-18023 (1989).
13. Futaki, S., *et al.* Arginine-rich peptides. An abundant source of membrane-permeable peptides having potential as carriers for intracellular protein delivery. *J Biol Chem* **276**, 5836-5840 (2001).
14. Martin, R.M., Tunnemann, G., Leonhardt, H. & Cardoso, M.C. Nucleolar marker for living cells. *Histochem Cell Biol* **127**, 243-251 (2007).
15. Mitchell, D.J., Kim, D.T., Steinman, L., Fathman, C.G. & Rothbard, J.B. Polyarginine enters cells more efficiently than other polycationic homopolymers. *J Pept Res* **56**, 318-325 (2000).
16. Harris, A.L., *et al.* Synthesis, characterization, and cytotoxicity of a novel highly charged trinuclear platinum compound. Enhancement of cellular uptake with charge. *Inorg Chem* **44**, 9598-9600 (2005).
17. Komeda, S., *et al.* A Third Mode of DNA Binding: Phosphate Clamps by a Polynuclear Platinum Complex. *Journal of the American Chemical Society* **128**, 16092-16103 (2006).
18. Calnan, B.J., Tidor, B., Biancalana, S., Hudson, D. & Frankel, A.D. Arginine-mediated RNA recognition: the arginine fork. *Science* **252**, 1167-1171 (1991).

19. Mangrum, J.B. & Farrell, N.P. Excursions in polynuclear platinum DNA binding. *Chemical Communications* **46**, 6640-6650 (2010).
20. Terrier, P., Tortajada, J., Zin, G. & Buchmann, W. Noncovalent Complexes Between DNA and Basic Polypeptides or Polyamines by MALDI-TOF. *Journal of the American Society for Mass Spectrometry* **18**, 1977-1989 (2007).
21. Grummt, I. Life on a planet of its own: regulation of RNA polymerase I transcription in the nucleolus. *Genes Dev* **17**, 1691-1702 (2003).
22. Learned, R.M., Cordes, S. & Tjian, R. Purification and characterization of a transcription factor that confers promoter specificity to human RNA polymerase I. *Molecular and Cellular Biology* **5**, 1358-1369 (1985).
23. Radebaugh, C.A., *et al.* TATA box-binding protein (TBP) is a constituent of the polymerase I-specific transcription initiation factor TIF-IB (SL1) bound to the rRNA promoter and shows differential sensitivity to TBP-directed reagents in polymerase I, II, and III transcription factors. *Mol Cell Biol* **14**, 597-605 (1994).
24. Zomerdijk, J.C., Beckmann, H., Comai, L. & Tjian, R. Assembly of transcriptionally active RNA polymerase I initiation factor SL1 from recombinant subunits. *Science* **266**, 2015-2018 (1994).
25. Cully, M.J. & Leever, S.J. RNA interference pinpoints regulators of cell size and the cell cycle. *Genome Biol* **7**, 219 (2006).
26. Klein, J. & Grummt, I. Cell cycle-dependent regulation of RNA polymerase I transcription: the nucleolar transcription factor UBF is inactive in mitosis and early G1. *Proc Natl Acad Sci U S A* **96**, 6096-6101 (1999).

27. Rubbi, C.P. & Milner, J. Disruption of the nucleolus mediates stabilization of p53 in response to DNA damage and other stresses. *EMBO J* **22**, 6068-6077 (2003).
28. El-Deiry, W.S. The role of p53 in chemosensitivity and radiosensitivity. *Oncogene* **22**, 7486-7495 (0000).
29. Volland, C., *et al.* Repression of cell cycle-related proteins by oxaliplatin but not cisplatin in human colon cancer cells. *Molecular Cancer Therapeutics* **5**, 2149-2157 (2006).
30. Elisabetta Pani, L.S., Mahmoud El-Shemerly, Josef Jiricny and Stefano Ferrari Mismatch Repair Status and the Response of Human Cells to Cisplatin. *Cell Cycle* **6**, 1796 - 1802 (2007).
31. Toyoshima, H. & Hunter, T. p27, a novel inhibitor of G1 cyclin-Cdk protein kinase activity, is related to p21. *Cell* **78**, 67-74 (1994).
32. Derenzini, M., *et al.* Key role of the achievement of an appropriate ribosomal RNA complement for G1-S phase transition in H4-II-E-C3 rat hepatoma cells. *J Cell Physiol* **202**, 483-491 (2005).
33. Häcker, G. The morphology of apoptosis. *Cell and Tissue Research* **301**, 5-17 (2000).
34. Harris, A.L., Ryan, J.J. & Farrell, N. Biological consequences of trinuclear platinum complexes: comparison of [[trans-PtCl(NH<sub>3</sub>)<sub>2</sub>]<sub>2</sub>μ-(trans-Pt(NH<sub>3</sub>)<sub>2</sub>(H<sub>2</sub>N(CH<sub>2</sub>)<sub>6</sub>-NH<sub>2</sub>)<sub>2</sub>)]<sub>4</sub><sup>+</sup> (BBR 3464) with its noncovalent congeners. *Mol Pharmacol* **69**, 666-672 (2006).
35. Riedl, S.J. & Shi, Y. Molecular mechanisms of caspase regulation during apoptosis. *Nat Rev Mol Cell Biol* **5**, 897-907 (2004).

36. S J Korsmeyer, M.C.W., M Saito, S Weiler, K J Oh, and P H Schlesinger. Pro-apoptotic cascade activates BID, which oligomerizes BAK or BAX into pores that result in the release of cytochrome c. *Cell Death and Differentiation* **7**, 1166-1173 (2000).



## Appendix B: Pre-association of polynuclear platinum anticancer agents on a protein, human serum albumin. Implications for drug design†

Eva I. Montero, Brad T. Benedetti, John B. Mangrum, Michael J. Oehlsen, Yun Qu and  
Nicholas P. Farrell\*

*Department of Chemistry, Virginia Commonwealth University, Richmond, VA 23284*

† Based on the presentation given at Dalton Discussion No. 10, 3–5<sup>th</sup> September 2007,  
University of Durham, Durham, UK.

Dalton Trans. 2007 November 21; (43): 4938–4942.

ICP-OES Binding Studies performed by Brad T. Benedetti

### **Abstract**

The interactions of polynuclear platinum complexes with human serum albumin were studied. The compounds examined were the “non-covalent” analogs of the trinuclear BBR3464 as well as the dinuclear spermidine-bridged compounds differing in only the presence or absence of a central  $\text{-NH}_2^+$  (BBR3571 and analogs). Thus, closely-related compounds could be compared. Evidence for pre-association, presumably through electrostatic and hydrogen-bonding, was obtained from fluorescence and circular dichroism spectroscopy and Electrospray Ionization Mass Spectrometry (ESI-MS). In the case of those compounds containing Pt-Cl bonds, further reaction took place presumably through displacement by sulfur nucleophiles. The

implications for protein pre-association and plasma stability of polynuclear platinum compounds are discussed.

## **Introduction**

Polynuclear platinum complexes (PPCs) containing two or three platinum units linked by alkanediamine or polyamine chains comprise a structurally distinct class of anticancer active platinum compounds, Figure B.1.<sup>1</sup> A distinct feature of these compounds is the presence of a central moiety capable of pre-association or “non-covalent” (hydrogen-bonding and electrostatic) interactions with biomolecular targets. The three global pharmacological factors controlling platinum drug cytotoxicity and antitumor activity are cellular uptake, the frequency and structure of DNA adducts, and the extent of metabolizing interactions. The presence of the central unit (platinum-tetraam(m)ine coordination sphere or the polyamine nitrogen) in polynuclear platinum compounds allows for modulation of these pharmacological factors and may affect drug efficacy.

The role of pre-association in dictating the final products of reaction of PPCs with biomolecules has been assisted greatly in the trinuclear case by the synthesis and evaluation of “non-covalent” analogs where the Pt-Cl bonds are displaced by a substitution-inert  $\text{NH}_3$  or a “dangling” amine  $\text{H}_2\text{N}(\text{CH}_2)_6\text{NH}_3^+$  (structures Ia or Ib, Figure B.1).<sup>2-3</sup> Similar strategies can be used for polyamine-bridged dinuclear compounds. Further, the synthetic strategies involved in producing linear polyamine-bridged species automatically give rise to a precursor where the central nitrogen is blocked, usually by a carbamate such as *t*-butyl (Boc).<sup>4</sup> This pair of compounds then only differs in charge

and the presence or absence of a central protonated nitrogen atom. The central nitrogen atom is susceptible to selective attack using, for example, various carbamate or amide blocking groups (structures II, IIa, and IIb, Figure B.1).<sup>5</sup>

The rate of DNA platination as well as the amount of long-range interstrand crosslinks (where the sites of platination are separated by up to 4 intervening base pairs) is affected by charge and hydrogen-bonding capacity of the linker.<sup>6</sup> For 1,4 interstrand crosslink directional isomers ( $3' \rightarrow 3'$  and  $5' \rightarrow 5'$  crosslinks) are formed. The relative proportion of these adducts is dependent on hydrogen-bonding and charge effects within the linker.<sup>7-8</sup> The X-ray crystal structure of a duplex DNA co-crystallized with Ib demonstrated a new mode of DNA ligand binding—a phosphate clamp—where hydrogen-bonding interactions with the phosphate backbone may be arranged in a modular manner.<sup>9</sup>

Intracellular platinum accumulation and cytotoxicity are also affected by charge. In this case, a perhaps counter-intuitive observation is that cell uptake actually increases with charge.<sup>3,10-11</sup> Interestingly, cellular uptake of the spermidine-bridged dinuclear compound II is greater than that of the blocked derivative IIa.<sup>11</sup> In these cases enhanced cytotoxicity is always correlated with greater cellular uptake.<sup>11-12</sup> In mechanistic studies with phospholipids, a “non-covalent” interaction of Ia was also observed, suggesting one possible mechanism for membrane transport of these highly charged species.<sup>13</sup>

In this contribution we examine the reactions of polynuclear platinum compounds with human serum albumin (HSA) and show for the first time the presence of a pre-associated or “non-covalent” interaction of a platinum drug on the protein. Reactions in

plasma, and especially with HSA, are generally considered responsible for the metabolic deactivation of platinum-based drugs. Understanding the molecular details of such interactions may allow for strategies to manipulate their extent with consequent effects on cellular uptake and even therapeutic index.

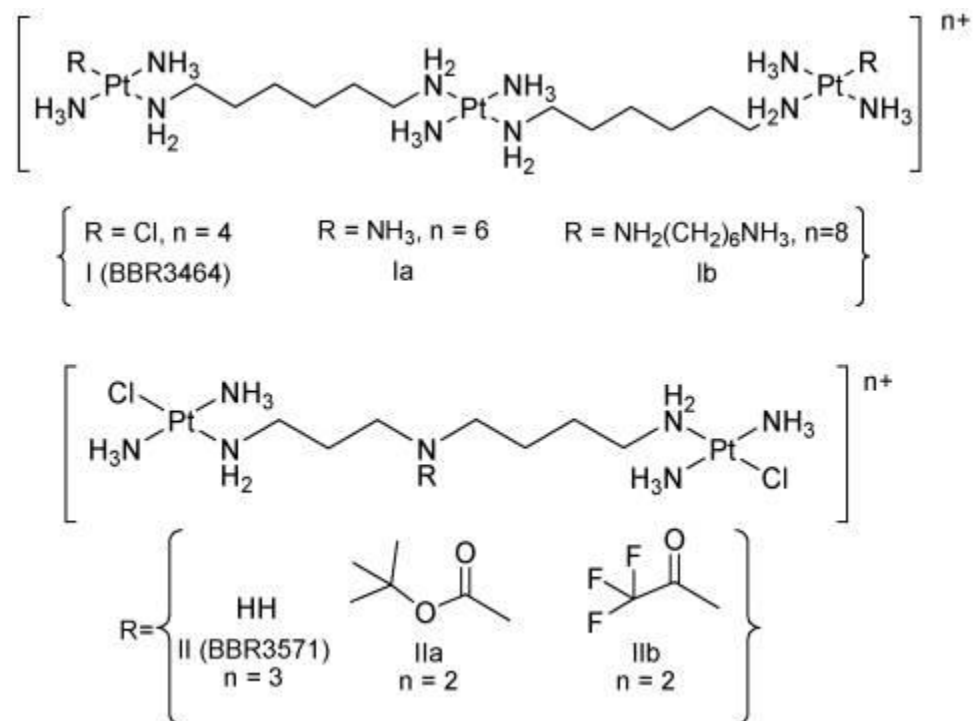


**Figure B.1** Structures of pairs of trinuclear (BBR3464 I, Ia, Ib) and dinuclear (BBR3571 II, IIa, IIb) studied for pre-association effects on human serum albumin (HSA).

## **Results and Discussion**

The effects of charge on polynuclear platinum complex binding to human serum albumin (HSA) were examined with two sets of compounds. Firstly, the trinuclear BBR3464 I was compared with its non-covalent analog Ia and secondly, the effect of blocking groups in the central nitrogen of the spermidine-linked dinuclear species was evaluated (II, IIa, IIb). See Figure B.1 for structures. Global changes in protein conformation can be assessed by circular dichroism (CD) and fluorescence spectroscopy.<sup>14-15</sup> The CD spectrum of HSA exhibits two negative bands in the ultraviolet region at 208 and 220 nm characteristic of an  $\alpha$ -helical structure of the protein. The fluorescence from excitation of HSA at 298 nm reflects changes in the microenvironment of the tryptophan 214 residue, serving as a tool to obtain information about conformational changes of the protein.<sup>14</sup> A decrease in fluorescence of the lone tryptophan of HSA is interpreted as a conformational change making the amino acid more accessible to water quenching.

### **Trinuclear platinum complexes**

#### *Fluorescence spectroscopy*

At  $t = 0$  the relative decrease in fluorescence is concentration dependent for both BBR3464 and the “non-covalent” analog Ia. Over time the relative decrease for BBR3464 is significantly greater than at  $t = 0$  for all concentrations whereas for the “non-covalent” analog there is little or no further perturbation of the system, Figure B.2.

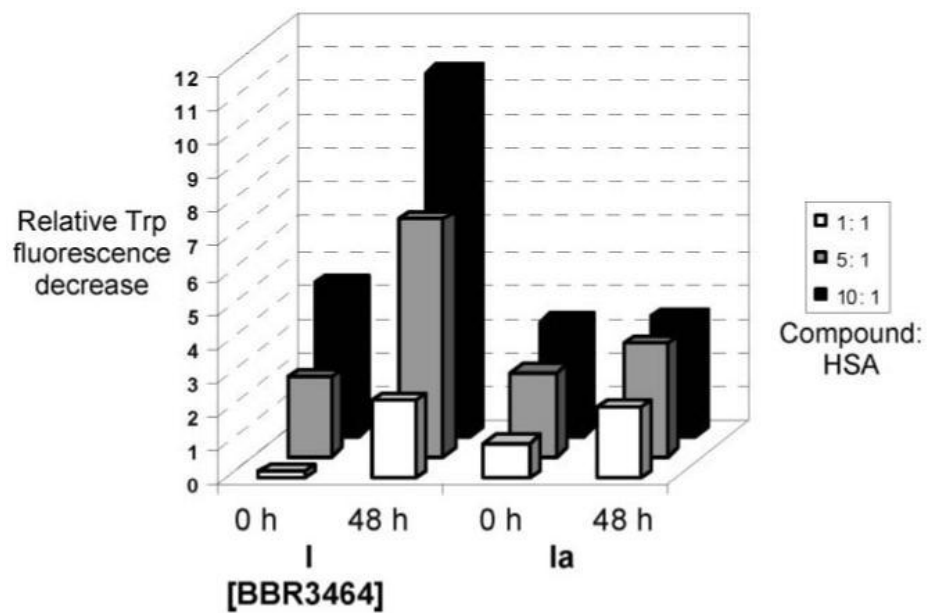


**Figure B.2** Changes in fluorescence of HSA treated with trinuclear platinum compounds. Note no significant change for the “non-covalent” analog over time.

### CD Spectroscopy

The CD spectrum of HSA incubated with PPCs is time and concentration-dependent. Immediately upon mixing 1:1 ratios of Pt complex:HSA the ellipticity of the negative band at 208 nm is increased (to more negative values) and the spectra do not change over a 24 h time period, Figure B.3. At  $t = 0$  the spectra for BBR3464 (3) and Ia (4) are superimposable. In contrast when 10:1 ratios are used, the spectrum corresponding to the BBR3464 reaction (1) changes and the ellipticity is reduced (less negative values). In fact the spectra become similar to those observed for 20-fold excesses of either c-DDP or its *trans* isomer upon extensive incubation with HSA and diminution of the  $\alpha$ -helical content of the protein.<sup>15</sup> Likewise, the binding of the ruthenium antitumor drug *trans*-[RuCl<sub>4</sub>(Im)<sub>2</sub>]<sup>-</sup> (Im = imidazole) induces considerable concentration-dependent change (up to 15%) of the secondary structure upon binding.<sup>16</sup> These results and others<sup>17-18</sup> are therefore consistent for the concept of bond-formation at the higher concentration. The most likely binding sites in all cases remain the sulfur amino acids and the CD results in general are consistent structural transitions of HSA being dependent on the state of the cysteine Cys34.<sup>19</sup> In contrast to all these cited cases where bond formation is expected to occur, there is little or no change for the “non-covalent” analog (5) at the higher ratio, Figure B.3. Thus, the pre-association is also indicated to actually increase the order of the secondary structure with an enhancement of  $\alpha$ -helical content.



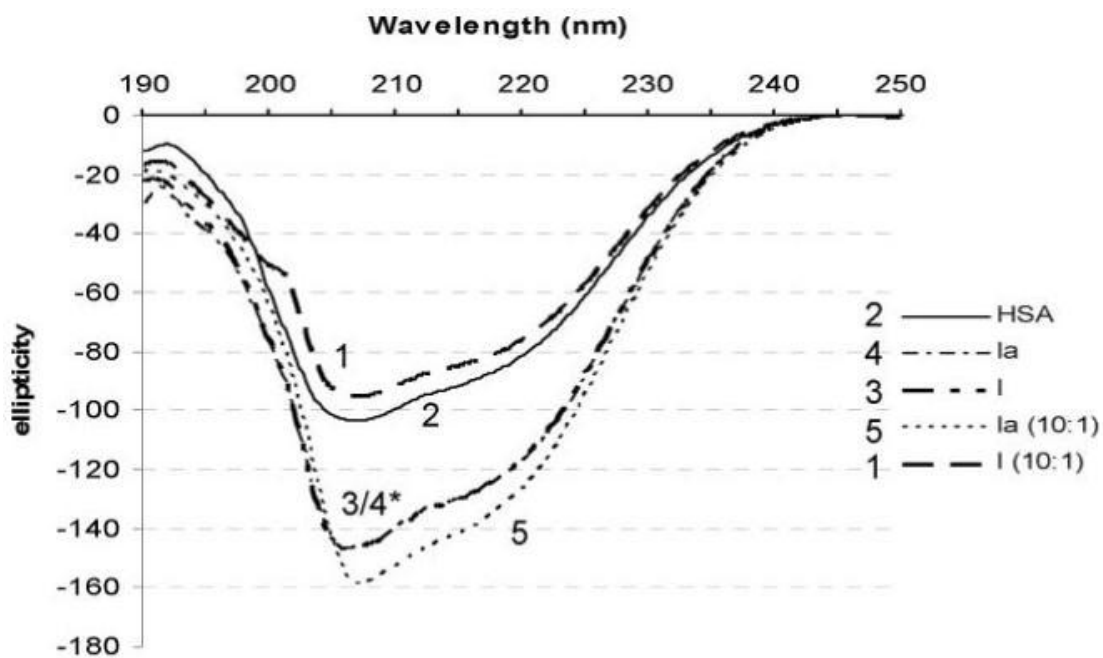


**Figure B.3** CD spectra of HSA incubated with compounds I or Ia at different ratios; drug:HSA, 1:1 and 10:1 after 24 h. Note no significant change for the “non-covalent” analog after 24 h. (\*) Spectra of I (3) and Ia (4) overlap from 195-250 nm.

### *ESI-Mass spectrometry*

It is reasonable to conclude from both the fluorescence and CD data that the spectral changes induced by Ia, which are invariant over time, represent a “pre-association” or non-covalent binding to the protein. At  $t = 0$  the binding of BBR3464 also represents a significant contribution from the non-covalent “pre-association” and that further changes are due to bond formation. To confirm the presence of this interaction, the compound Ia was incubated with rHSA and the mixture examined by ESI-mass spectrometry, Figure B.4. It is observed in the mass spectrum that a noncovalent interaction between the polynuclear platinum compound Ia and rHSA takes place after a very short incubation period. There is a 1015 Da shift in the deconvoluted spectrum (Figure B.4B) obtained after incubation reveals that rHSA which corresponds to a 1:1 complex Ia with rHSA with the presence of one of  $\text{NO}_3^-$  counter ion from the complex. Mass spectrometry has also been used to directly observe c-DDP binding<sup>20</sup> and also Cys34 binding to gold of gold-based antiarthritic drugs.<sup>21</sup> In the present case initial studies with BBR3464 caused precipitation and no clean spectra were obtained—further studies are in progress.

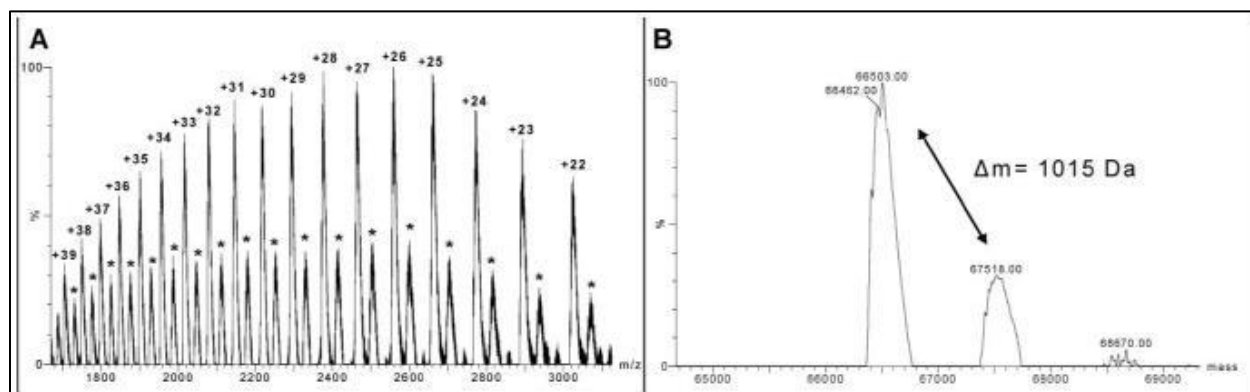


**Figure B.4** (A) Nano-ESI-MS of rHSA incubated with Ia. rHSA-ligand bound peaks are designated with (\*). (B) Deconvoluted mass spectrum showing a mass shift of 1015 Da, corresponding to the addition of Ia + one  $\text{NO}_3^-$ .

## Dinuclear spermidine-linked compounds

Designed synthesis of polyamine backbones gives a series of exceptionally potent compounds which mimic successfully the biological activity of BBR3464.<sup>4,12,22</sup> The critical feature in the biological activity is linked to the presence of a central charged  $\text{-NH}_2^+$  on the polyamine linker. The role of pre-association in dinuclear polyamine-linked compounds can be examined by comparing the reactions of the charged species and its uncharged or blocked analog. Interestingly, the relative decrease in fluorescence at 1:1 ratios was significantly less for the blocked derivatives. In this case, however the presence of Pt-Cl bonds does mean that over time platinum-protein bond formation may take place and this is reflected in an enhanced fluorescence decrease over time for all compounds, Figure B.5. It is of interest to note however, that this decrease is not as great as that seen for BBR3464. In agreement with the changes in fluorescence the CD spectrum of HSA bound to BBR3571 after 48 h appears similar to that of BBR3464 at high Pt:HSA (10:1) ratios (data not shown).

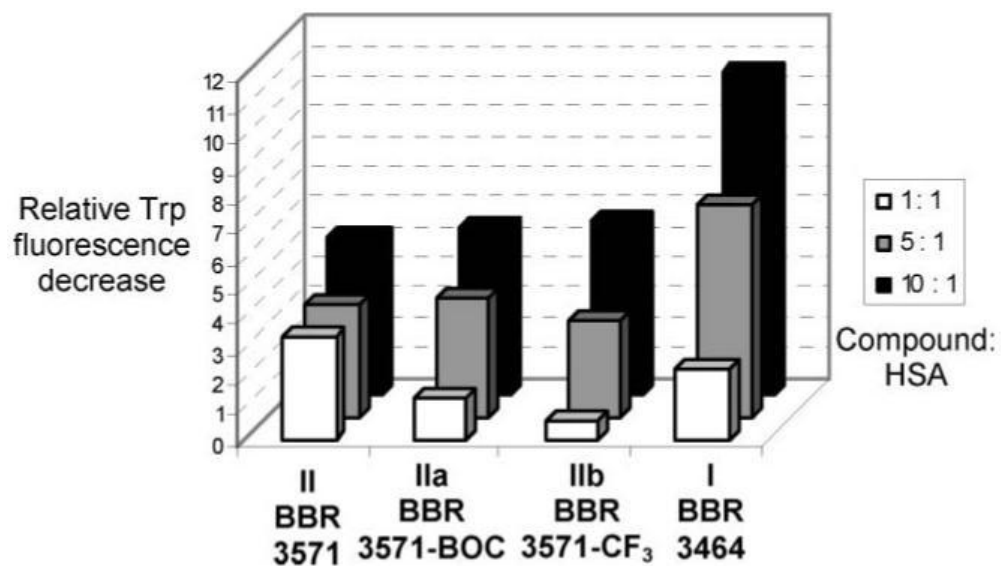


**Figure B.5** Changes in fluorescence of HSA treated with dinuclear platinum compounds.

It is generally considered that chemical changes of platinum compounds on HSA lead to deactivation.<sup>14,23</sup> A study of a series of mononuclear and dinuclear derivatives of *meso*-1,2-bis(4-fluorophenyl)ethylenediamine showed strong binding to HSA by hydrophobic and electrostatic interactions, leading to reduced cellular uptake and decreased potency.<sup>24</sup> A pharmacological principle is that free (non-protein-bound) drug is active, being able to diffuse readily to tissue. Therefore to evaluate and quantitate the binding of PPCs to HSA, BBR3464 and Ia were incubated and the ultrafilterable protein unbound fraction was quantified for selected time points, Figure B.6. Analysis by ICP-OES shows a decrease in Pt content immediately upon mixing,  $t = 0$ , for both BBR3464 and Ia. This initial decrease in Pt content represents the non-covalent, “pre-association” of the Pt complex with protein. The Pt content corresponding to BBR3464 decreases with time, representing a displacement of the Pt-Cl bond and a formation of the covalently bound Pt-protein species (where covalent is used to indicate Pt-amino acid residue formation independent of strict contributions of covalent or coordinate bonding). In contrast, ICP-OES analysis of Ia shows a constant Pt concentration from  $t = 0$  through  $t = 24$  h. Due to the presence of the substitution-inert  $-NH_3$  group, the initial pre-association is not followed by a covalent Pt-protein interaction. Similar behavior was observed for Ib.

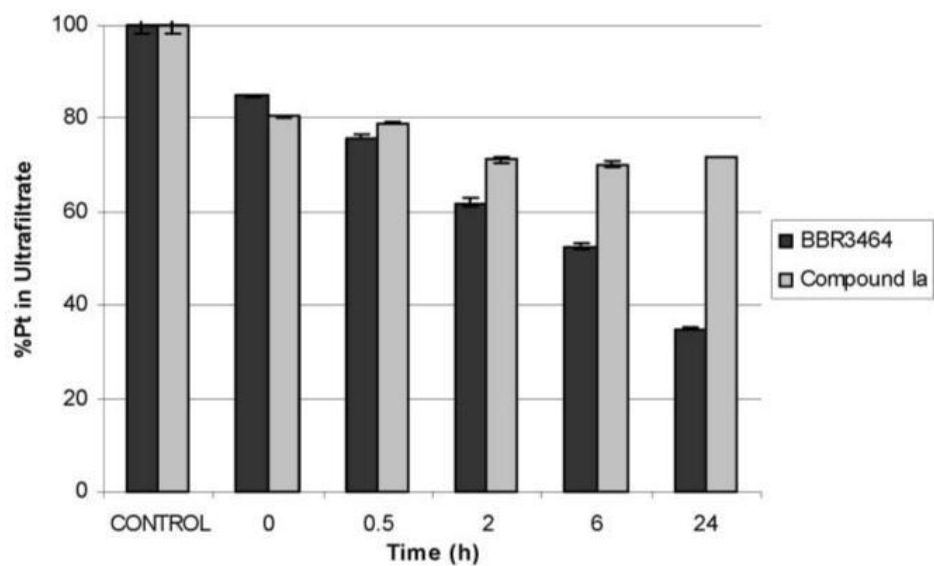


**Figure B.6** ICP-OES analysis of Pt content in ultrafiltrate of BBR3464 and Ia after incubation with HSA for selected time points.

## Conclusions

The results show that the initial reaction of human serum albumin with trinuclear platinum compounds is one of “pre-association”, similar to that observed for DNA and phospholipids. The mass spectral confirmation is the first, to our knowledge shown for platinum antitumor agents. The strength of binding is apparently stronger than that seen for free spermine, spermidine or the cation  $[\text{Co}(\text{NH}_3)_6]^{3+}$ , where the CD changes upon incubation were minimal compared to free HSA.<sup>25</sup> The “pre-association” observed for I and Ia can be also observed for complexes II—where the presence of a blocking group diminished the initial interaction as a cause of diminished charge and hydrogen-bonding capacity of the central nitrogen. The proposed binding sites for platinum on HSA are the Cys-34 and Met-298, located on the exterior of the protein in sub-domains I and II.<sup>14-15,20,23</sup>

There are a number of interesting points to consider based on this understanding. Human serum albumin is a versatile transport protein and receptor for a variety of ligands and drugs. The primary function of HSA is the transport of fatty acids but since it carries a negative 17 charge, it is also responsible for shuttling a wide variety of metal ions, steroids, and a variety of pharmaceuticals. The crystal structure of human serum albumin has allowed the identification of the principal ligand-binding domains located in the hydrophobic cavities of sub-domains IIA and IIIA.<sup>26-27</sup> In principle the receptor sites for the highly-charged cations as represented by PPCs in this study should be distinct from the Cys and Met covalently-binding sites. It may, therefore, eventually be possible to plot the migration of the pre-associated form to the platinated species. Secondly, the identified metabolic products of BBR3464 can be



mimicked by reactions with small sulfur nucleophiles such as glutathione and methionine.<sup>28-30</sup> HSA constitutes roughly 60% of the mass of plasma proteins with a concentration of  $\sim 40 \text{ mg mL}^{-1}$ . It is highly likely therefore that HSA binding could contribute to these metabolic deactivation reactions, as suggested also for some similar dinuclear complexes.<sup>24</sup> Finally, as a corollary, the results for Ia and Ib suggest that these non-covalent compounds may “by-pass” the deactivation associated with Pt-S bond formation. This is especially important for Ib. This 8+ compound is taken up into cells in a significantly greater concentration than either BBR3464 or Ia, and as a result has demonstrated *in vitro* cytotoxicity equivalent to cisplatin. The “non-covalent” compounds have shown a new mode of DNA binding distinct from intercalation and minor-groove binding. The interaction, but not deactivation, on HSA suggests a new and promising profile for a polynuclear platinum drug.

## **Experimental**

### **Sample preparation**

All platinum compounds were as prepared previously.<sup>2-5</sup> Human serum albumin (essentially fatty acid free) was purchased from Aldrich/Sigma. Recombinant human serum albumin (rHSA) (Recombunin®), expressed in *Saccharomyces cerevisiae*, was a generous gift from Delta Biotechnology Limited (Nottingham, UK). A stock solution of phosphate buffered saline ([phosphate] = 150 mM, pH 7.35 at 37 °C, [NaCl] = 120 mM, [KCl] = 2.7 mM) (PBS) was prepared and used for all reaction solutions in order to mimic physiological conditions. HSA was incubated with platinum reactions at a

constant temperature of 37.5 °C prior to obtaining spectroscopic data, which was acquired at room temperature.

### **UV-Visible spectroscopy (UV-Vis)**

Absorption spectra were recorded on a JASCO V-550 UV-Vis spectrophotometer. HSA concentration was determined from the absorption spectrum, taking the absorbance of a 1 mg mL<sup>-1</sup> solution at 280 nm ( $\lambda_{\text{max}}$  Trp-214) as 0.55.<sup>15</sup>

### **Circular dichroism (CD)**

CD spectra were measured on a Jasco J-600 UV dichrometer using a 0.3 mm (open-ended side plate) quartz crystal cuvette. A bulk solution of HSA was prepared at a 38.5 mg mL<sup>-1</sup> ( $1.12 \times 10^{-4}$  M) concentration. HSA/Pt reactions were conducted at a 1:1 and 10:1 (drug:HSA) stoichiometry. Spectral measurements were recorded at  $t = 0$  and selected time intervals.

### **Fluorescence spectroscopy**

Fluorescence measurements were conducted on a Cary Eclipse Fluorimeter with the excitation and emission wavelengths set at 279 and 310 nm, respectively, with a scan rate 120 of nm min<sup>-1</sup>. PMT voltage was set manually to 409 V. The reactions of platinum compounds were studied at various reactant ratios, predominantly 1:1 and 10:1 (Pt:HSA). An initial concentration for a 10:1 reaction was prepared for each drug. Each solution was then diluted to the specific concentration needed for the desired ratio. Each

reactant was incubated in a shaker bath at 37.5 °C for 45 min prior to reacting. Separate measurements were taken at  $t = 0$  and appropriate time intervals.

### **Electrospray Ionisation Mass Spectrometry (ESI-MS)**

Experiments were conducted on a Waters/Micromass (Manchester, UK) QTOF-2 mass spectrometer. A custom built nano-ESI source was used with a capillary voltage of 2.1 kV and a cone voltage of 36 V. Source block temperature was maintained at 150 °C. ESI-solutions consisted of methanol:water (50:50 v/v) with 0.1% formic acid. The solutions were infused at 0.5  $\mu\text{L min}^{-1}$  using a Harvard Apparatus Model 22 syringe pump (Harvard Apparatus, Holliston, MA). Data acquisition and processing were carried out using the MassLynx 4.0 software. Stock solution of AH 44 was 500  $\mu\text{M}$  in water and made fresh before ESI-MS experiments. Aliquots from the stock solution of rHSA, 139  $\mu\text{M}$ , were mixed with the polynuclear platinum compound Ia in a 1:2 molar ratio in water and incubated at 37 °C, for 15 min. Incubated samples were mixed in the ESI solution to give a final rHSA concentration of approximately 40  $\mu\text{M}$ .

### **Inductively Coupled Plasma-Optical Emission Spectroscopy (ICP-OES)**

1.8 mM solutions of each complex were prepared in phosphate buffer and added to 0.6 mM HSA such that the final concentration of complex was 0.9 mM; (3:1; drug:HSA) The mixture was reacted at 37 °C and 100  $\mu\text{L}$  aliquots were removed at  $t = 0, 0.5, 2, 6,$  and 24 h. Aliquots were then centrifuged through a Microcon YM-10 10 000 kDa membrane filter at 14 000  $g$  for 30 min to isolate ultrafiltrate. The centrifuge cup was upturned in a second eppendorf and then centrifuged at 1000  $g$  for 3 min to isolate the protein-bound

fraction. Samples were digested following published methods. Pt content was recorded at 214 nm and 265 nm, at each time point, using a Varian ICP-OES. Data are reported as percentage of Pt in control vs. Pt per time point.

**Acknowledgements:** This work was supported by a grant NIH RO1CA78754 to NF.

### List of References

1. Farrell, N. *Metal Ions in Biological Systems*, (Marcel Dekker, Inc., New York, 2004).
2. Harris, A., Qu, Y. & Farrell, N. Unique Cooperative Binding Interaction Observed between a Minor Groove Binding Pt Antitumor Agent and Hoeschst Dye 33258. *Inorg Chem* **44**, 1196-1198 (2005).
3. Harris, A.L., *et al.* Synthesis, Characterization, and Cytotoxicity of a Novel Highly Charged Trinuclear Platinum Compound. Enhancement of Cellular Uptake with Charge. *Inorg Chem* **44**, 9598-9600 (2005).
4. Rauter, H., *et al.* Selective Platination of Biologically Relevant Polyamines. Linear Coordinating Spermidine and Spermine as Amplifying Linkers in Dinuclear Platinum Complexes. *Inorg Chem* **36**, 3919-3927 (1997).
5. Hegmans, A., *et al.* Amide-based prodrugs of spermidine-bridged dinuclear platinum. Synthesis, DNA binding, and biological activity. *J Med Chem* **51**, 2254-2260 (2008).
6. McGregor, T., *et al.* A comparison of DNA binding profiles of dinuclear platinum compounds with polyamine linkers and the trinuclear platinum phase II clinical agent BBR3464. *J Biol Inorg Chem* **7**, 397-404 (2002).
7. Hegmans, A., *et al.* Long Range 1,4 and 1,6-Interstrand Cross-Links Formed by a Trinuclear Platinum Complex. Minor Groove Preassociation Affects Kinetics and Mechanism of Cross-Link Formation as Well as Adduct Structure. *J Am Chem Soc* **126**, 2166-2180 (2004).

8. Kasparkova, J., Zehnulova, J., Farrell, N. & Brabec, V. DNA Interstrand Cross-links of the Novel Antitumor Trinuclear Platinum Complex BBR3464. *J Biol Chem* **277**, 48076-48086 (2002).
9. Komeda, S., *et al.* A third mode of DNA binding: Phosphate clamps by a polynuclear platinum complex. *J Am Chem Soc* **128**, 16092-16103 (2006).
10. Harris, A.L., Ryan, J.J. & Farrell, N. Biological consequences of trinuclear platinum complexes: comparison of  $[\{\text{trans-PtCl}(\text{NH}_3)_2\}_2\mu\text{-(trans-Pt}(\text{NH}_3)_2(\text{H}_2\text{N}(\text{CH}_2)_6\text{-NH}_2)_2)]^{4+}$  (BBR 3464) with its noncovalent congeners. *Mol Pharmacol* **69**, 666-672 (2006).
11. Roberts, J.D., *et al.* Comparison of cytotoxicity and cellular accumulation of polynuclear platinum complexes in L1210 murine leukemia cell lines. *J Inorg Biochem* **77**, 47-50 (1999).
12. Farrell, N. *Platinum-Based Drugs in Cancer Therapy*, (Humana Press, 2000).
13. Liu, Q., Qu, Y., Van Antwerpen, R. & Farrell, N. Mechanism of the Membrane Interaction of Polynuclear Platinum Anticancer Agents. Implications for Cellular Uptake†. *Biochemistry* **45**, 4248-4256 (2006).
14. Timerbaev, A.R., Hartinger, C.G., Aleksenko, S.S. & Keppler, B.K. Interactions of Antitumor Metallodrugs with Serum Proteins: Advances in Characterization Using Modern Analytical Methodology. *Chemical Reviews* **106**, 2224-2248 (2006).
15. Trynda-Lemiesz, L., Kozlowski, H. & Keppler, B.K. Effect of cis-, trans-diamminedichloroplatinum(II) and DBP on human serum albumin. *J Inorg Biochem* **77**, 141-146 (1999).

16. Trynda-Lemiesz, L., Keppler, B.K. & Kozlowski, H. Studies on the interactions between human serum albumin and imidazolium [trans-tetrachlorobis(imidazol)ruthenate(III)]. *J Inorg Biochem* **73**, 123-128 (1999).
17. Ohta, N., et al. Aggregation of [gamma]-globulin by cis-diamminedichloroplatinum(II): Alteration of Fc region and restoration by diethyldithiocarbamate. *International Journal of Pharmaceutics* **124**, 165-172 (1995).
18. Trynda-Lemiesz, L. & Pruchnik, F.P. Studies on the interaction between human serum albumin and  $[Rh_2(OAc)_2(bpy)_2(H_2O)_2](OAc)_2$ . *J Inorg Biochem* **66**, 187-192 (1997).
19. Christodoulou, J., Sadler, P.J. & Tucker, A. A New Structural Transition of Serum Albumin Dependent on the State of Cys34. *European Journal of Biochemistry* **225**, 363-368 (1994).
20. Ivanov, A.I., et al. Cisplatin binding sites on human albumin. *J Biol Chem* **273**, 14721-14730 (1998).
21. Chang, P.S., Absood, A., Linderman, J.J. & Omann, G.M. Magnetic bead isolation of neutrophil plasma membranes and quantification of membrane-associated guanine nucleotide binding proteins. *Analytical Biochemistry* **325**, 175-184 (2004).
22. Billecke, C., et al. Polynuclear platinum anticancer drugs are more potent than cisplatin and induce cell cycle arrest in glioma. *Neuro-Oncology* **8**, 215-226 (2006).

23. Esposito, B.P. & Najjar, R. Interactions of antitumoral platinum-group metallodrugs with albumin. *Coordin Chem Rev* **232**, 137-149 (2002).
24. Kapp, T., Dullin, A. & Gust, R. Mono- and Polynuclear [Alkylamine]platinum(II) Complexes of [1,2-Bis(4-fluorophenyl)ethylenediamine]platinum(II): Synthesis and Investigations on Cytotoxicity, Cellular Distribution, and DNA and Protein Binding. *Journal of Medicinal Chemistry* **49**, 1182-1190 (2006).
25. Ouameur, A.A., *et al.* Effects of organic and inorganic polyamine cations on the structure of human serum albumin. *Biopolymers* **73**, 503-509 (2004).
26. Curry, S., Mandelkow, H., Brick, P. & Franks, N. Crystal structure of human serum albumin complexed with fatty acid reveals an asymmetric distribution of binding sites. *Nat Struct Biol* **5**, 827-835 (1998).
27. Petitpas, I., Grune, T., Bhattacharya, A.A. & Curry, S. Crystal structures of human serum albumin complexed with monounsaturated and polyunsaturated fatty acids. *J Mol Biol* **314**, 955-960 (2001).
28. Oehlsen, M., Hegmans, A., Qu, Y. & Farrell, N. Effects of geometric isomerism in dinuclear antitumor platinum complexes on their interactions with N-acetyl-L-methionine. *J Biol Inorg Chem* **10**, 433-442 (2005).
29. Oehlsen, M.E., Hegmans, A., Qu, Y. & Farrell, N. A Surprisingly Stable Macrochelate Formed from the Reaction of Cis Dinuclear Platinum Antitumor Compounds with Reduced Glutathione. *Inorg Chem* **44**, 3004-3006 (2005).
30. Oehlsen, M.E., Qu, Y. & Farrell, N. Reaction of polynuclear platinum antitumor compounds with reduced glutathione studied by multinuclear ( $^1\text{H}$ ,  $^{15}\text{N}$



gradient heteronuclear single-quantum coherence, and  $^{195}\text{Pt}$  NMR spectroscopy. *Inorg Chem* **42**, 5498-5506 (2003).

## Vita

Brad Thomas Benedetti was born on July, 10<sup>th</sup>, 1984, in North Adams, Massachusetts, and is an American citizen. He graduated from West Carteret High School, Morehead City, North Carolina in 2002. He received his Bachelor of Science in Chemistry from Hampden-Sydney College, Hampden-Sydney, Virginia in 2006. He then continued his studies in the Ph.D. Chemistry programs at Virginia Commonwealth University.

### EDUCATION

#### **Doctorate of Philosophy, Chemistry; May 2011**

Virginia Commonwealth University (VCU)

Massey Cancer Center and Dept. of Chemistry, Richmond, VA

**Dissertation:** Drug Design, Biological Activity, and Metabolic Consequences of Cytotoxic Platinum Compounds: Utilizing Fluorescent Tagging to Understand Drug Action and Metabolism

Advisor: Nicholas P. Farrell

#### **Bachelor of Science, Chemistry; May 2006**

Hampden-Sydney College, Hampden-Sydney, VA

### AWARDS/AFFILIATIONS

Altria Excellence in Research Fellowship Award, 2010-2011

Phillip Morris Graduate Research Scholarship, 2008

American Chemical Society Member, 2008-Present

### RELATED EXPERIENCE

#### **Research**

Pre-Doctoral Fellow/Ph.D. Research, Massey Cancer Center, Virginia Commonwealth University, Richmond, VA

June 2006 - present

- Designed, synthesized and evaluated a fluorescently tagged TriplatinNC derivative, which led to the discovery of a novel nucleolar DNA/RNA targeting platinum drug.
- Designed and evaluated a novel fluorescent based trans-platinum compound with greater cytotoxicity, cellular uptake and DNA binding than cisplatin.
- Developed metabolic assays and conducted experiments to understand and improve the pharmacokinetic properties of platinum based chemotherapeutics.

- Skilled in biochemical techniques including: 1D, 2D, Exotic Nuclei NMR Spectroscopy, ICP-OES/MS, UV-Vis, Isothermal Titration Calorimetry (ITC), Protein/Peptide Modification, and Gel Electrophoresis.
- Skilled in biological techniques including: Fluorescent/Confocal Laser Scanning Microscopy, Immunohistochemistry, Cell Culture, DNA/RNA Extraction, Rational Drug Design and Synthesis, Cytotoxicity Assays, and Drug/Protein Labeling/Tagging.

NMR Facility Technician, VCU Dept. of Chemistry, Richmond, Va  
March 2007 - Present

- Refill He bi-monthly and N<sub>2</sub> weekly in 300MHz, 400MHz, and 600MHz NMR.
- Assist in setup and analysis of 1-D and 2-D NMR Spec. techniques.

### **Teaching**

Teaching Instructor, VCU Dept. of Chemistry, Richmond, VA  
October 2008

- Taught two classes of graduate BioInorganic Chemistry
- Taught two classes of undergraduate Inorganic Chemistry

Laboratory Instructor, VCU Dept. of Chemistry, Richmond, VA  
August 2006 – May 2007

- Taught and organized four laboratory sections for undergraduate Chemistry 101 and Chemistry 102; 25 students/section.

## **PUBLICATIONS**

Benedetti, B. T., Peterson, E. J., Kabolizadeh. P., Martinez, A., Kipping, R., Farrell, N. F.; **Effects of non-covalent platinum drug-protein interactions on drug efficacy: Use of fluorescent conjugates as probes for drug metabolism.** *Molecular Pharmaceutics*. 2011. *In Press*

Menon, V., Kabolizadeh, P., Peterson, E., Benedetti, B., Kipping, R., Ryan, J., Farrell, N.; **A Nucleolar Targeting Platinum Drug, TriplatinNC, Inhibits rRNA Transcription, Causing G1 Arrest And p53-Independent Apoptosis.** *Proc. Nat. Acad. Sci*. 2011. *In Submission*

Benedetti, B. T., Farrell, N. F.; **Modulation of serum metabolic deactivation through ligand modification in a series of cytotoxic trans-platinum planar amine compounds.** *Inorg. Chem*. 2011. *In Submission*

Martinez, A., Benedetti, B. T., Farrell, N. F.; **Synthesis and Biological Activity of FluoroPlatin in A2780 and HCT116 Cell Lines.** *J. Am. Chem. Soc*. 2011. *Manuscript in Preparation*

Montero, E.; Benedetti, B. T.; Mangrum, J.; Oehlsen, M.; Qu, Y.; Farrell, N.; **Pre-association of polynuclear platinum anticancer agents on a protein, human serum albumin. Implications for drug design.** *Dalton Trans.* 2007; (43): 4938-4942.

## PRESENTATIONS

Benedetti, B.T.; Mangrum, J.; Bulluss, G.; Qu, Y.; Farrell, N.; **Pharmacokinetic Studies of Polynuclear Platinum Complexes with Plasma and Human Serum Albumin: Implications for Drug Design and Delivery.** Poster Presentation at *Xth International Symposium on Platinum Coordination Compounds in Cancer Chemotherapy (ISPCC)*, 2007, Verona, Italy.

Benedetti, B.T.; Peterson, E.; Martinez, A.; Farrell, N.; **TriplatinNC, a non-covalent platinum chemotherapeutic circumvents serum protein metabolic deactivation in A2780 ovarian carcinoma cells.** Poster Presentation at *VCU Massey Cancer Center: Cancer Research Retreat*. 2010, Richmond, Va.

Benedetti, B.T.; Farrell, N.; **Pharmacokinetic Studies of Anti-Tumor Platinum Compounds: Effects of Ligand Substitution on Protein Binding and Free Drug Availability.** Poster Presentation at *VCU Chemistry Department Poster Session*. 2009, Richmond, Va.

Benedetti, B.T.; Farrell, N.; **Metabolic Studies of Anti-Tumor Platinum Compounds: Drug Deactivation Vs. Drug Delivery.** Poster Presentation at *VCU Chemistry Department Poster Session*. 2010, Richmond, Va.